IDŐJÁRÁS

QUARTERLY JOURNAL
OF THE HUNGARIAN METEOROLOGICAL SERVICE

Special Issue: Application of information and communication technologies in environmental sciences: towards a sustainable future

Guest Editor: **Kálmán Kovács**

CONTENTS

****

http://www.met.hu/Journal-Idojaras.php

VOL. 118 * NO. 4 * OCTOBER – DECEMBER 2014

IDŐJÁRÁS

Quarterly Journal of the Hungarian Meteorological Service

Editorial Office: Kitaibel P.u. 1, H-1024 Budapest, Hungary
P.O. Box 38, H-1525 Budapest, Hungary
E-mail: journal.idojaras@met.hu
Fax: (36-1) 346-4669

Indexed and abstracted in Science Citation Index Expanded™ and Journal Citation Reports/Science Edition
Covered in the abstract and citation database SCOPUS®

Subscription by mail:
IDŐJÁRÁS, P.O. Box 38, H-1525 Budapest, Hungary
E-mail: journal.idojaras@met.hu

Editorial

Special Issue: Application of information and communication technologies in environmental sciences: towards a sustainable future

The Future Information and Communication Project (FuturICT) was launched by the European Union within the frame of Seventh Framework Programme. The ultimate goal of the FuturICT project is to understand and manage complex, global, socially interactive systems, with a focus on sustainability and resilience. Revealing the hidden laws and processes underlying societies probably constitutes the most pressing scientific grand challenge of our century and is equally important for the development of novel robust, trustworthy, and adaptive information and communication technologies, based on socially inspired paradigms. FuturICT is at heart of a revolutionary 21st century science, which will use and develop information and communication technologies to create a decision support system, combining data with models in order to solve the grand challenges humanity is facing. FuturICT is expected to lift our knowledge of social and economic systems to a new level of understanding, enabling us to discover promising paths towards a sustainable future.

In close connection to the goals above, the FuturICT.hu project was initiated and performed within the framework of TÁMOP-4.2.2.C-11/1/KONV-2012-0013 project involving cooperating partners from leading Hungarian universities as well as private research sector. Some results of the project relevant to the environmental aspects of application of ICT and their relation to social issues are presented in five papers in present thematic issue. The first paper discusses the assessements of greenhouse gas emissions and trends in Hungary related to the national policies and measures. In the second paper, the trends of precipitation and drought-related climate indices and the return period of the daily precipitation amount are analyzed based on the results of 11 regional climate models (RCMs) after applying a bias-correction procedure. The authors of the third paper deal with the trend analysis of a new MODIS satellite based drought severity index with emphasis on the Carpathian Basin. In the fourth paper, some important aspects of the impact of meteorological forecast uncertainties on environmental dispersion prediction are discussed. The final paper of this issue presents a statistical analysis of relationships between road accidents involving personal injury and meteorological variables in Hungary on the basis of a 20 years long database, and provides a qualitative outlook for the future expectations.

Kálmán Kovács
Guest Editor

IDŐJÁRÁS
Quarterly Journal of the Hungarian Meteorological Service
Vol. 118, No. 4, October – December, 2014, pp. 293–304

Progress towards emission targets through the development of climate change policies and measures in Hungary

Márk Molnár[1], **Sándor Molnár,**[2] and **Anita Csábrági**[2]

[1] *Szent István University, Faculty of Economics and Social Sciences*
H-2100 Gödöllő, Páter Károly u. 1.

[2] *Szent István University, Faculty of Mechanical Engeneering,*
H-2100 Gödöllő, Páter Károly u. 1.

**Corresponding author E-mail: Molnar.Sandor@gek.szie.hu;*

(Manuscript received in final form May 14, 2014)

Abstract—Parties included in Annex I to the UNFCCC are requested to regularly submit National Communications to the Secretariat. This report presents an overview of the results of the 6th National Communication (NC6) of Hungary with respect to the relevant provisions of the Convention and Article 8 of the Kyoto Protocol.

Key-words: mitigation scenarios, emission reduction, national reporting

1. Introduction

Hungary, as a Member State of the European Union and a Party to the Kyoto Protocol, considers efforts against climate change to be one of the most important challenges. Implementing, adopting, and planning measures and policies to tackle climate change related threats, designing mechanisms and plans to adapt to climate change, and pursuing scientific activities to assess, monitor, and decrease climate change vulnerability are in the focus of the Hungarian Government and the experts.

The recent findings outlined in the Fifth Assessment Report of the IPCC conclude that human activities are highly likely to be causing climate change and that actions against global warming are indispensable. In accordance with these results and responding to the 19th Conference of Parties in Warsaw in 2013, Hungary presents the future commitments, the progress made and other relevant topics in the 6th National Communication (*Ministry of National Development,* 2013), where Hungary provides information on greenhouse gas emissions and trends, quantified emission reduction targets, and progress towards their accomplishment, and gives an overview of emissions projections and financial and technical support provided to developing countries (*Molnár S. et al.*, 2012).

2. Information on GHG emissions and trends

In 2011, total emissions of greenhouse gases in Hungary were 66.1 million tons carbon dioxide equivalents (excluding the LULUCF – land use, land use change, and forestry – sector), which is the lowest value in the whole time series (1985–2011). Considering the carbon sinks in the LULUCF sector, the net emissions of Hungary were 62.4 million tons CO_2 equivalents in 2011. Being about 6–7 tons, the Hungarian per capita emissions are below the European average.

By far, the biggest emitting sector was the energy sector, contributing 71.6% to the total GHG emission in 2011. Agriculture was the second largest sector with 13.2%, while emissions from industrial processes (with solvent and other product use) accounted for 9.8%, and the waste sector contributed 5.3%. Compared to the base year, emissions were significantly reduced in the energy (–40.3%), agriculture (–54.0%), and industrial processes (–57.7%) sectors. In contrast, emissions in the waste sector have increased since 1985 (+14.5%). Solvent and other product use and land use, land use change and forestry (LULUCF) sectors show fluctuating behavior.

The most important greenhouse gas is carbon dioxide, accounting for 75.2% of the total GHG emissions. The main source of CO_2 emissions is burning of fossil fuels for energy purposes, including transport. CO_2 emissions have decreased by 41.8% since the middle of the 80's. Methane represents 12.8% in the GHG inventory. Methane is generated mainly at waste disposal sites and in animal farms, but the fugitive emissions of natural gas are also important sources. CH4 emissions are by 37.2% lower than in the base year. Nitrous oxide contributes 10.2% to the total GHG emissions. Its main sources are agricultural soils and manure management. N_2O emissions are 60.4% lower compared to the base year. The total emissions of fluorinated gases amount to 1.8%, but their steadily growing tendency seems to level off since 2008.

By ratifying the Kyoto Protocol, Hungary has committed to reduce its GHG emissions by 6%. Now, our emissions are 43.2% lower than in the base

year (average of 1985–87). For the most part, this significant reduction was a consequence of the economic transition in Hungary (1989–1990), which brought significant decline in the output of the national economy. The production decreased in almost every economic sector including also the GHG relevant sectors like energy, industry, and agriculture. Then, between 2005 and 2011, after a period of about 14 years of relatively stagnant emission levels (1992–2005), GHG emissions fell again quite significantly by 16.7 per cent.

The global financial and economic crises exerted a major impact on the output of the Hungarian economy, consequently on the level of GHG emissions as well. After a quite significant drop of 8.4% between 2008 and 2009, our emissions in the following three years (2009–2011) remained the lowest in the entire time series. Although the decline in economic output stopped in the first quarter of 2010 and Hungary had a moderate growth of 1.6%, emissions fell again by 2.6% in 2011, after a slight increase (+0,8%) in 2010.

Compared to the base year, emissions were significantly reduced in the energy (–40.3%), agriculture (–54.0%), and industrial processes (–57.7%) sectors. In contrast, emissions in the waste sector have increased since 1985 (+14.5%). Solvent and other product use and land use, land-use change and forestry (LULUCF) sectors show fluctuating behavior.

3. Assessment of the current situation

Under the EU's Climate and Energy Package, Hungary as an EU member is committed to a quantified economy-wide GHG emission reduction target of 20% by 2020, compared to the 1990 levels. This target is coupled with a renewable penetration rate of 14.65% for Hungary and an energy efficiency improvement of 20%; while the RED Directive (2009/28/EC) of the EU set the renewable target for Hungary as minimum 13% of the total gross final energy consumption, the objective defined by the NREAP is 14.65%.

This means that Hungary committed herself to a reduction of 20% of the 96 961,78 kt CO_2 equivalents emissions of 1990 (incl. LULUCF), the target to be achieved is 77 568,8 kt by 2020.

Sectors under the EU ETS are forecasted to provide a basis of GHG emissions savings until 2025. Beginning with 2013, from the third trading period onwards, a single EU-wide cap determines the amount of emissions allowed to be emitted by the EU ETS sectors. Furthermore, from 2013 onwards, a linear reduction factor of –1.74 % per annum applies to achieve a total of 21% of reduction in the ETS sectors. Under the joint Effort Sharing Decision (ESD) of the EU, Hungary took the commitment of a maximum 10% increase of the non-ETS sectors greenhouse gas emissions compared to their 2005 levels by 2020.

Hungary is also influenced by the Kyoto second period target of the EU. The EU has also committed to reduce its emissions by 20% under the Kyoto Protocol's second period, which runs from 2013 to 2020. Despite its identical nature, this commitment differs in several important respects from the EU's unilateral 2020 commitment:

- The Kyoto commitment is measured against base years, not 1990.
- LULUCF: the LULUCF sector in the EU is not included in the 20 % target under the Climate and Energy Package, but is accounted for under the KP according to the relevant decisions made in Durban.
- Inclusion of nitrogen trifluoride (NF3): NF3 is not included in the Climate and Energy Package, whereas the scope of the second commitment period has been extended to include the additional gas. The impact of NF3 on aggregate EU emissions is insignificant.
- It requires the EU to keep its emissions at an average of 20% below base-year levels over the whole period, not only in 2020.
- It differs in scope (for instance, it does not cover emissions from international aviation, since these are outside the scope of the Protocol, but it does cover emissions and their removals from land use, land use change and forestry, which is not covered by the unilateral commitment).
- The EU will meet its Kyoto commitment jointly with Iceland.

4. Policies and measures

Legislative and policymaking activities in climate change and the energy sector have been united under the auspices of the Ministry of National Development with the establishment of a sovereign State Secretariat of Climate Change and Energy Policy with two aides of the state secretary – a deputy state secretary for energy policy and another deputy for green economy development and climate change. The most important task of the Secretariat was the formation of the long-term energy strategy of Hungary, as well as submission of the National Action Plan for Renewable Energy to the European Commission. Recently, the administration was reformulated into a State Secretariat of Development, Climate Policy, and Key Public Services.

In the following section, the framework of climate change policies will be outlined. Details are provided in Chapter 4 of the 6th National Communication of Hungary.

The general context of policy development is the Programe of National Cooperation. Although in itself the Programe of National Cooperation is not focused on the GHG mitigation, the implementation of the Programe includes several similar elements, and the Programe itself has some priorities that serve this purpose. Some relevant key elements are:

- Promotion of the European initiative to employ "green" technologies and to research the energy efficiency of buildings and construction materials;
- Launching of a large scale energy efficiency program aiming at reconstruction of pre-fab buildings, thermal insulation projects of other building types, reconstruction of public buildings, etc.;
- Encouragement of renewable energy investments.

A cornerstone of climate change policy is the National Climate Change Strategy which was revised in 2013. Its key characteristics are as follows:

- Main areas of intervention are:
  - — Energy efficiency in buildings;
  - — Renewable energy utilization;
  - — Transport (road tolls, other economic incentives, modal split change);
  - — Afforestation.
- New element is increased emphasis on adaptation to climate change.
- The responsibility of the government is to create the necessary regulatory-legal framework; to review and adjust the subsidy systems; to raise the awareness of the society by giving priority to sustainability and providing good example.
- The residential sector is a key field of change: peoples' lifestyle needs to be changed; a large-scale reduction of demands for energy and materials must be achieved (by subsidized energy efficiency projects, among others);
- Industry and other enterprises also need to reduce their energy consumption, adopt emission reduction measures, "green" their profile, products, and services.
- NGOs, civil organizations shall have increased role in the dissemination of information, awareness raising, and civil control.

As the new EU Sustainable Development Strategy adopted by the European Council requires, Hungary prepares and regularly updates its National Sustainable Development Strategy (NSDS). The new NSDS has been adopted by the Hungarian Parliament in 2013.

Beginning from 1995, a regularly (every six year) revised and updated National Environmental Protection Programe (NEP) is prepared. The recent National Environmental Protection Programe 2009–2014 (NEP-III) was adopted by the Parliament in 2009. Similarly to the previous programes, the NEP-III identifies general objectives, which are then broken down to specific actions, the so-called thematic action programes or TAPs. The general objectives are the following:

- Improving the quality of the environment and life locally;

- Preservation of natural resources;
- Promotion of sustainable lifestyle, production, and consumption;
- Improvement of environmental safety.

The following TAPs are relevant from the aspect of GHG mitigation:

- Reinforcing environmental awareness:
  - — Education, training within the education system from the elementary school to the university;
  - — Environmentally conscious production and consumption;
  - — Access to environment-related information, information dissemination;
  - — Combating climate change;
  - — Reduction of GHG emissions (EU-ETS system, improvement of energy efficiency [NEEAP]);
  - — Reducing the environmental impact of transport (reducing demand, restructuring modal split, alternative fuels);
  - — Reducing emissions from the agriculture (improvement of production efficiency);
  - — Afforestation according to the National Afforestation Programe.
- Environment and health:
  - — Transport and environment (reversing the tendency of shifting to individual transport).
- Protection and sustainable utilization of waters:
  - — Utilization of the energy of geothermal waters.
- Waste management:
  - — Prevention (reduction of waste quantities);
  - — Utilization of wastes and recycling;
  - — Reduction of landfill waste.

The National Sustainable Development Strategy has recently been reformulated and accepted by the government, and it is an important element together with the National Environmental Programe. The New Széchenyi Plan (NSZP) is an economic development programe providing an operative background for the realization of strategic objectives.

The programes of the NSZP concerning GHG mitigation are as follows:

- Energy policy:
  - — Energy policy is to serve economic growth and job creation, together with security of supply, resource diversification, and the reduction of import dependence;

— Production and utilization of renewable energies are to be encouraged.

- Transport:
  - — Creating the financial resources necessary for a sustainable transport system;
  - — Encouraging intermodal transports;
  - — Enforcing environmental and climate policy considerations;
  - — Transformation of the primary energy mix – a greater proportion of renewable energy is necessary;
  - — Development of an adequate traffic and transport system, nodes as well as intermodal and multifunctional logistics centers and related industrial parks established in these nodes to reduce road transit.

The Green Investment Scheme (GIS) is considered to be a key source of funding GHG mitigation projects and efforts. Several of the policies described in this report have been or will be financed at least partly from GIS sources. The GIS is planned to be restructured with the following priorities in mind:

- Complex (deep) energy efficiency revamp of multi-flat and family houses, to increase the approximately 40% energy saving achieved by GIS programes so far to at least 60%;
- Support for the construction of new highly efficient buildings;
- Loan guarantee for the investors of the above projects, so that they could take loans at better conditions to provide their own share for the other supports from the GIS.

Maximum 5% of the GIS revenues can be used for covering the administrative costs of the GIS. It is also required by the regulation that the supported project should be additional (i.e., not implemented without the support).

The impact of policies and measures are summarized in *Table 1*.

Table 1 The impact of policies and measures in CO_2 equivalent

	Policy name	Status	2015 ($ktCO_2eq./yr$)	2020 ($ktCO_2$ eq./yr)	2025 ($ktCO_2$ eq./yr)	2030 ($ktCO_2$ eq./yr)
1	Promotion of renewables	implemented	5 600.2	8 821.2	11 299.1	13 061.0
2	Nuclear power	adopted	2 762.6	5 172.8	7 875.8	10 593.8
3	"Liveable panel buildings" sub-program	implemented	509.7	953.5	1 374.1	1 592.7
4	"Our home" reconstruction sub-program	implemented	402.9	844.4	1 324.6	1 861.8
5	"Power saving households" program	implemented	535.4	1 117.1	1 439.7	1 573.6
6	Renewable public institutions sub-program	implemented	366.6	722.1	1 058.1	1 360.4
7	Reduction of power demand of public institutions	implemented	495.3	972.8	1 451.6	1 866.4
8	District heating efficiency sub-program	implemented	135.1	242.0	312.7	347.2
9	Reducing the energy use of enterprises	implemented	655.9	1 477.6	2 182.0	2 737.5
10	Horizontal measures	implemented	126.3	336.7	547.2	757.7
11	Reducing the energy demand of cargo and passenger transport	implemented	38.7	98.2	111.8	122.4
12	Directing transport to railways	planned	51.3	80.6	89.7	89.7
13	Directing transport to public transport and developing public transport	planned	19.6	52.4	84.7	106.5
14	Reducing road transport emissions	adopted	727.5	1 549.7	2 578.0	3 622.7
15	Environmental awareness in agriculture	adopted	NA	NA		
16	Less nitrate get into water and N-cycle	implemented	NA	NA		
17	Draw attention to decrease GHG emission in agriculture	implemented	NA	NA		
18	National Forest Programe for increasing forest area	implemented	500.00	700.00	1 000.00	1 300.00
19	Frame for forestry management and forest protection	implemented	NA	NA		
20	Mitigation of agricultural emissions with partial change of nitrogen fertilizer utilization and cultivations change	implemented	200.00	NA		
21	Support for perennial herbaceous energy plantation by the European Agricultural Fund	implemented	NA	NA		
22	Complementary financing to support the plantation of energy crops by the European Agricultural Fund	implemented	NA	NA		
23	Rural development for sustainable and modern agriculture	implemented	NA	NA		
24	Climate protection by efficient manure management and biogas	implemented	135.00	NA		
25	New waste management instruments	adopted	2.14	4.62	12.70	16.96
26	Setting up regional waste management projects	implemented	17.14	20.77	34.29	51.83
27	Packaging waste governmental regulation	adopted	6.43	23.08	39.37	58.43
28	Budapest municipal door-to-door separate waste collection	adopted	12.86	20.77	31.75	45.24
29	Landfill recultivation, remediation	adopted	2.14	4.62	11.43	16.02
30	Prevention	adopted	0.00	9.23	25.40	29.22
31	Waste landfill tax	implemented	4.29	13.85	31.75	39.58

Source: *Ministry of National Development* (2013)

The total effect from policies and measures is summarized in *Table 2*.

Table 2. Total effects of policies and measures until 2030

Gg CO_2 equivalent per year	2015	2020	2025	2030
Estimated emission savings from PAMs	13 307.19	23 237.98	32 915.95	41 250.61

5. Projections and the total effect of policies, measures, and supplementarity relating to the Kyoto Protocol mechanisms

Average 2008–2011 emissions in Hungary were 40.8 % lower than the base-year level, well below the Kyoto target of -6 % for the period 2008–2012. In the sectors not covered by the EU ETS, emissions were significantly lower than their respective target, by an amount equivalent to 33.6 % of the base-year emissions. LULUCF activities are expected to reduce net emissions by an annual amount equivalent to 1.9 % of base-year level emissions. Hungary intends to use flexible mechanisms at governmental level by selling an amount of Kyoto units equivalent to 3.5% of base-year emissions per year. Taking all these effects into account, average emissions in the sectors not covered by the EU ETS in Hungary were standing below their target level, by a gap representing 31.1 % of the base-year emissions. Therefore Hungary was on track towards its Kyoto target by the end of 2011.

6. Progress towards EU 20/20/20 goals (ESD)

Total GHG emissions of Hungary decreased by 3.7% between 2011 and 2012, based on approximated GHG inventories for the year 2012 (see *Table 3*). When considering the scope of the EU's climate and energy package, which includes emissions from international aviation, Hungarian emissions in 2012 are approximately 55% lower compared to 1990 levels (98 980.69 Mt). Thus Hungary reaches its 20% reduction target, eight years ahead of 2020. This should not mean that the country has no dedicated tasks, as the reduction of emissions can be accounted to the decline in economic activity and economic growth beyond expectations.

Aggregated projections from Hungary indicate that the total emissions will further decrease between 2012 and 2020 (and 2025, see the Biennial Report for forecast figures). With the current set of national domestic measures in place, emissions are expected to reach a level in 2020 which is 65% below the 1990 level. Implementing the additional measures (at planning stage or realized at lower implementation levels) it is expected to achieve a reduction of 74% below the 1990 level in 2020.

Table 3. Hungary's emissions in the first commitment period

	Mt CO_2 equiv.	2008	2009	2010	2011	2012	Average of 2008-2012	Total of 2008-2012
1	Total GHG emissions	73.6	67.4	67.9	66.1	63.7	67.7	338.7
2	Verified emissions under the EU ETS	27.2	22.4	23.0	22.5	21.3	23.3	116.4
3	Non-ETS emissions	46.4	45.0	45.0	43.7	42.4	44.5	222.4
4	Initial Assigned Amounts (AAUs)	108.5	108.5	108.5	108.5	108.5	108.5	542.4
5	Allowances issued under the EU ETS	25.1	23.9	25.7	25.0	32.8	26.5	132.5
6	Non-ETS target	83.3	84.6	82.8	83.5	75.7	82.0	409.9
7	Difference between target and actual emissions (non-ETS domestic)	37.0	39.6	37.8	39.8	33.3	37.5	187.5
8	Expected carbon sequestration from LULUCF	2.2	2.2	2.2	2.2	2.2	2.2	11.1
9	Difference between target and actual emissions (non-ETS domestic) incl. carbon sequestration	39.2	41.8	40.0	42.0	35.5	39.7	198.6
10	Planned use of Kyoto mechanisms by government (net transfer of AAUs + purchase of CERs+ERUs)	–4.0	–4.0	–4.0	–4.0	–4.0	–4.0	–20.0
11	Emission reduction units (ERUs issued in JI projects)	0.0	1.2	1.4	1.6	3.1	1.5	7.3
12	Difference between target and actual emissions (non-ETS, domestic, incl. Kyoto mechanisms and carbon sinks)	35.2	36.6	34.7	36.4	28.4	34.3	171.3

Source: EEA Report (2013)

The projected reductions are to be achieved both in the sectors covered by the EU ETS (mostly energy supply and industry), where an emission cap is determined at EU level, and in the other sectors covered by national emission targets under the Effort Sharing Decision (ESD). Beyond the EU ETS itself, the largest reductions are expected via measures supporting renewable energy under the Renewable Energy Directive (RED) and implementation of efficiency and energy saving measures.

The average annual emissions and removals from LULUCF in the 2008–2011 are as follows: –1.15 Mt CO_2 equivalent for the average net carbon stock change (Art 3.3.), and –1.06 Mt from forest management (Art 3.4).

Concerning non-ETS emissions in Hungary, the absolute gap between the average non-ETS emissions in 2008–2012 and the Kyoto targets are 37.5 Mt CO_2 equivalents (excluding carbon sinks), which is 32.5% less than the targeted value.

Thus, the average 2008–2012 emissions in sectors not covered by the EU ETS, including the effect of carbon sinks, are less than the target for non-ETS sectors.

Despite these promising results, energy efficiency measures in the residential and services sectors are of key importance in the provision of further emission reductions by 2020.

Concerning the national GHG targets under the ESD: 2012 non-ETS emissions were below the 2013 ESD targets and 2020 non-ETS emissions are projected to be lower than the 2020 ESD target with the existing measures. Concerning the national targets for the RES share in the gross final energy consumption, the 2011 RES share was above the RED and NREAP 2011–2012 trajectories.

Concerning energy efficiency, some progress is made in reducing energy consumption, but further improvements are necessary to further develop policies or to better implement the existing ones.

Regarding the current progress towards 2013 ESD targets, the following conclusions can be drawn. Considering the proportional targets of 2020 by 2013 – the so-called 2013 ESD targets – then the reduction of -5% is the proportional goal until 2013 and +10% by 2020 for non-ETS sectors is allowed. The actual emissions from non-ETS sectors are 18% less in 2012 than the 2005 values and the 6.9 Mt (13%) below the 2013 ESD target.

Considering the projected emissions in 2020 in non-ETS sectors and comparing them with the targets for 2020, the With Existing Measures scenario forecasts a –8% aggregate emission reduction (a 11 Mt reduction) compared to the target, whilst the With Additional Measures scenario forecasts a 21 Mt reduction and a –16% relative gap.

Overall, the projections show that with the current measures, the non-ETS emissions in 2020 will be below the 2020 targets.

The projections presented herewith are developed for the years 2015, 2020, and 2025. The projections rely on energy demand forecasts, latest emission factors, and technological data, and use parametric assumptions. The detailed sectoral impact of measures is enumerated in Chapter 5 of the NC for the industry, energy, and power sector, transportation, public sector, agriculture, and forestry sectors.

Throughout the development of the projections, the impacts of EU level policy requirements and specific domestic policies were considered (e.g., Renewable Energy Directive, EU ETS). For the sake of a concise and methodologically sound forecast, the HUNMIT model was developed and adapted to the present forecast, which is a bottom up model enlisting all measures, their technical and economical characteristics. The model is capable of selecting an optimal set of measures allowing for a cost efficient emission reduction.

Table 4 summarizes total emissions for the two scenarios (with and without LULUCF).

Table 4. Total emissions in the WEM and WAM scenarios (Gg. CO_2 equivalent)

	2010	2015	2020	2025
Without measures scenario	67 679.0	63 568.7	65945.7	69473.6
WOM including LULUCF	63 694.3	66 193.0	68731.3	69473.6
With existing measures	67 679.0	63 475.5	59 840.2	58 598.0
WEM including LULUCF	63 694.3	60 680.0	58 046.5	56 391.1
With additional measures	67 679.0	61 515.1	56 774.2	55 400.2
WAM including LULUCF	63 694.3	58 719.6	54 980.5	53 193.4

It is visible that the two scenarios do not differ significantly at the end of the forecasting period. This indicates that the WEM scenario already incorporates a large share of potential abatament measures and mitigation options.

7. Conclusions and recommendations

Bringing together the results of the current progress towards the 2013 targets (based on 2012 proxy data) and projected progress to 2020 targets (based on Member States projections) allows for an overall assessment of the progress achieved so far by Hungary towards her objectives under the ESD. Thus, Hungary is presently considered to be on track towards her respective 2013 ESD targets, i.e., 2012 non-ETS emissions were below these targets.

If a modified base year (2005) would be set for the 2020 ESD targets (adjusted according to Art. 10) for Hungary it would mean a 16% reduction target or a 57 Mt CO_2 equivalent emission cap in the non-ETS sectors until 2020. This is expected to be reached already under the assumptions of the WEM scenario, which forecasts 43 Mt emission, while the WAM forecasts GHG emissions equivalent to 40 Mt of CO_2 by 2020. Thus Hungary is expected to reach her 2020 target with the current set of policies and measures through domestic emission reductions alone, even if a more demanding base year is chosen.

Overall, combining the above findings Hungary is well on track towards the ESD targets with 2012 emissions below 2013 ESD targets, and current policies and measures are sufficient to achieve 2020 targets through domestic emission limitations or reductions only.

References

Ministry of National Development, 2013: 6th National Communication of Hungary to the UNFCCC, Biennial Report of Hungary to the UNFCCC (as an Annex to the 6th National Communication).

Molnár, S. and *Molnár, M.*, 2012: Comprehensive assessment of climate change policies and measures in Hungary: concerns and tasks in an underestimated challenge. *Időjárás 116*, 297–321.

IDŐJÁRÁS

Quarterly Journal of the Hungarian Meteorological Service
Vol. 118, No. 4, October – December, 2014, pp. 305–321

Estimation of future precipitation conditions for Hungary with special focus on dry periods

Rita Pongrácz*, Judit Bartholy, and **Anna Kis**

Department of Meteorology, Eötvös Loránd University,
Pázmány Péter sétány 1/A, H-1117 Budapest, Hungary

E-mail: prita@nimbus.elte.hu, bartholy@caesar.elte.hu,
kisanna@nimbus.elte.hu

**Corresponding author*

(Manuscript received in final form August 25, 2014)

Abstract—In this paper, estimated trends of precipitation- and drought-related climate indices and the return period of the daily precipitation amount are analyzed. For this purpose 11 regional climate model (RCM) simulations from the ENSEMBLES project with 25 km horizontal resolution for the emission scenario A1B are used after applying a bias-correction procedure. According to the results, the summer 10- and 20-year return periods will increase by a factor of 1.2–2 by the late 21st century relative to the 1961–1990 reference period. The projected changes are considerably smaller for the other three seasons compared to future summer changes. Furthermore, drought-related climate indices in summer are projected to increase significantly in Hungary as well as in Central/Eastern Europe by the end of the 21st century. Additionally, precipitation-related indices are projected to decrease in summer by 2071–2100 compared to 1961–1990.

Key-words: precipitation index, dry period, return period, bias correction, regional climate model simulation

1. Introduction

Climate change is most often referred as higher temperature values and more frequent heat waves (e.g., *Pongrácz et al.*, 2013). However, it usually involves more intense and more frequent extreme events related to excess or lack of precipitation (e.g., severe dry spells, heavy precipitation, intense thunderstorms), too (*IPCC*, 2012). This highlights the importance of climate research in quantifying the detected past and the projected future changes from global to local scales. Frequent hot weather in summer and overall increasingly warm climatic conditions are quite straightforward consequences of global warming. Global and regional warming induced effects on precipitation are not as clear as on temperature, because the higher spatial and temporal variabilities might hide any robust changing signal. Nevertheless, precipitation is one of the most important meteorological variables, since it considerably affects natural ecosystems and cultivated vegetation as well as most of human activities. Extreme precipitation events – both excessive, intense rainfalls and severe droughts – may result in several environmental, agricultural, economical, and natural disasters. The lack of precipitation for extended period and coincidental intense heat wave often lead severe drought events. For instance, in 2003 a long-lasting, devastating heat wave occurred throughout Europe (*Stott et al.*, 2004), causing death of hundreds of people (*Bouchama*, 2004). In Hungary, the year 2003 was generally dry with 17% less annual precipitation than the 1971–2000 average (*Schirokné Kriston*, 2004). The Europe-wide heat wave in the summer superposed to these overall dry conditions, resulting in severe drought. The estimated monetary damage in the Hungarian agriculture reached 50–55 billion HUF by the end of the year (*Faragó et al.*, 2010). Another hot and dry summer from the past decades occurred in 2007, this drought resulted in reduced harvest of maize in Hungary and caused at least 80 billion HUF loss (*Faragó et al.*, 2010). On the contrary, in May 2010, the total rainfall in Hungary largely exceeded the average monthly precipitation of the 1971–2000 baseperiod for May, namely, almost three times more precipitation occurred than usual (*Móring*, 2011). The excessive precipitation led to inland inundation and floods on Sajó, Hernád, Bodrog, and Bódva rivers resulting in more than 10 billion HUF of defence and recovery costs (*KSH*, 2011). Overall, the year 2010 became the wettest year in Hungary since 1901 with 959 mm annual precipitation amount exceeding the annual mean of the 1971–2000 period by 65% (*Móring*, 2011). Besides Hungary, a large majority of the Central/Eastern European region was hit at the same time by severe floods (*Bissolli et al.*, 2011; *WMO*, 2011). After the year of excessive precipitation, Hungary experienced the driest year in 2011 since 1901 with only 407 mm annual total precipitation amount, being only 72% of the annual average in the 1971–2000 period (*Móring*, 2012), which affected the agricultural production quite negatively. The very

next year, 2012 was also dry in Hungary, the annual total precipitation was only 470 mm (*Horváth et al.*, 2012; *Rajhonáné Nagy*, 2013) resulting in more losses in agriculture than in 2011 (e.g., by 24% less harvested cereal and 20% less production of sunflower and grape) (*KSH*, 2013). Due to the large temporal variability of precipitation, after two consecutive very dry years, in late May and early June in 2013 large precipitation occurred again in Central Europe and resulted in extreme water levels, with record high peak levels on several Central European rivers, i.e., the Danube, the Elbe, and the Vltava (*BBC News*, 2013; *van der Schrier et al.*, 2013; *WMO*, 2014). Besides the great amount of precipitation, the large spatial extension and the strong intensity (exceeding 100 mm/24 hours) also contributed to this extreme event (*Horváth et al.*, 2013). Overall, this flood affected several countries in Central and Eastern Europe (e.g., Germany, Austria, Czech Republic, Hungary, Serbia) with 16 billion EUR losses and 22 deaths altogether (*Munich Re*, 2013).

In order to avoid or at least reduce the effects of these precipitation related hazards, national and local communities need to develop regional adaptation strategies (*IPCC*, 2012; *Motha*, 2009; *Sivakumar* and *Stefanski*, 2009; *Anwar et al.*, 2013), and then, act according to them. For this purpose, results of global climate model (GCM) simulations must be downscaled to regional and local scales, hence better serving end-users' needs. Downscaling of coarse resolution GCM simulation outputs is especially important in case of precipitation because of the large temporal and spatial variabilities, and consequently, since appropriate precipitation impact assessment studies require fine resolution information (e.g., *Marengo* and *Ambrizzi*, 2006; *Fowler et al.*, 2007; *Maurer et al.*, 2007; *Serinaldi* and *Kilsby*, 2014). From the agricultural point of view, especially potential dry conditions induce long-term planning, for which estimation of precipitation is evidently the key element.

Sheffield and *Wood* (2008) analyzed global and regional trends of drought using a moisture-based drought index for 1950–2000. According to their results, soil moisture has increased globally with regional differences. In Africa, a significant drying can be identified, whereas increasing trend is detected in North America. The annual precipitation sum in Hungary decreased in the 1901–2009 period; in Budapest the mean change is –20.5%, which is statistically significant (*Lakatos* and *Bihari*, 2011). Precipitation measurements in the Carpathian Basin suggest that both the overall intensity and frequency of extreme precipitation events – related to both excess and lack of precipitation – increased in the 20th century, whereas the mean climate became slightly drier (*Bartholy* and *Pongrácz*, 2005; *Lakatos et al.*, 2011). For the future, 50 km horizontal resolution regional climate model (RCM) experiments of the PRUDENCE project (*Christensen et al.*, 2007a) suggest that the annual distribution of precipitation will be totally restructured

in Hungary both in case of A2 and B2 emission scenarios (*Nakicenovic* and *Swart*, 2000), namely, the wettest season (currently summer) will become the driest, and the driest season (currently winter) is likely to be the wettest by the end of the 21st century (*Bartholy et al.*, 2008). The projected changes for Central/Eastern Europe involve large uncertainity, therefore, further analysis is necessary. In order to successfully adapt to the changing climatic and environmental conditions, appropriate assessment of possible changes is essential.

In the current study, fine (25 km) resolution RCM experiments of the ENSEMBLES project are analyzed taking into account the A1B intermediate emission scenario for the entire 21st century. First, the data and the bias correction method applied to the raw RCM outputs are presented. Then, the precipitation-related characteristics, return period of daily precipitation, and various climate indices are defined. Section 3 discusses projected changes in the seasonal return period of daily precipitation, and estimated seasonal changes of climate indices with special focus on dry conditions. Finally, Section 4 summarizes the main conclusions.

2. *Data and methods*

2.1. Data used in the analyses

In this paper, simulations of 25 km horizontal resolution RCMs nested in coarse resolution GCMs are used to estimate the future precipitation- and drought-related climatic conditions in Central/Eastern Europe covering the region 43.625°–50.625°N, 13.875°–26.375°E. The assessment focuses on analysis of daily precipitation outputs of 11 RCM simulations (listed in *Table 1*) from the ENSEMBLES project (*van der Linden* and *Mitchell*, 2009). This European Union funded project aimed and successfully completed to run several climate models between 2004 and 2009 in order to improve the reliability of climate projections, measure uncertainty, and help decision-makers with reliable information. All of the RCM simulations selected for this study cover the entire 1951–2100 period and apply the intermediate A1B emission scenario, according to which the estimated CO_2 concentration level will be 532 ppm and 717 ppm by 2050 and 2100, respectively (*Nakicenovic* and *Swart*, 2000). The necessary initial and boundary conditions are provided by three different GCMs: ECHAM (*Roeckner et al.*, 2006) developed at the Max Planck Institute, HadCM (*Gordon et al.*, 2000) developed at the UK MetOffice, and ARPEGE (*Déqué et al.*, 1998) developed at Météo-France.

Table 1. List of the selected RCMs, their main references, their driving GCMs, and the responsible institutes used in this analysis.

RCM (Reference)	Driving GCM	Institute
HadRM3Q0 (*Jones et al.*, 1995; 2004)	HadCM3Q	HC (Hadley Centre), United Kingdom
RCA3 (*Samuelsson et al.*, 2011)	HadCM3Q (high sensitivity version)	C4I (Community Climate Change Consortium for Ireland), Ireland
CLM (*Böhm et al.*, 2006)	HadCM3Q	ETHZ (Eidgenössische Technische Hochschule Zürich), Switzerland
RCA3 (*Samuelsson et al.*, 2011)	HadCM3Q (low sensitivity version) ECHAM5	SMHI (Swedish Meteorological and Hydrological Institute), Sweden
RACMO (*van Meijgaard et al.*, 2008)	ECHAM5	KNMI (Koninklijk Nederlands Meteorologisch Instituut), Netherlands
REMO (*Jacob* and *Podzun*, 1997)	ECHAM5	MPI (Max Planck Institut), Germany
RegCM (*Giorgi* and *Bi*, 2000)	ECHAM5	ICTP (International Centre for Theoretical Physics), Italy
HIRHAM (*Christensen et al.*, 2007b)	ECHAM5 ARPEGE	DMI (Danmarks Meteorologiske Institut), Denmark
ALADIN (*Radu et al.*, 2008)	ARPEGE	CNRM (Centre National de Recherches Météorologiques), France

2.2. Bias correction of RCM outputs

The evaluation of raw precipitation outputs of RCMs for 1961–1990 suggests that simulated values usually significantly overestimate the observations in Central/Eastern Europe, except in summer when mostly underestimations were found (*Pongrácz et al.*, 2011). In case of precipitation indices associated with specific thresholds, it is particularly important to use the most accurate simulations, as close to measurements as possible. For this purpose, before the analyses, a bias correction method should be applied to the raw simulated data. The biases of the raw RCM outputs are corrected using quantile matching technique. This is based on the assumption that two datasets are considered similar if their distributions are close to each other (and the closer is the more similar), therefore, the monthly empirical distribution functions of daily precipitation at each grid cell should be fitted (*Formayer* and *Haas*, 2010) to the observed distribution represented by the gridded E-OBS (*Haylock et al.*, 2008) data for a baseperiod, i.e., 1951–2000 in this study. These fitting procedures provide the multiplicative bias-correcting factors for each month, for each grid cell. Then, these calculated factors are applied to the raw daily outputs of RCM experiments both for the past (1951–2000) and the target (2000–2100) period.

Fig. 1 illustrates the successful fitting of the bias-correction for January for a selected grid cell, where the percentile values of the raw and bias-corrected simulations are compared to the percentiles of E-OBS data. The Q-Q plot clearly shows that after the correction, the distribution of the simulated precipitation fits perfectly to the distribution of the reference data (i.e., all the percentile value pairs are located along the y = x line).

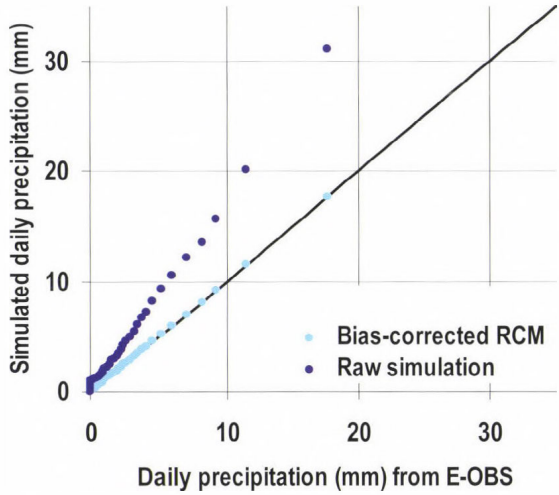

Fig. 1. Q-Q plot for raw and bias corrected simulation data, 1951–2000. Results for January daily data from the grid cell located at 47.625°N, 19.125°E using the ARPEGE-driven HIRHAM experiment are shown.

2.3. The return period and the selected climate indices

After the bias-correction, both the 10- and 20-year return periods of the daily precipitation amount are analyzed. The return period (τ) is defined as the inverse of the expected average number of occurrences (P) in a year (τ=1/P). *Fig. 2* shows an example for how to determine the change of the 10-year return period. First, the 90th percentile of the daily precipitation ($P_{0.9}$(1961–1990)) is calculated for the reference period (1961–1990) in each grid cell. Then, this daily precipitation amount should be compared to the future (2071–2100) percentile values, and that one (P_X(2071–2100)) is selected, which equals to this $P_{0.9}$(1961–1990) daily precipitation. In the example of *Fig. 2*, X = 0.94 since the 94th percentile value of the future period equals to $P_{0.9}$(1961–1990). So $\tau_{10\text{years, }1961\text{–}1990}$ = 100/(100–94) = 16.67 years, which implies a substantial increase of the return period, and hence, drier climatic conditions.

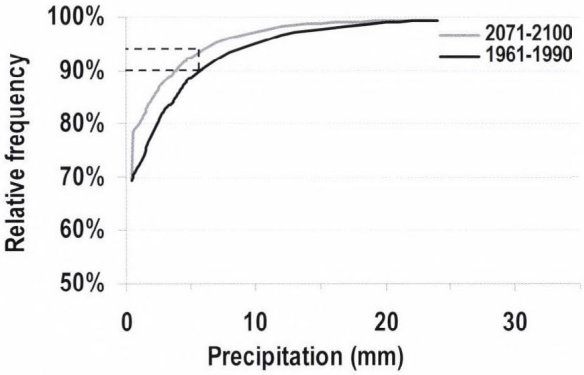

Fig. 2. Calculation of the projected value of the 10-year return period ($\tau_{10years,\ 1961-1990}$). Empirical distributions of summer daily data from the grid cell located at 47.625°N, 19.125°E using the ARPEGE-driven HIRHAM experiment are shown.

In order to assess future climate tendencies in the Central/Eastern European region, several precipitation-related indices are also analyzed on seasonal scales. *Table 2* lists the names, definitions, and units of the selected climate indices. Three indices are directly related to drought (DD, MDS, CDD), the other three indices refer to wet conditions using small precipitation thresholds (RR1, RR5, MWS). The grid cell values of all the six indices are calculated from the bias-corrected simulated precipitation data sets for the entire selected domain covering the latitude 43.625°–50.625°N and longitude 13.875°–26.375°E for the whole simulation period (1951–2100) using all the 11 RCM experiments. Overall projected seasonal changes by 2021–2050 and 2071–2100 periods relative to the 1961–1990 reference period are also calculated. Furthermore, spatial average changes for Hungary represented by the grid cells located within the country border are estimated for all the seasons both for mid to late 21st century.

Table 2. Drought- and precipitation-related climate indices used in the current analysis

Index	Definition	Unit
DD	Number of dry days ($R_{day} < 1$ mm)	day
MDS	Mean length of dry spell ($R_{day} < 1$ mm)	day
CDD	Maximum length of dry spell, i.e., maximum number of consecutive dry days ($R_{day} < 1$ mm)	day
RR1	Number of precipitation days exceeding 1 mm ($R_{day} \geq 1$ mm)	day
RR5	Number of precipitation days exceeding 5 mm ($R_{day} \geq 5$ mm)	day
MWS	Mean length of wet spell ($R_{day} \geq 1$ mm)	day

3. *Results and discussion*

First, we focus on the 10-year and 20-year return periods of the daily precipitation amount. The projected seasonal changes generally show similar patterns for the whole selected domain. According to our results, a slight decrease of the return period is likely to occur in winter, namely, the 10-year return period may change to 8–9 years by the end of the 21st century (*Fig. 3*). This implies wetter climatic conditions for winter. In spring and autumn, individual RCM experiments suggest slightly more diverse changes than in winter, which results in larger uncertainty but very small changes overall. In case of summer, the results for the 2071–2100 period clearly suggest that the return period of daily precipitation occurred once in a decade on average in the recent past is very likely to increase by a factor of 1.2–2, so drier climatic conditions are projected. Larger increase of the 10-year return period is estimated in the southern parts (exceeding 8 years) of the selected domain than in the northern subregions (less than 4 years).

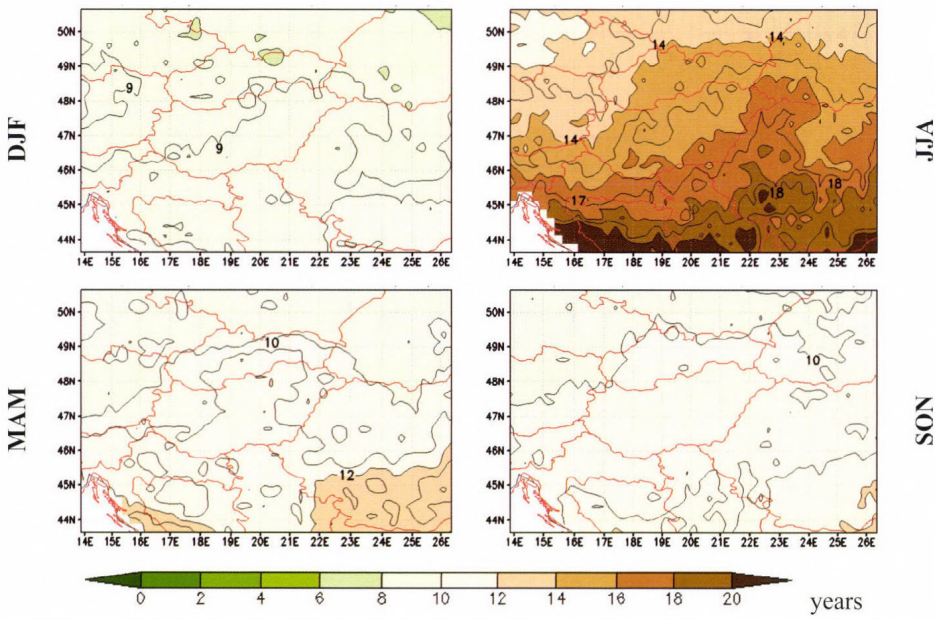

Fig. 3. Composite maps of 11 RCM simulations indicating the estimated seasonal mean changes of the 10-year return period by 2071–2100 relative to the reference period 1961–1990.

Besides the average return periods, the seasonal uncertainties for nine subregions are also determined (*Fig. 4*). Whisker-Box plot diagrams are used for

indicating the highest (maximum) and the lowest (minimum) values, and the lower and upper quartiles, i.e., the 25th and 75th percentiles of the 10-year return period of daily precipitation amount for each subregion based on the 11 individual RCM simulations. According to these results, the return period increases in summer, thus implying an overall future drying trend by almost all of the RCM simulations in every subregion (only a few RCM simulations project slight decrease in the northwestern subregions). Although the projected tendency is clear, the RCM-based projections cover a wide range of return periods, thus, the uncertainty of the estimation is quite large. The estimated changes are clearly larger as proceeding from the northwestern to the southeastern part of the domain. In Hungary and Slovenia, the doubling of the return period is estimated by only a couple of RCM simulations (using CLM for instance), whereas in the southern subregions (Romania, Croatia, and northern Serbia) 25% of the RCM simulations suggest larger increase than by a factor of 2. In the other three seasons, the overall uncertainties of the projections are smaller than in summer, however, even the signs of the estimated changes are not identical, especially in spring and autumn. In winter, most of RCM simulations suggest considerable decrease of the return period, thus implying wetter conditions in all subregions (only two RCM simulations project increase of winter return periods, namely, ALADIN and HIRHAM driven by ARPEGE).

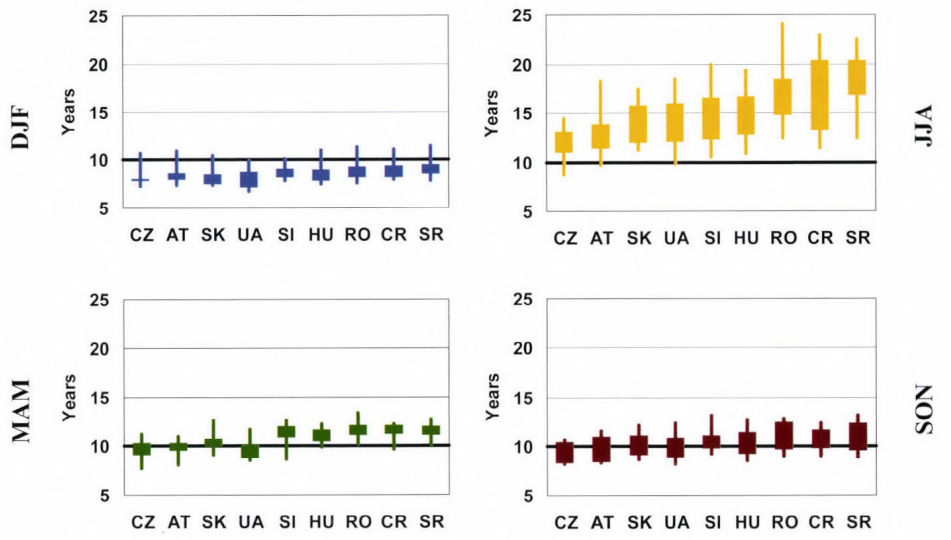

Fig. 4. The maximum, minimum, upper, and lower quartile values of the 10-year seasonal return period of the daily precipitation amount for nine subregions (CZ: southeastern Czech Republic, AT: eastern Austria, SK: Slovakia, UA: southwestern Ukraine, SI: Slovenia, HU: Hungary, RO: Romania, CR: Croatia and SR: northern Serbia).

The projected seasonal changes of 10- and 20-year return periods are compared for Hungary in *Fig. 5*. In general, the signs of the projected changes by one particular RCM simulation are identical for both return periods. It can be clearly seen that all the RCM simulations suggest clear increasing return period in summer. Most of the RCM simulations project similar rate of changes, except three RCM simulations (HIRHAM driven by ARPEGE, CLM driven by HadCM, and HadRM3Q driven by HadCM), when, when extremely large changes (larger than twofold increasing) is projected for Hungary in case of the 20-year return period of daily precipitation sum. The projected changes are considerably smaller for the other three seasons than for summer. Nevertheless, the estimated changes of the 10-year return period are slightly larger than the changes of the 20-year return period in winter and autumn.

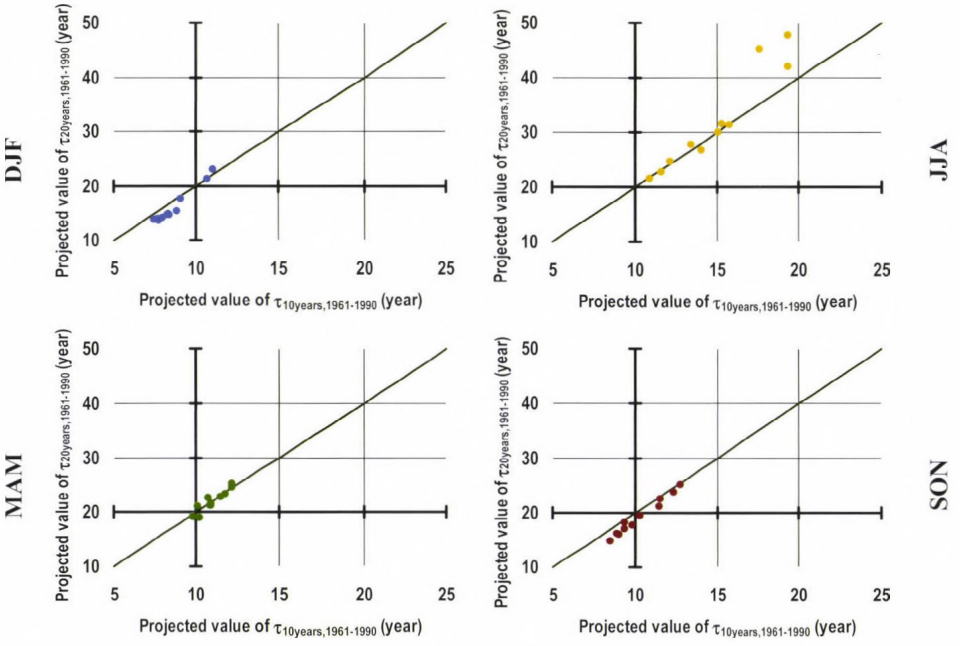

Fig. 5. Scatter-plot diagrams based on the 11 RCM simulations of the 10- and 20-year seasonal return periods for Hungary by 2071–2100 relative to the reference period, 1961–1990. Each dot represents the results of one RCM simulation.

In the second part of this section, we analyze the projected changes of the selected precipitation indices focusing on Hungary. According to the 11 bias-corrected RCM simulations in the 2021–2050 period, smaller changes are projected than in the 2071–2100 period (*Fig. 6*). By the mid-century, only a few

RCM simulations project statistically significant seasonal changes and the average estimated changes do not exceed 11%. In most of the indices, the signs of the projected changes are identical, which implies that the tendencies are likely to continue throughout the 21st century. In general, RR1 and RR5 (precipitation days exceeding 1 mm and 5 mm, respectively) are projected to decrease in summer and increase in winter. However, by the late century, almost all RCM simulations estimate significant decrease in summer (the average projected decrease is 27% relative to the reference period both for RR1 and RR5), and increase in winter for RR5 (the average projected increase is 25%). CDD and MDS in summer are projected to increase significantly in Hungary by the end of the 21st century (by 42% and 41% on average, respectively), clearly implying considerably drier future summers. Similar conclusions were found in *Bartholy et al.* (2013).

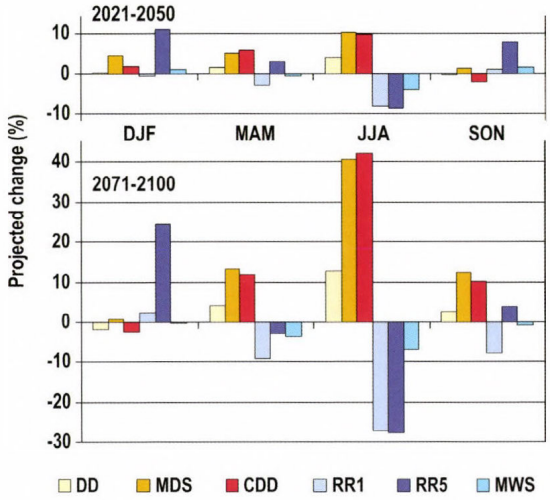

Fig. 6. Projected seasonal mean changes of climate indices for Hungary by 2021–2050 (upper panel) and 2071–2100 (lower panel) relative to the reference period, 1961–1990. Definitions of these indices are listed in *Table 2*.

The spatial pattern of the projected mean seasonal changes by the mid to late century are shown for CDD in *Fig. 7* (this index focuses on long dry periods when precipitation does not exceed 1 mm). The spatial averages of the estimated changes for the whole domain are –0.1%, +11%, +42%, and +10% in winter, spring, summer, and autumn, respectively (for Hungary the average projected changes are as follows: –2%, +12%, +42%, and +11%). In all the four seasons, larger increases are projected for the southern parts of the selected domain than

for the northern regions. For instance, the estimated mean increase of CDD in summer is about 50% in Serbia and Romania by 2071–2100, whereas it is less than 40% in southeastern Czech Republic. In Hungary, the average summer value of CDD is 14 days in 1961–1990, which is projected to increase by 42%, and thus, exceeding 20 days by the end of the 21st century.

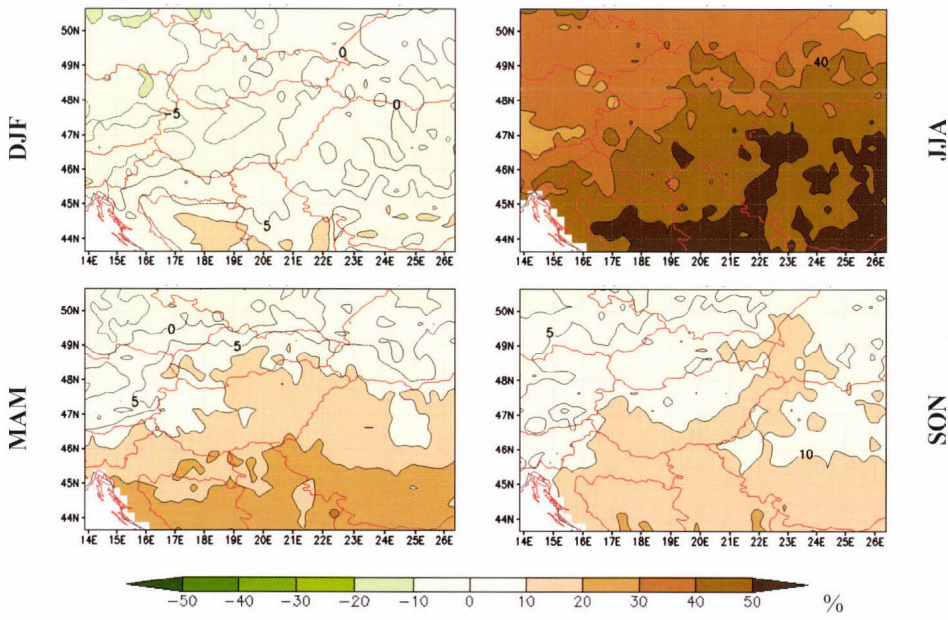

Fig. 7. Composite maps of 11 RCM simulations indicating the projected seasonal mean changes of CDD by 2071–2100 relative to the reference period 1961–1990.

Besides the multimodel seasonal averages, the standard deviations of estimated changes (characterizing the differences between the individual RCM projections) are also important, especially in terms of assessing the uncertainty of projections. The largest standard deviation values of the seasonal changes are found in summer, namely 15–30% depending on the location, with larger standard deviation in the northern regions and smaller in the southern regions of the domain. The smallest standard deviations of the late century changes are in spring (5–15%), however, winter and autumn standard deviation values are roughly in the same range. To present the inter-model uncertainty on decadal scale covering the whole 1951–2100 period, spatial average CDD values taking

into account all the gridcells within Hungary are shown in *Fig. 8* for winter and summer. According to the statistical analysis (t-test), the summer increasing trend is significant at 0.05 level, which implies future lengthening of consecutive dry days highly affecting agriculture in the region. The longest seasonal dry periods lasted 15 days on average in summer in the 1950s (only one individual RCM simulation resulted in CDD values for Hungary over 20 days). The RCM simulation ensemble projects dry periods lasting 22 days on average by the last decade of the 21st century, and one of the RCM simulations even resulted in 40-day-long summer dry periods in the 2090s.

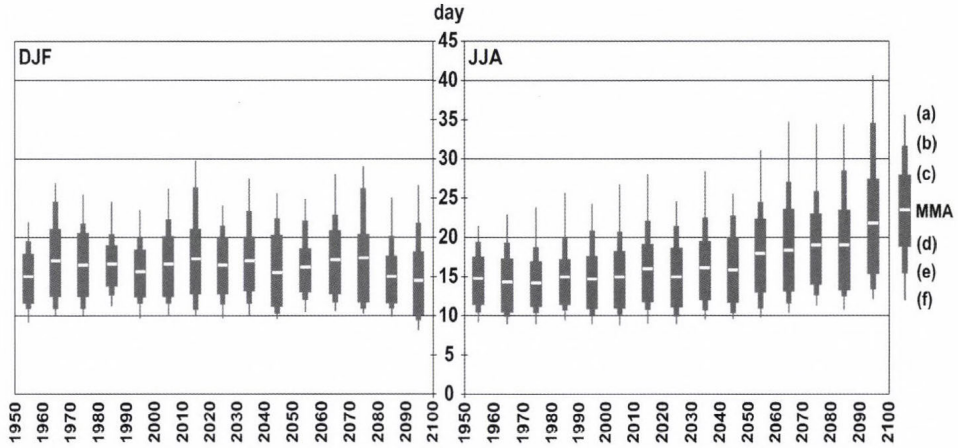

Fig. 8. Average decadal values of CDD in Hungary in winter (left panel) and summer (right panel), 1951–2100. MMA indicates the multi-model average. (a) and (f) indicate the maximum and minimum CDD values, respectively. (b) and (e) indicate the second largest and smallest CDD values, respectively. (c) and (d) indicate the third largest and smallest CDD values, respectively.

The mean length of dry spells is estimated to increase in Hungary in all seasons during the 21st century (*Fig. 9*). The largest change is projected for summer: MDS will increase by 41%, so the 5-day-long mean dry spells of the reference period are likely to lengthen by 3 days and last for 8 days on average by the end of the 21st century. The mean dry spells were the longest in autumn in the reference period (MDS average value is about 8 days), and the RCM simulations suggest that they will remain the longest in 2071–2100 when MDS is likely to exceed 9–10 days. Smaller and only slight changes are estimated in winter and spring.

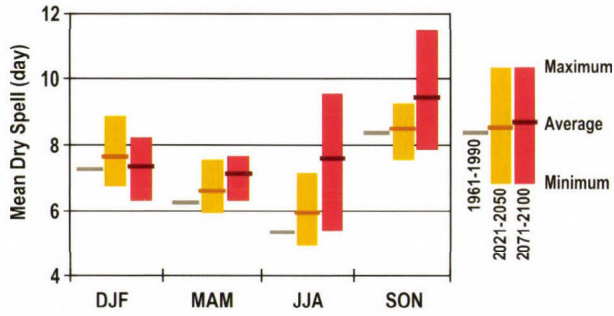

Fig. 9. Spatial average values of MDS in Hungary for three time slices: 1961–1990, 2021–2050, and 2071–2100. Columns represent the projections of the multi-model ensemble.

4. Conclusions

Projected changes of precipitation tendencies for Central/Eastern Europe have been analyzed for the 21st century using bias-corrected outputs of 11 RCM simulations available from the ENSEMBLES database. All the simulations applied 25 km horizontal resolution and took into account the intermediate SRES A1B emission scenario. In order to eliminate the systematic errors, we completed a bias-correction procedure using quantile matching technique. After the correction, we analyzed the return period of daily precipitation amount and different precipitation- and drought-related climate indices for nine subregions. In this paper we focused on the changes of the 10-year return period of daily precipitation amount, the maximum number of consecutive dry days, and the mean length of dry spells in Hungary. The main results can be summarized as follows:

(1) The RCM simulations suggest that the 10- and 20-year return periods will increase in summer by a factor of 1.2–2. Larger increases of the return periods are estimated in the southern parts of the domain than in the northern subregions. The projected changes are considerably smaller for the other three seasons compared to future summer changes. Nevertheless, the estimated changes of the 10-year return period are slightly larger than the changes of the 20-year return period in winter and autumn.

(2) Our results clearly suggest drier summers and wetter winters in the future, especially at the end of the 21st century. In summer, the maximum number of consecutive dry days, the mean length of dry spell, and the total number of dry days are all projected to increase significantly. Furthermore, the mean length of wet spell, the number of wet days, and the number of precipitation days exceeding 5 mm are projected to decrease in Hungary as well as in Central/Eastern Europe. In winter, opposite changes are very likely.

Acknowledgements: Research leading to this paper has been supported by the following sources: the Hungarian Scientific Research Fund under grant grants K-78125 and K109109, the European Union and the European Social Fund through project FuturICT.hu (TÁMOP-4.2.2.C-11/1/KONV-2012-0013). The ENSEMBLES data used in this work was funded by the EU FP6 Integrated Project ENSEMBLES (Contract number 505539) whose support is gratefully acknowledged. Furthermore, we acknowledge the E-OBS dataset from the EU-FP6 project ENSEMBLES (http://ensembles-eu.metoffice.com), and the data providers in the ECA&D project (http://eca.knmi.nl).

References

Anwar, M.R., Liu, D.L., Macadam, I., and *Kelly, G.*, 2013: Adapting agriculture to climate change: a review. *Theor. Appl. Climatol. 133*, 225–245.

Bartholy, J. and *Pongrácz, R.*, 2005: Tendencies of extreme climate indices based on daily precipitation in the Carpathian Basin for the 20th century. *Időjárás 109*, 1–20.

Bartholy, J., Pongrácz, R., Gelybó, Gy., and *Szabó, P.*, 2008: Analysis of expected climate change in the Carpathian Basin using the PRUDENCE results. *Időjárás 112*, 249–264.

Bartholy, J., Pongrácz, R., and *Hollósi, B.*, 2013: Analysis of projected drought hazards for Hungary. *Adv. Geosci. 35*, 61–66.

BBC News, 2013: Thousands flee flood-hit parts of Germany and Hungary. Available online at http://www.bbc.com/news/world-europe-22835154

Bissolli, P., Friedrich, K., Rapp, J., and *Ziese, M.*, 2011: Flooding in eastern central Europe in May 2010-reasons, evolution and climatological assessment. *Weather 66*, 147–153.

Böhm, U., Kücken, M., Ahrens, W., Block, A., Hauffe, D., Keuler, K., Rockel, B., and *Will, A.*, 2006: CLM - the Climate Version of LM: Brief Description and long-term Applications. *COSMO Newsletter 6*, 225–235.

Bouchama, A., 2004: The 2003 European heat wave. *Intens. Care Med. 30*, pp. 1–3.

Christensen, J.H., Carter, T.R., Rummukainen, M., and *Amanatidis, G.*, 2007a: Evaluating the performance and utility of regional climate models: The PRUDENCE project. *Climatic Change 81*, 1–6.

Christensen, O.B., Drews, M., Christensen, J.H., Dethloff, K., Ketelsen, K., Hebestadt, I., and *Rinke, A.*, 2007b: The HIRHAM Regional Climate Model Version 5 (beta). Techn. Report 06-17.

Déqué, M., Marquet, P., and *Jones, R.G.*, 1998: Simulation of climate change over Europe using a global variable resolution general circulation model. *Clim. Dynam. 14*, 173–189.

Faragó, T., Láng, I., and *Csete, L.*, 2010: Climate change and Hungary: mitigating the hazard and preparing for the impacts (the „VAHAVA Report"). MTA, Budapest.

Formayer, H. and *Haas, P.*, 2010: Correction of RegCM3 model output data using a rank matching approach applied on various meteorological parameters. Deliverable D3.2 RCM output localization methods (BOKU-contribution of the FP 6 CECILIA project). http://www.cecilia-eu.org/

Fowler, H.J., Blenkinsop, S., and *Tebaldi, C.*, 2007: Linking climate change modelling to impacts studies: recent advances in downscaling techniques for hydrological modelling. *Int. J. Climatol. 27*, 1547–1578.

Giorgi, F. and *Bi, X.Q.*, 2000: A study of internal variability of a regional climate model. *J. Geophys. Res. 105(D24)*, 29503–29521.

Gordon, C., Cooper, C., Senior, C.A., Banks, H., Gregory, J.M., Johns, T.C., Mitchell, J.F.B., and *Wood, R.A.*, 2000: The simulation of SST, sea ice extents and ocean heat transports in a version of the Hadley Centre coupled model without flux adjustments. *Clim. Dynam. 16*, 147–168.

Haylock, M.R., Hofstra, N., Klein Tank, A.M.G., Klok, E.J., Jones, P.D., New, M., 2008: A European daily high-resolution gridded dataset of surface temperature and precipitation. *J. Geophys. Res 113 (D20)*, 27.

Horváth, Á., Kerényi, J., Lakatos, M., Nagy, A., Németh, Á., and *Szenyán, I.*, 2012: Extreme drought in 2012 – weather circumstances. *Erdészeti Lapok CXLVII*, 347–348. (in Hungarian).

Horváth, Á., Nagy, A., and *Simon, A.*, 2013: Flooding on the Danube in June 2013 – weather circumstances. OMSZ, Budapest. Available online at http://met.hu/ismeret-tar/erdekessegek-_tanulmanyok/index.php?id=709&hir=A_2013._juniusi_dunai_arviz_idojarasi_hattere. (in Hungarian)

IPCC, 2012: Managing the Risks of Extreme Events and Disasters to Advance Climate Change Adaptation. A Special Report of Working Groups I and II of the Intergovernmental Panel on Climate Change. (Eds. *Field, C.B., Barros, V., Stocker, T.F., Dahe, Q., Dokken, D.J., Plattner, G-K., Ebi, K.L., Allen, S.K., Mastandrea, M.D., Tignor, M., Mach, K.J., Midgley, P.M.*), Cambridge University Press, Cambridge, UK and New York, NY, USA.

Jacob, D. and *Podzun, R.*, 1997: Sensitivity studies with the regional climate model REMO. *Meteorol. Atmos. Phys. 63*, 119–129.

Jones, R.G., Murphy J.M. and *Noguer, M.*, 1995: Simulation of climate change over Europe using a nested regional-climate model. I: Assessment of control climate, including sensitivity to location of lateral boundaries. *Q. J. Roy. Meteorol. Soc. 121*, 1413–1449.

Jones, R.G., Noguer, M., Hassell, D.C., Hudson, D., Wilson, S.S., Jenkins, G.J., and *Mitchell, J.F.B*, 2004: Generating high resolution climate change scenarios using PRECIS. Met Office Hadley Centre, Exeter, UK.

KSH, 2011: A 2010. évi árvíz Borsod-Abaúj-Zemplén megyében. (szerk. Szalainé H.A.) Központi Statisztikai Hivatal Miskolci Igazgatósága. ISBN 978-963-235-328-9 (in Hungarian)

KSH, 2013: Output of Hungary's agriculture in 2012 (Economic accounts for agriculture, 2012). *Statistical Reflections, 48 (7)*, 5.

Lakatos, M. and *Bihari, Z.*, 2011: A közelmúlt megfigyelt hőmérsékleti- és csapadéktendenciái. In (Eds: *Batholy, J., Bozó L., Haszpra, L.*): Klímaváltozás – 2011: Klímaszcenáriók a Kárpát-medence térségére. Magyar Tudományos Akadémia és Eötvös Loránd Tudományegyetem Meteorológiai Tanszék, Budapest, 146–169. (in Hungarian).

Lakatos, M., Szentimrey, T., and *Bihari, Z.*, 2011: Application of gridded daily data series for calculation of extreme temperature and precipitation indices in Hungary. *Időjárás 115*, 99–109.

van der Linden, P. and *Mitchell, J.F.B.*, (Eds)., 2009: ENSEMBLES: Climate Change and Its Impacts: Summary of research and results from the ENSEMBLES project. UK Met Office Hadley Centre, Exeter, UK.

Marengo, J.A. and *Ambrizzi, T.*, 2006: Use of regional climate models in impacts assessments and adaptations studies from continental to regional and local scales. Proceedings of 8 ICSHMO, Foz do Iguaçu, Brazil, April 24–28, 2006, INPE, 291–296.

Maurer, E.P., Brekke, L., Pruitt, T., and *Duffy, P.B.*, 2007: Fine-resolution climate projections enhance regional climate change impact studies. Eos, *Transactions American Geophysical Union 88* (47),. 504.

van Meijgaard, E., van Ulft, L.H., van de Berg, W.J., Bosveld, F.C., van den Hurk, B.J.J.M., Lenderink, G., and *Siebesma, A.P.*, 2008: The KNMI regional atmospheric climate model RACMO version 2.1. *Techincal Report*, 43p.

Móring, A., 2011: Weather of 2010 (in Hungarian). *Légkör 56*, 38–42. . (in Hungarian)

Móring, A., 2012: Weather of 2011 (in Hungarian). *Légkör, 57,* 38–42. (in Hungarian)

Motha, R.P., 2009: Developing an adaptation strategy for sustainable agriculture. *Időjárás 113*, 117–127.

Munich RE NatCatSERVICE, 2013: Natural catastrophes first half of 2013. 1p.
Available online at http://www.munichre.com/site/corporate/get/documents_E-2004907462/mr/assetpool.shared/Documents/0_Corporate%20Website/6_Media%20Relations/Press%20Releases/2013/2013_07_09_natcat_en.pdf

Nakicenovic, N. and *Swart, R.*, 2000: Emissions Scenarios. A special report of IPCC Working Group III. Cambridge University Press, UK, 570p.

Pongrácz, R., Bartholy, J. and *Miklós, E.*, 2011: Analysis of projected climate change for Hungary using ENSEMBLES simulations. *Appl. Ecol. Environ. Res. 9*, 387–398.

Pongrácz, R., Bartholy, J., and *Bartha, E.B.*, 2013: Analysis of projected changes in the occurrence of heat waves in Hungary. *Adv. Geosci. 35*, 115–122.

Radu, R., Somot, S. and *Déqué, M.*, 2008: Spectral nudging in a spectral regional climate model. *Tellus Ser. A - Dyn. Meteorol. Oceanol. 60*, 898–910.

Rajhonáné Nagy, A., 2013: Weather of 2012. *Légkör, 58*, 35–39. (in Hungarian)

Roeckner, E., Brokopf, R., Esch, M., Giorgetta, M., Hagemann, S., Kornblueh, L., Manzini, E., Schlese, U., and *Schulzweida, U.*, 2006: Sensitivity of simulated climate to horizontal and vertical resolution in the ECHAM5 atmosphere model. J. Climate, 19, pp. 3771–3791.

Samuelsson, P., Jones, C.G., Willén, U., Ullerstig, A., Gollvik, S., Hansson, U., Jansson, C., Kjellström, E., Nikulin, G., and *Wyser, K.*, 2011: The Rossby Centre Regional Climate model RCA3: model description and performance. *Tellus 63A*, 4–23.

Schirokné Kriston, I., 2004: Weather of 2003. *Légkör 49*, 36–39. (in Hungarian)

van der Schrier, G., van den Besselaar, E., Leander, R., Verver, G., Klein Tank, A., Beersma, J., van Oldenborgh, G.J., Plieger, M., Renshaw, R., and *Bissoli, P.*, 2013: Central European flooding 2013. EURO4M Climate Indicator Bulletin.
Available online at http://cib.knmi.nl/mediawiki/index.php-/Central_European_flooding_2013

Serinaldi, F. and *Kilsby, C.G.*, 2014: Simulating daily rainfall fields over large areas for collective risk estimation. *J. Hydrol. 512*, 285–302.

Sheffield, J. and *Wood, E.F.*, 2008: Global trends and variability in soil moisture and drought characteristics, 1950-2000, from observation-driven simulations of the terrestrial hydrologic cycle, *J. Climate 21*, 432–458.

Sivakumar, M.V.K. and *Stefanski, R.*, 2009: Climate change mitigation, adaptation, and sustainability in agriculture. *Időjárás 113*, 89–102.

Stott, P.A., Stone, D.A., and *Allen, M.R.*, 2004: Human contribution to the European heatwave of 2003. *Nature 432*, 610–614.

WMO, 2011: WMO statement on the status of the global climate in 2010. WMO-No. 1074. Geneva, Switzerland.
Available online at http://www.wmo.int/pages/publications/-showcase/documents/1074_en.pdf

WMO, 2014: WMO statement on the status of the global climate in 2013. WMO-No. 1130. Geneva, Switzerland. Available online at https://drive.google.com/file/d/0BwdvoC9AeW-jUeEV1cnZ6QURVaEE/edit?usp=sharing

IDŐJÁRÁS

Quarterly Journal of the Hungarian Meteorological Service
Vol. 118, No. 4, October – December, 2014, pp. 323–333

Trend analysis of a new MODIS drought severity index with emphasis on the Carpathian Basin

Péter I. Orvos[1,2], **Viktória Homonnai**[2], **Anita Várai**[3], **Zoltán Bozóki**[4], and **Imre M. Jánosi**[2,3]*

[1]*Department of Optics and Quantum Electronics, University of Szeged, Dóm tér 9, H-6720 Szeged, Hungary*

[2]*Regional Research Center, Eötvös Loránd University, Irányi Dániel u. 4, H-8000 Székesfehérvár, Hungary*

[3]*Department of Physics of Complex Systems, Eötvös Loránd University, Pázmány Péter sétány 1/A, H-1117 Budapest, Hungary*

[4]*MTA-SZTE Research Group on Photoacoustic Spectroscopy, University of Szeged, Dóm tér 9, H-6720 Szeged, Hungary*

**Corresponding author E-mail: imre.janosi@ttk.elte.hu*

(Manuscript received in final form July 15, 2014)

Abstract—Recently, *Mu et al.* (2013) have compiled an open access data base of a remotely sensed global drought severity index (DSI) based on MODIS satellite measurements. Observations cover a continuous period of 12 years between January 1, 2000 and December 31, 2011 with a temporal resolution of 8 days. The highest spatial resolution is around 5 km in the geographic band between 60°S and 80°N latitudes (more than 4.9 million locations over land). Here we extend the global trend analysis by *Orvos et al.* (2014) of these satellite based DSI time series in order to locate geographic areas where either positive or negative trends are statistically significant. Significance is established by a standard perturbation test, where each individual record is cut into annual pieces, and the statistics of 1000 randomly shuffled and glued time series is compared with the original record. We exhibit three regions of significant wetting and/or drying trends over extended geographic ranges and try to correlate them with recent reports of local climate shifts. We are fully aware of the fact that 12 years are too short for linking the findings to global climate change. Most probably, the identified significant trends can be considered as a component of natural climate variability on decadal time scales, however, a full explanation will require to identify a couple of explanatory variables.

We demonstrate that drying and wetting trends are weakly significant in the Carpathian Basin. Nevertheless, the observations can serve as benchmark for regional climate simulations, projections can be accepted when the test period is properly reproduced considering also high resolution DSI data.

Key-words: drought indices, linear trend analysis, high resolution mapping, statistical significance tests, remote sensing

1. Introduction

Severe droughts or floods are devastating events for both ecosystems and human society. There are several indices used widely for drought assessment integrating large amounts of data (precipitation, snowpack, stream-flow, etc.). Probably, the best known is the Palmer drought severity index (PDSI) (*Palmer*, 1968; *Alley*, 1984) determined by monthly water supply (precipitation), water outputs (evaporation and runoff), and preceding soil water status. New variants of the original approach have been emerged in order to overcome some limitations of the Palmer model (*Alley*, 1984; *Keyantas* and *Dracup*, 2002), such as the self-calibrating PDSI by *Wells et al.* (2004) or PDSI incorporating improved formulations for potential evapotranspiration (*Heim*, 2002). Remote sensing data from the Moderate Resolution Imaging Spectroradiometer (MODIS) combined with NCEP reanalysis records and statistical procedures together have supported to develop an evaporative drought index (EDI) by *Yao et al.* (2010, 2014) with 4 km spatial and 1 month temporal resolutions. Nevertheless, the development and improvement of drought indices are incomplete tasks, and numerous challenges remain for the future (*Vicente-Serrano et al.*, 2011).

In order to better exploit the strengths of continuous satellite observations, *Mu et al.* (2013) have recently developed a remotely sensed global drought severity index (DSI), and compiled an open access data base spanning 12 years between 2000 and 2011 at a temporal resolution of 8 days. The highest spatial resolution is around 5 km ($0.05° \times 0.05°$) with an almost global coverage. Permanently unvegetated locations such as deserts, high mountains, lakes, or large cities cannot provide input for DSI data, because the computation algorithm incorporates the following MODIS products (*Parkinson* and *Greenstone*, 2000):

1. The normalized difference vegetation index (MOD 13) determined as (NIR-VIS)/(NIR+VIS), where NIR and VIS denote the spectral reflectances in the near-infrared and visible (practically red) regions.
2. The surface resistance and evapotranspiration (MOD 16) calculated using land surface temperature data (MOD 11), the previously mentioned NDVI index (MOD 13) and incident radiation. For details, see *Mu et al.* (2011, 2013).

To our best knowledge, the most comprehensive and longest PDSI trend analysis has been provided by *Dai et al.* (2004). A monthly PDSI dataset from 1870 to 2002 has been derived using historical precipitation and temperature data for global land areas on a grid of $2.5° \times 2.5°$. An empirical orthogonal function (EOF) analysis resulted in a linear trend in the twentieth century, with drying over northern and southern Africa, the Middle East, Mongolia, and eastern Australia, and moistening over the United States, Argentina, and parts of Eurasia (*Dai et al.*, 2004). A follow-up study by *Dai* (2011) compared the

original and three other variants of PDSI records, but the main conclusion remained the same: warming in the second half of the last century is responsible for much of the drying trend over several land areas. Increased heating itself from global climate change may not cause droughts, but it is expected that when droughts occur they are likely to set in quicker and be more intense (*Trenberth et al.*, 2014). However, similarly to the open questions on an optimal definition of a drought index, debates on the trends are also not entirely closed (*Sheffield et al.*, 2012; *Damberg* and *AghaKouchak*, 2013; *Spinoni et al.*, 2013).

2. *Locations of significant DSI trends*

Here we extend the global trend analysis by *Orvos et al.* (2014) of the remotely sensed DSI data base by *Mu et al.* (2013). Records at 4 914 440 geographic locations are evaluated in order to identify linear trends. Each individual record consists of 552 points covering 12 years from January 1, 2000 to December 31, 2011. The basic time-step is 8 days, apart from the necessary cuts at the end of each year. Statistical significance of slopes is verified by the standard permutation test (*Manly*, 2007). Since most of the DSI signals exhibit marked seasonality, the basic unit of data shuffling was one whole calendar year. We cut a given record into 12 pieces, and built a test set from randomly shuffled and glued years. The mean slope and standard deviation were determined, and we accepted a fitted slope of a measured record to be significant when its distance from zero was larger than 2σ of its own test set. *Orvos et al.* (2014) demonstrated that a test set of 100 samples provides essentially the same statistics as 100 000 random samples, however, for the sake of minimizing errors, we fixed the size of test sets at 1000 samples. The larger the test sample size the closer the histogram of obtained slopes to a pure Gaussian, however, the mean and standard deviation do not show detectable sensitivity to the size of the test sets (*Orvos et al.* 2014). Statistically significant slopes are obtained for 852 373 data points (17.34%) at 2σ level, the numbers for 2.5σ and 3σ thresholds are 269 900 (5.49%) and 16 321 (0.33 %), respectively.

The main result of the global trend analysis is illustrated in *Fig. 1*. There are several geographically connected areas exhibiting drying (South America, Middle Asia, or Sub-Equatorial Africa) or wetting (Middle and North Africa, Indian Peninsula, or eastern Spain) tendencies. We emphasize that the remotely sensed DSI is a standardized variable (12-year mean value is removed and normalized by the standard deviation), thus values and trends provide local information: the same numerical value can be connected to very different local circumstances. In order to demonstrate the power of high resolution mapping, we illustrate zooms in three different regions where extended changes are clearly observable.

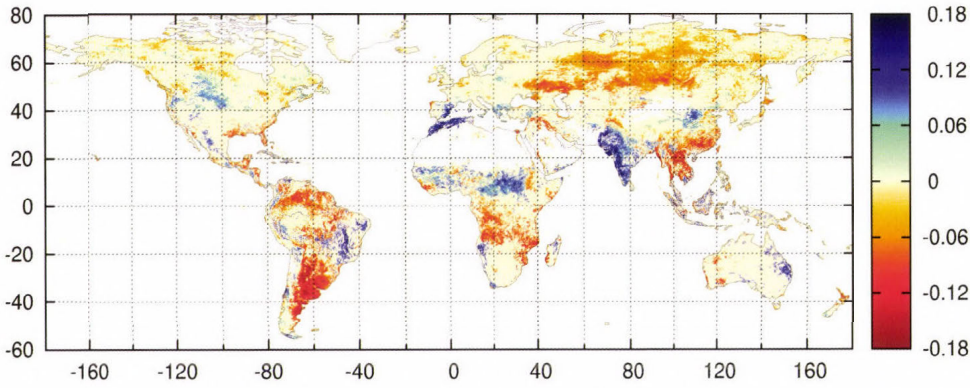

Fig. 1. Geographic locations of statistically significant drying (red) or wetting (blue) trends. Slopes are color coded in units of DSI/year. White color indicates missing data. (*Orvos et al.*, 2014)

Fig. 2 illustrates a detailed map of the southern part of the Asian subcontinent. As for climate shifts in India, *Kothyari* and *Singh* (1996) studied long-term time series of summer monsoon rainfall and identified decadal departures above and below the long-time average alternatively for three consecutive decades. *Singh* and *Sontakke* (2002) reported on an increase in extreme rainfall events over northwest India during the summer monsoon and a decline of the number of rainy days along east coastal stations in the past decades, resulting in a westward shift in rainfall activities. Similarly, *Murumkar* and *Arya* (2014) demonstrated by means of wavelet analysis that prominent annual rainfall periods exist ranging from 2 to 8 years at all the studied stations after 1960s. Large-scale spatial and temporal correlations between the trends of rainfall and temperature are found by *Subash* and *Sikka* (2013), without a direct relationship between increasing rainfall and increasing temperature of monthly or seasonal patterns over meteorological subdivisions of India. As for the particular area, even glaciers can be listed as candidate explanatory factors, since they influence runoff into lowland rivers, and recharge river-fed aquifers (*Bolch et al.*, 2012). In order to illustrate the difficulties of interpreting DSI trends, *Panda* and *Kumar* (2014) also found increasing trends of extreme rainfall indices based on the percentile and absolute values, simultaneously with a significantly increased length of dry spells over northern and central regions of India, suggesting a serious threat to the Indian agriculture.

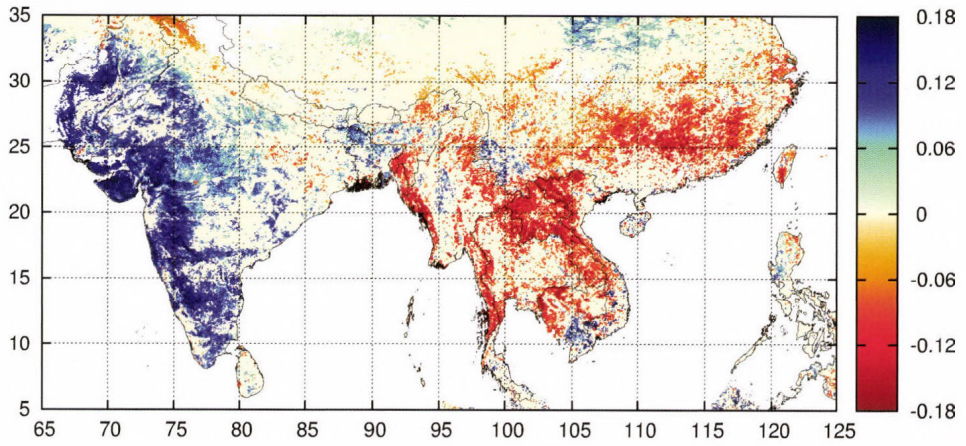

Fig. 2. Geographic locations of statistically significant drying (red) or wetting (blue) trends in Southern Asia. Slopes are color coded in units of DSI/year.

At the other side of the Bay of Bengal, the largest part of Laos, Northern Vietnam, and extended territories in South China are affected by an opposite, drying trend. *Nguyen et al.* (2014) studied a total of 40 years of data from 60 stations around Vietnam. They concluded that dominant trends for annual rainfall are declines, but not in a statistically significant way (they used the Mann-Kendall test). Among the eight climate regions, five of them in Northern Vietnam show decreasing trends, but only the sub-region around Ha Noi has statistically significant decreases. Note that DSI is not a direct measure of precipitation, however, the spatial and temporal coincidences indicate a strong relationship between them. *Hsu et al.* (2014) reviewed the variability of East Asian, Indochina, and Western North Pacific Summer Monsoon on time scales ranging from diurnal to interannual and interdecadal. They concluded that one of the largest challenges is to understand the observed long-term changes and regime shifts in terms of global monsoon. Regional climate model runs by *Zhou et al.* (2013) suggest that the high-speed emission of SO_2 and its uneven distribution over eastern China can contribute to the change in the May-August rainfall over eastern China between the two decades of 1999–2008 and 1989–1998, especially to the decrease of rainfall in the Yangtze River valley.

As a next example, *Fig. 3* demonstrates also an interesting large-scale pattern in DSI trends at the opposite sides of the equator. Large regions in Sudan and in the Central African Republic exhibit positive (wetting), while Eastern Congo, Angola, and Mozambique suffer from negative (drying) tendencies. Various regions in Africa are commonly accepted to be among the most vulnerable territories considering global climate change, the climatological literature is quite controversial and uneven. One reason is that Africa has the

lowest density and quality observational network, therefore, most of the studies are based on reanalysis data or numerical modeling. Since the DSI strongly depends on NDVI data, a proper interpretation would require reliable information on local circumstances such as land use changes, shepherding, large-scale migrations, etc.

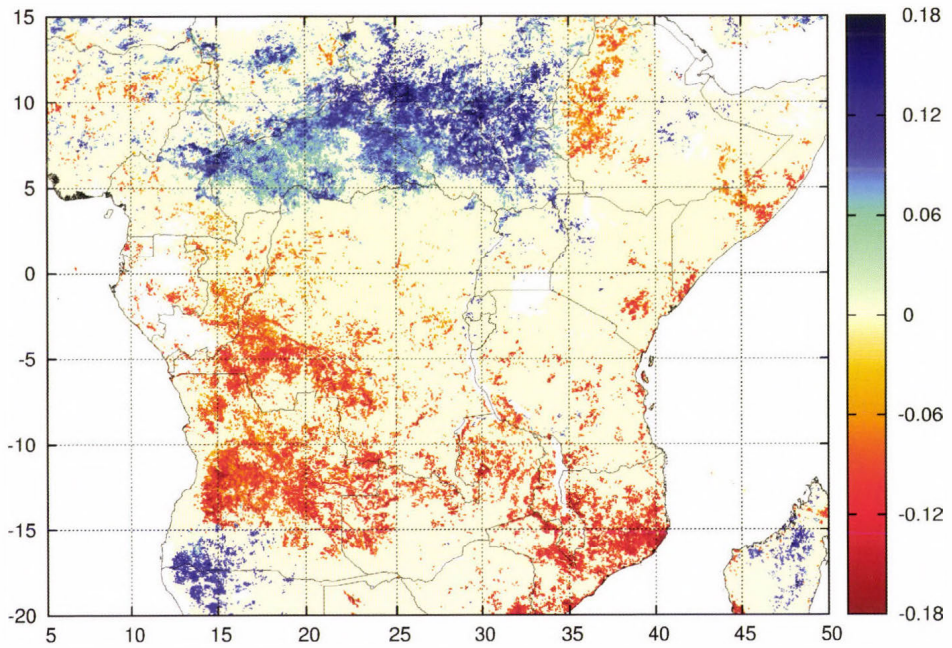

Fig. 3. Geographic locations of statistically significant drying (red) or wetting (blue) trends in Middle Africa. Slopes are color coded in units of DSI/year.

Fig. 4 demonstrates remarkable tendencies around the western Mediterranean basin: northern Morocco, Algeria, and Eastern Spain exhibit strong and significant wetting trends. The main characteristic of the region is the strong gradient between two large-scale systems, namely the North Atlantic (Azores) anticyclone and the low pressure monsoon system over the Indian Ocean and Middle East. This strong gradient establishes a flow from north to south during all seasons that is enhanced by the differential heating between the land of North Africa and South Europe with the Mediterranean waters. It is interesting to note that a recent collaborative assessment on regional climate change (see: *Navarra* and *Tubiana*, 2013) concluded that no basin-wide trends in precipitation and droughts are detectable for the second half of the twentieth century.

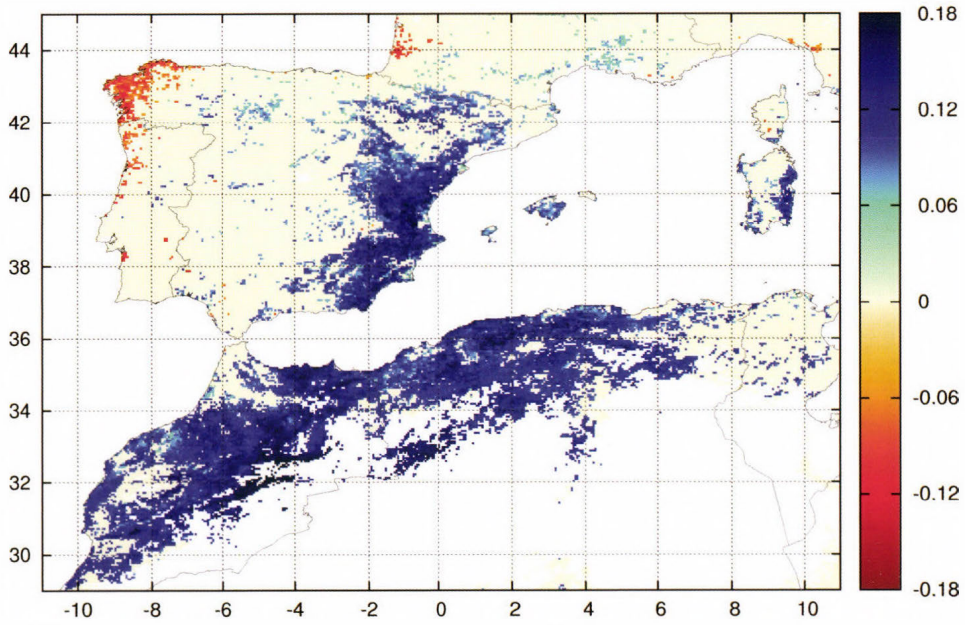

Fig. 4. Geographic locations of statistically significant drying (red) or wetting (blue) trends around the western Mediterranean region. Slopes are color coded in units of DSI/year.

3. Weak DSI trends in the Carpathian basin

Since the drought severity index basically conveys local information, it is worth to check regions where trends are not such significant as in the examples in the previous Section. As a case study, *Fig. 5* shows the geographic distribution of DSI trends in the Carpathian Basin, Central Europe. Locations are plotted where measured slopes passed the significance test by at least 1σ level (the number of sites obeying 2σ significance is not more than 1.1%). While an isolated point of weak DSI trend can easily be a consequence of statistical uncertainties, larger connected regions of similar tendencies support the existence of real effects in the background.

Representative locations are indicated in *Fig. 5*. Sites around České Budějovice (Czech Republik), Szombathely (Hungary), or Pula (Croatia) obey weak wetting, while weak drying is characteristic in the surroundings of Doboj (Bosnia and Herzegovina) or the diagonal band between 49°N–23.5°E and 48°N–25°E (see *Fig. 5*). The latter band coincides with a by and large unpopulated region of Carpathian Mountains in Ukraine, where the observed tendencies are probably consequences of forest cover loss (*Dezső et al.*, 2005).

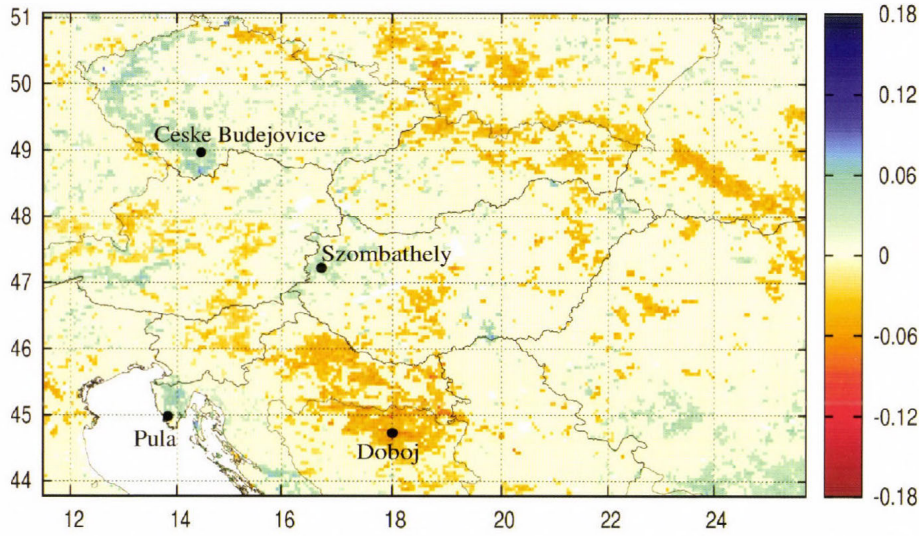

Fig. 5. Geographic locations of weakly significant drying (red) or wetting (blue) trends at 1σ level in the Carpathian Basin. Slopes are color coded in units of DSI/year (note that the range of the color scales is identical for all maps). Locations of a few cities are indicated for an easier orientation.

Repeated analyses and projections of regional climate change are in focus of several research projects also in the Carpathian Basin (*Gálos* and *Jacob*, 2007; *Szépszó* and *Horányi*, 2008; *Krüzselyi et al.*, 2011; *Torma et al.*, 2011; *Bartholy et al.*, 2012; *Bartholy et al.*, 2013; *Mezősi et al.,* 2013). The results are somewhat controversial similarly to other efforts in regional climate modeling: warming and drying tendencies are often identified with various intensities for different geographic sub-regions. However, it should be emphasized that a direct comparison of numerical simulation with empirical results such as illustrated in *Fig. 5* is not really possible, simply because the models cannot determine the very drought severity index analyzed in this work (*Rummukainen,* 2010).

4. Discussion

We have shortly described the way of obtaining DSI records in Section 1. Clearly, any drought severity index is related to precipitation in some way, however, we have illustrated in *Orvos et al.* (2014) that several other local factors, most importantly changing land-use, contribute to a given index value. As a further illustration we show in *Fig. 6* that precipitation trends are not directly related to local DSI trends. Two locations from the map of *Fig. 5* are chosen, where the weakly significant DSI trends of opposite signs are not related to daily precipitation time series at all.

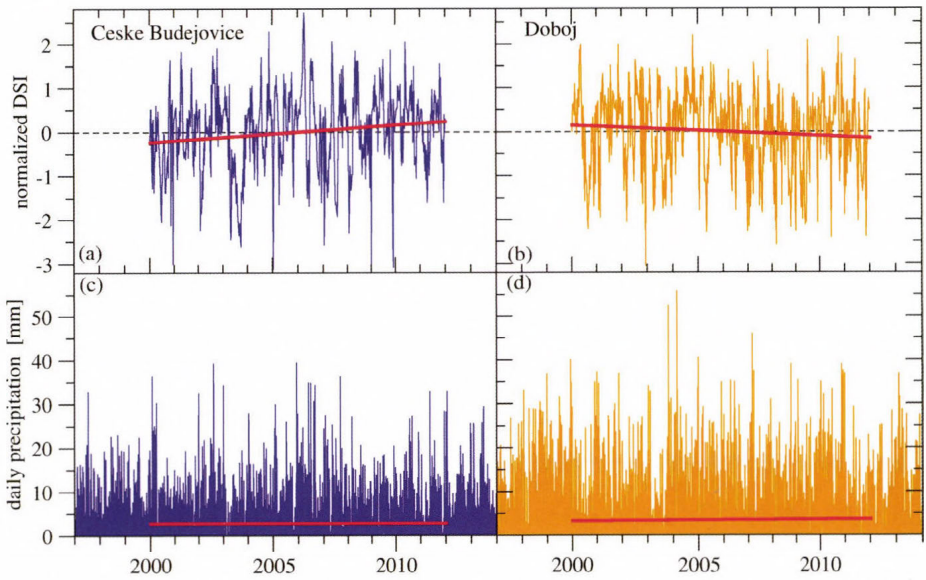

Fig. 6. Weakly significant wetting/drying trends at 1σ level at (a) České Budějovice (49.5°N, 14.5°E) and (b) Doboj (44.5°N, 18.5°E). Red lines indicate slopes of +0.0394 and -0.0243 DSI/year, respectively. (c) and (d) show daily precipitation time series in units of mm for the same geographic locations. Note that fitted trends for the same 12-year period (red lines) are statistically not significant, however the slopes are opposite: –0.0042 mm/year for České Budějovice (c) and +0.0317 mm/year for Doboj (d).

As for the Carpathian Basin, our findings are in agreement with a high spatial resolution trend analysis of monthly self-calibrating PDSI records by *van der Schrier et al.* (2005). Trends in summer moisture availability over Europe for the 1901–2002 period failed to be statistically significant, both in terms of spatial means of the drought index and the area affected by drought. While the time interval of our analysis has a negligible overlap with the cited study (*van der Schrier et al.,* 2005), we also found that the MODIS DSI time series have non-significant local trends in the middle of the European continent.

Nevertheless, we think that the DSI defined by *Mu et al.* (2013) can be implemented in numerical models. Considering the high temporal and spatial resolutions of the data set, it can serve as an exceptional tool for model parameterization and benchmarking.

Acknowledgements: This work was partially supported by the European Union and the European Social Fund through the project FuturICT.hu (grant no. TAMOP-4.2.2.C-11/1/KONV-2012-0013), furthermore the project StratoClim (grant no. 603557-FP7-ENV.2013.6.1-2), and the Hungarian Science Foundation (grant no. OTKA NK100296).

References

Alley, W. M., 1984: The Palmer drought severity index: Limitations and assumptions. *J. Climate Appl. Meteor. 23*, 1100–1109.

Bartholy, J, Pongrácz R, Nagy, J., Pieczka, I., and *Hufnagel, L.*, 2012: Regional climate change impacts on wild animals' living territory in Central Europe. *Appl. Ecol. Environ. Res. 10*, 107–120.

Bartholy, J., Pongrácz, R., and *Hollósi, B.*, 2013: Analysis of projected drought hazards for Hungary. *Adv. Geosci. 35*, 61–66.

Bolch, T., Kulkarni, A., Kääb, A., Huggel, C., Paul, F., Cogley, J.G., Frey, H., Kargel, J.S., Fujita, K., Scheel, M., Bajracharya, S., and *Stoffel, M.*, 2012: The state and fate of Himalayan glaciers. *Science 336*, 310–314.

Dai, A., 2011: Characteristics and trends in various forms of the Palmer Drought Severity Index during 1900–2008. *J. Geophys. Res. 116*, D12115.

Dai, A., Trenberth, K.E., and *Qian, T.*, 2004: A global dataset of Palmer drought severity index for 1870–2002: Relationship with soil moisture and effects of surface warming, *J. Hydrometeor. 5*, 1117–1130.

Damberg, L. and *AghaKouchak, A.*, 2013: Global trends and patterns of drought from space. *Theor. Appl. Climatol.*, early view, doi: 10.1007/s00704-013-1019-5.

Dezső, Z., Bartholy, J., Pongrácz, R., and *Barcza, Z.*, 2005: Analysis of land-use/land-cover change in the Carpathian region based on remote sensing techniques. *Phys. Chem. Earth. 30*, 109–115.

Gálos, B., Lorenz, Ph., and *Jacob, D.*, 2007: Will dry events occur more often in Hungary in the future? *Environ. Res. Lett. 2*, 034006.

Heim, R.R. Jr., 2002: A review of twentieth-century drought indices used in the United States. *Bull. Amer. Meteor. Soc. 83*, 1149–1165.

Hsu, H-H., Zhou, T., and *Matsumoto, J.*, 2014: East Asian, Indochina and Western North Pacific Summer Monsoon - An Update. *Asia-Pac. J. Atmos. Sci. 50*, 45–68.

Keyantash, J., and Dracup, J.A., 2002: The quantification of drought: An evaluation of drought indices. *Bull. Amer. Meteor. Soc. 83*, 1167–1180.

Kothyari, U.C. and *Singh, V.P.*, 1996: Rainfall and temperature trends in India. *Hydrol. Process. 10*, 357–372.

Krüzselyi, I., Bartholy, J., Horányi, A., Pieczka, I., Pongrácz, R., Szabó, P., Szépszó, G., and *Torma, Cs.*, 2011: The future climate characteristics of the Carpathian Basin based on a regional climate model mini-ensemble. *Adv. Sci. Res. 6*, 69–73.

Manly, B.F.J., 2007: Randomization, Bootstrap and Monte Carlo Methods in Biology. 3rd Ed., Chapman and Hall/CRC, Boca Raton.

Mezősi, G., Meyer, B.C., Loib, W., Aubrecht, l Ch., Csorba, P., and *Bata, T.*, 2013: Assessment of regional climate change impacts on Hungarian landscapes. *Reg. Environ. Change 13*, 797–811.

Mu, Q., Zhao, M., and *Running, S.W.*, 2011: Improvements to a MODIS Global Terrestrial Evapotranspiration Algorithm. *Remote Sens. Environ. 115*, 1781–1800.

Mu, Q., Zhao, M., Kimball, J.S., McDowell, N.G., and *Running, S.W.*, 2013: A remotely sensed global terrestrial drought severity index. *B. Am. Meteorol. Soc. 94*, 83–98.

Murumkar, A. R. and *Arya, D.S.*, 2014: Trend and periodicity analysis in rainfall pattern of Nira basin, Central India. *Am. J. Clim. Change 3*, 60–70.

Navarra, A. and *Tubiana L. (Eds.)*, 2013: Regional Assessment of Climate Change in the Mediterranean. Volume 1: Air, Sea and Precipitation and Water. Springer Science+Business Media, Dordrecht.

Nguyen, D-Q., Renwick, J., and *McGregor, J.*, 2014: Variations of surface temperature and rainfall in Vietnam from 1971 to 2010. *Int. J. Climatol. 34*, 249–264.

Orvos, P.I., Homonnai, V., Várai, A., Bozóki, Z., and *Jánosi, I.M.*, 2014: Global trend analysis of the MODIS drought severity index with local statistical significance tests. Submitted to *Geosci. Instr. Methods Data Syst.*

Palmer, W.C., 1968: Keeping track of crop moisture conditions, nationwide: The new crop moisture index. *Weatherwise 21*, 156–161.

Panda, D.K. and *Kumar, A.*, 2014: The changing characteristics of monsoon rainfall in India during 1971–2005 and links with large scale circulation. *Int. J. Climatol.*, early view, doi: 10.1002/joc.3948

Parkinson, C.L. and Greenstone, R. (Eds.), 2000: EOS Data Product Handbook (Vol. 2), NASA Goddard Space Flight Center, Greenbelt, Maryland.

Rummukainen, M., 2010: State-of-the-art with regional climate models. *Wiley Interdisciplinary Reviews: Climate Change, 1,* 82–96.

Sheffield, J., Wood, E.F., and *Roderick, M.L.*, 2012: Little change in global drought over the past 60 years. *Nature 491*, 435–438.

Singh, N. and *Sontakke, N.A.*, 2002: On climatic fluctuations and environmental changes of the Indo-Gangetic Plains, India. *Climatic Change 52*, 287–313.

Spinoni, J., Naumann, G., Carrao, H., Barbosa, P., and *Vogt, J.*, 2013: World drought frequency, duration, and severity for 1951-2010. *Int. J. Climatol.*, early view, doi: 10.1002/joc.3875

Subash, N. and *Sikka, A.K.*, 2013: Trend analysis of rainfall and temperature and its relationship over India. *Theor. Appl. Climatol.*, early view, doi: 10.1007/s00704-013-1015-9

Szépszó, G. and *Horányi, A.,* 2008: Transient simulation of the REMO regional climate model and its evaluation over Hungary. *Időjárás 112*, 203–231.

Torma, Cs., Coppola, E., Giorgi, F., Bartholy, J., and *Pongrácz, R.*,2011: Validation of a high-resolution version of the regional climate model RegCM3 over the Carpathian Basin. *J. Hydrometeorol. 12*, 84–100.

Trenberth, K. E., Dai, A., van der Schrier, G., Jones, P.D., Barichivich, J., Briffa, K.R., and *Sheffield, J.*, 2014: Global warming and changes in drought. *Nature Clim. Change 4*, 17–22.

van der Schrier, G., Briffa, K.R., Jones, P.D., and *Osborn, T.J.,* 2006: Summer moisture variability across Europe, *J. Climate 19*, 2828–2834.

Vicente-Serrano, S.M., Beguería, S., and *López-Moreno, J.I.*, 2011: Comment on "Characteristics and trends in various forms of the Palmer Drought Severity Index PDSI) during 1900–2008"' by Aiguo Dai, *J. Geophys. Res. 116*, D19112

Wells, N., Goddard, S., and *Hayes, M.J.*, 2004: A self-calibrating Palmer drought severity index. *J. Climate 17*, 2335–2351.

Yao, Y., Liang, S., Qin, Q., and *Wang, K.*, 2010: Monitoring drought over the conterminous United States using MODIS and NCEP Reanalysis-2 data. *J. Appl. Meteorol. Climatol. 49*, 1665–1680.

Yao Y., Liang, S., Zhao, S., Zhang, Y., Qin, Q., Cheng, J., Jia, K., Xie, X., Zhang, N., and *Liu, M.*, 2014: Validation and application of the modified satellite-based Priestley-Taylor algorithm for mapping terrestrial evapotranspiration. *Remote Sens. 6*, 880–904.

Zhou, Y., Jiang, J., Huang, A., La, M., Zhao, Y., and *Zhang, L.,* 2013: Possible contribution of heavy pollution to the decadal change of rainfall over eastern China during the summer monsoon season. *Environ. Res. Lett. 8*, 044024.

IDŐJÁRÁS

Quarterly Journal of the Hungarian Meteorological Service
Vol. 118, No. 4, October – December, 2014, pp. 335–347

Some aspects of the impact of meteorological forecast uncertainties on environmental dispersion prediction

Tímea Haszpra[1*] and **András Horányi**[2]

[1]*MTA–ELTE Theoretical Physics Research Group,*
Pázmány Péter sétány 1/A, H-1117 Budapest, Hungary,
hatimi@caesar.elte.hu

[2]*Hungarian Meteorological Service,*
Kitaibel Pál u. 1., H-1024 Budapest, Hungary,
Currently on leave at the European Centre for Medium-Range Weather Forecasts,
Shinfield Park, Reading, RG2 9AX, United Kingdom
Andras.Horanyi@ecmwf.int

**Corresponding author*

(Manuscript received in final form August 25, 2014)

Abstract—There are several types of uncertainties related to the simulation of the dispersion of pollutants in the atmosphere. For a dispersion forecast, one of the most important error sources is the meteorological data produced by a numerical weather prediction model and utilized by the dispersion model. In this paper, we will present the results of an ensemble dispersion forecast created by using an ensemble meteorological forecast and the high-resolution forecast for 2.5 days. The dispersion simulations are carried out by the RePLaT Lagrangian dispersion model for particles of different radii. Significant deviations appear both in the extension and location of the ensemble of pollutant clouds consisting of particles of the same size. Differences appear also between the dispersion scenarios which use the unperturbed meteorological forecasts with different resolutions. The difference among the ensemble members increases for small particles. The area where at least one ensemble member predicts pollutant is much larger than the area covered by the pollutant cloud of the high-resolution forecast.

Key-words: dispersion, realistic particles, ensemble forecast, RePLaT model

1. Introduction

Pollutants from different sources may be advected far away from their initial position and cause pollution episodes at distant locations. The effects of ash clouds from volcano eruptions and of gases and aerosol particles from industrial accidents underline the need for investigating dispersion in the atmosphere as the emitted material can be hazardous. Volcanic ash can be dangerous, e.g., for air transport, and hence, may imply an economic hazard even if the eruption itself is not a strong one (for instance as it was the case for the Eyjafjallajökull's eruptions in 2010). The disaster of Chernobyl in 1986 and Fukushima in 2011 drew attention to the significance of the fact that radioactive materials from nuclear power plant accidents or air pollutants from other sources can also be a risk for health both in the atmosphere and as deposited material, therefore, the accurate prediction of their dispersion is essential.

As a consequence, the demand for more and more accurate tracking and forecasting of atmospheric pollutants has increased due to the growing interest in environmental problems.

However, dispersion simulations are subject to numerous uncertainties. There might be inaccuracies in the emission data for the dispersion model as the source term (the emitted amount, physical and chemical properties, emission height and period, initial extension and size distribution of the pollutant cloud) is only estimated. Obviously, in particular cases, e.g., for sudden and intense volcano eruptions, the 3-dimensional extent of the ash cloud and the size distribution of the aerosol particles can be estimated only with much more uncertainty than in other cases, like e.g., for a weak leaking from a plant close to the ground.

The other set of the input data on which the dispersion calculation is based, that is, the meteorological forecast data produced by the numerical solution of the atmospheric hydro-thermodynamic equations also include uncertainty. This is, on the one hand, the consequence of the inaccurate initial conditions of the forecasts that cannot be precisely determined due to the inaccuracies in the measurements and the approximations in the data assimilation procedures. On the other hand, the reason for the uncertainties in the meteorological data is also the fact that the meteorological weather prediction model is not fully precise as for instance it uses parameterizations for certain processes and applies numerical schemes. The uncertainty in the meteorological forecasts can be quantified by the ensemble technique including the execution of multiple meteorological forecasts (*Leutbecher* and *Palmer*, 2008). This meteorological uncertainty estimate can be carried forward to the dispersion models for assessing the implied uncertainties in the air pollution prediction.

The dispersion model itself also contains uncertainties. Its reliability depends on the processes taken into account (like advection, turbulent diffusion, dry and wet deposition, chemical reactions, etc.), their parameterizations, numerical approximations, and interpolations applied in the model. The importance of all the above-mentioned uncertainty sources is summarized in *Galmarini et al.* (2004).

Furthermore, it is important to emphasize that in 2D time-dependent flows or in 3D flows, as it is the case of the atmosphere, the advection of pollutants is chaotic. The typical characteristics of chaotic behavior are the sensitivity to the initial conditions, irregular motion, and complex but regular (fractal-like) structures (*Aref*, 1984). Thus, chaotic advection of pollutants amplifies the inaccuracies mentioned before.

It is a relevant question to understand the relative merits of the various uncertainty sources during the entire dispersion modeling process. The uncertainties related to the meteorological inputs can be minimized when such observation-related analysis meteorological fields are used as re-analysis (*Dee et al.*, 2011). With the use of re-analysis information, the meteorological inputs are considered to be perfect, therefore, only the other uncertainty sources play role in the overall uncertainty pattern of the dispersion model.

As an example, *Fig. 1* illustrates the dispersion of volcanic ash from the Eyjafjallajökull's eruption in the spring of 2010. In the beginning of the eruption period, northern flows were dominating south to Iceland, and a high pressure area was located in the Atlantic region. *Fig. 1* shows that, first, the volcanic ash becomes transported to south in the anticyclonic circulation. It is due to the northerly winds that the volcanic ash can reach even the Iberian Peninsula located about 2000 km away from Iceland. Some days later (not shown here) the volcanic ash is dispersed all over Europe. We compared the results of the simulation with satellite observation on May 10 (see right panel of *Fig. 1*). The shape of the ash cloud was found to be remarkably similar in the simulation and in the satellite image. Even the fat patch at the southwest "edge" of the ash cloud found in the simulation appears in the satellite image. Therefore, according to this comparison, there seems to be a satisfying agreement between the simulation and the measurement. This means that in this particular case, the dispersion simulation uncertainties are low, consequently, the non-meteorological related uncertainties have only a small impact. Based on this result, we consider that the uncertainties related to the meteorological inputs are presumably more important than the other ones.

Therefore, in this paper we focus on the impact of uncertainty of the meteorological forecasts on the dispersion calculation. This kind of variability was studied in different ways for gases (see, e.g., *Holt et al.*, 2009; *Lee et al.*, 2009; *Scheele* and *Sigmund*, 2001; *Straume et al.*, 1998; *Straume*, 2001). To our knowledge, no systematic investigation has been carried out for aerosol particles before the study of *Haszpra et al.* (2013). In order to study this problem we

carried out multiple dispersion simulations using 50+1 members of an ensemble forecast and the corresponding high-resolution forecast (HRES, referred as deterministic forecast in earlier references). The dispersion simulations were performed with particles of different sizes composing the pollutant clouds in order to investigate the dependence of the impact on the particle radius. This work serves as a complement to *Haszpra et al.* (2013) as the results are based on the same meteorological and emission data and, therefore, on the same dispersion simulations. Although, in contrast to that, this paper mostly concentrates on the properties of the individual pollutant clouds in the ensemble dispersion forecast rather than looking them altogether to characterize them with various statistical properties.

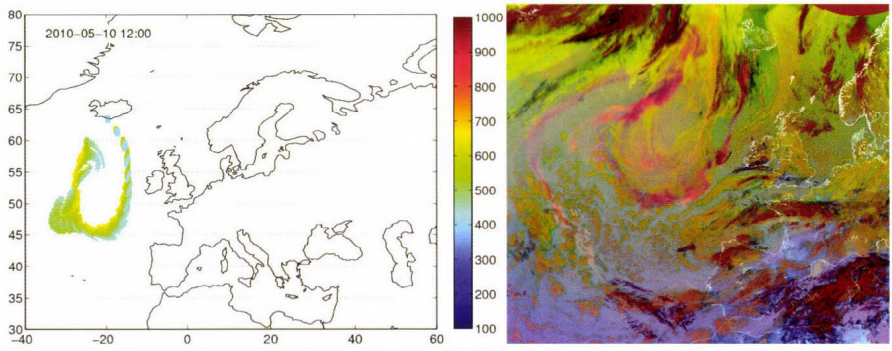

Fig. 1. Left: The dispersion of a sequence of volcanic ash puffs from the Eyjafjallajökull's eruption in RePLaT simulation (see Section 2). Each volcanic ash puff consists of 10^3 particles with radius $r = 1$ μm. The initial altitude of the centre of puffs is $p = 500$ hPa, the initial extension is 1°×1°×200 hPa. The puffs are emitted in every 6 hours from May 8, 00 UTC on. The color bar indicates the altitude of the particles in hPa. Right: Satellite image at 12 UTC, May 10, 2010. Volcanic ash is indicated by pink. [http://oiswww.eumetsat.org/WEBOPS/medialib/medialib/images/2010_05_10_1200_m8_rgb_24hmicro.jpg]

Section 2 gives a brief overview of the RePLaT dispersion model by which the dispersion simulations were carried out (it was also used for the computations shown in *Fig. 1*). In Section 3, the meteorological data utilized for the dispersion calculation is presented. Section 4 provides the results of the ensemble dispersion simulation, and Section 5 summarizes the main conclusions of the work.

2. *The RePLaT dispersion model*

The RePLaT (Real Particle Lagrangian Trajectory) dispersion model – as its name also suggests – is a Lagrangian trajectory model that tracks individual spherical aerosol particles with fixed, realistic radius r and density ρ_p. The velocity of a particle is equal to the velocity of the ambient air in horizontal, and in the vertical direction (owing to the impact of gravity), deposition has to be taken into account with the terminal velocity w_{term}. The effect of turbulent diffusion is built into the equations as a stochastic term. Thus, the equation of motion of a particle is the following:

$$\frac{d\mathbf{r}_p}{dt} = \mathbf{v} + w_{term}\mathbf{n} + \boldsymbol{\xi} \cdot \mathbf{K}, \tag{1}$$

where

$$w_{term} = -\frac{2}{9}\frac{\rho_p r^2 g}{\rho \nu}. \tag{2}$$

This follows from Stokes's law which is valid for small and heavy particles (ρ_p is in the order of 2000 kg m^{-3}, $r \leq 10$ μm). In Eq. (1) and (2), $\mathbf{r}_p(t)$ denotes the particle trajectory, $\mathbf{v} = (u, v, w)$ is the velocity of air, $\mathbf{n}$ is the vertical unit vector pointing upwards, g is gravitational acceleration, ρ and ν indicate the density and viscosity of the air, $\boldsymbol{\xi}$ is a random walk process and $\mathbf{K}$ represents the turbulent diffusivity in the different directions which might be location- and time-dependent.

RePLaT also takes into account the impact of scavenging of particles by precipitation. It is built into the model as a random process that results in a particle that is captured by a raindrop with a certain probability. The probability of the transformation from an aerosol particle to a raindrop depends on the precipitation intensity. The trajectory of the "new" particle (the particle that turned into a raindrop) is computed using the terminal velocity based on the new properties of the particle, typically using a terminal velocity w_{term} derived from the quadratic drag law for large particles:

$$w_{term} = -\frac{8}{3}\frac{\rho_{rain} r_{rain} g}{\rho C_d}, \tag{3}$$

where $C_d = 0.4$ is the drag coefficient for spheres. The transformed particle does not leave the atmosphere instantaneously, but as a raindrop falling through the air according to Eq. (1).

The meteorological data given on a grid are interpolated to the location of the particles using bicubic spline interpolation in horizontal and linear interpolation in vertical and in time. The equation of motion is solved by Euler's method. For more details about RePLaT, see *Haszpra* and *Tél* (2013).

3. Data and methods

In order to demonstrate the variability of an ensemble dispersion forecast, the RePLaT model was run with an ensemble meteorological forecast of the European Centre for Medium-Range Weather Forecasts (ECMWF) (*Molteni et al.*, 1996; *Leutbecher* and *Palmer*, 2008) including 50 perturbed members and the unperturbed control forecast (CF). Additionally, simulations were also carried out with the unperturbed high-resolution forecast (HRES). The horizontal resolution of the former ones is 0.25°×0.25°, while that of the latter is 0.125°×0.125°; the time resolution is 3 hours in both datasets. In vertical direction, the meteorological data utilized in the simulations are given on pressure levels (1000, 925, 850, 700, 500, 400, 300, 250, 200, 100, 50, 10 hPa). The dispersion calculation covers a 2.5-day period and starts at 00 UTC on March 12, 2011.

As a first approach, we are interested in the simplest case when the motion of the pollutants is determined only by advection and their terminal velocity, and the effects of turbulent diffusion and precipitation are neglected. These conditions are fulfilled in the free atmosphere with good approximation. Therefore, the simulations are carried out above the 850 hPa level (considered as the bottom of the free atmosphere), and particles sunk below this region are considered to "be deposited" and are no longer tracked.

4. Results

4.1. Ensemble evaluation of meteorological uncertainties

4.1.1. Evaluation of ensemble members

In order to study the impact of the uncertainty of the meteorological fields on the dispersion calculation, a hypothetical emission is considered centered at $\lambda = 141°$, $\varphi = 37.5°$, $p = 500$ hPa (above Japan). Initially, 9×10^4 particles of density $\rho_p = 2000$ kg m^{-3} are distributed uniformly in a horizontal square of size 1°×1°. The simulations are performed for particles of radius $r = 0, 1, 2, \ldots,$ 10 μm so that one can follow the size-dependence of the variability in the ensemble of dispersion forecast.

Particle dispersion patterns were determined in all the 50 ensemble members along with the HRES and CF members 2.5 days after the emission. However, for an easier overview, only some representative members of the whole ensemble dispersion simulation are presented here. *Fig. 2* illustrates the distribution of $r = 1$ μm aerosol particles, while *Fig. 3* is the same for $r = 4$ μm particles. The mean sea level pressure characteristics of each ensemble member are also displayed in the figures. The colors indicate the altitude of the particles

in hPa. In all dispersion simulations, the pollutant cloud of the particles is advected to east, over the Pacific Ocean. In most of them, the cloud stretches more or less in the west–east or southwest–northeast direction. This deformation is the consequence of a jet located east to Japan and some cyclones above the Pacific Ocean during these days: the strong wind shear and mixing effects related to them elongates most of the clouds (*Haszpra et al.*, 2013). The particles happen to sink in the first day. In some members, significant fraction of the $r = 1$ μm particles (having terminal velocity smaller than or of the same order as the vertical velocity component of the air) is captured by a cyclone passing towards the Californian coast. In the upwelling zone, particles lift higher in the atmosphere (green and light blue region), e.g., in members no. 6, 13, etc.

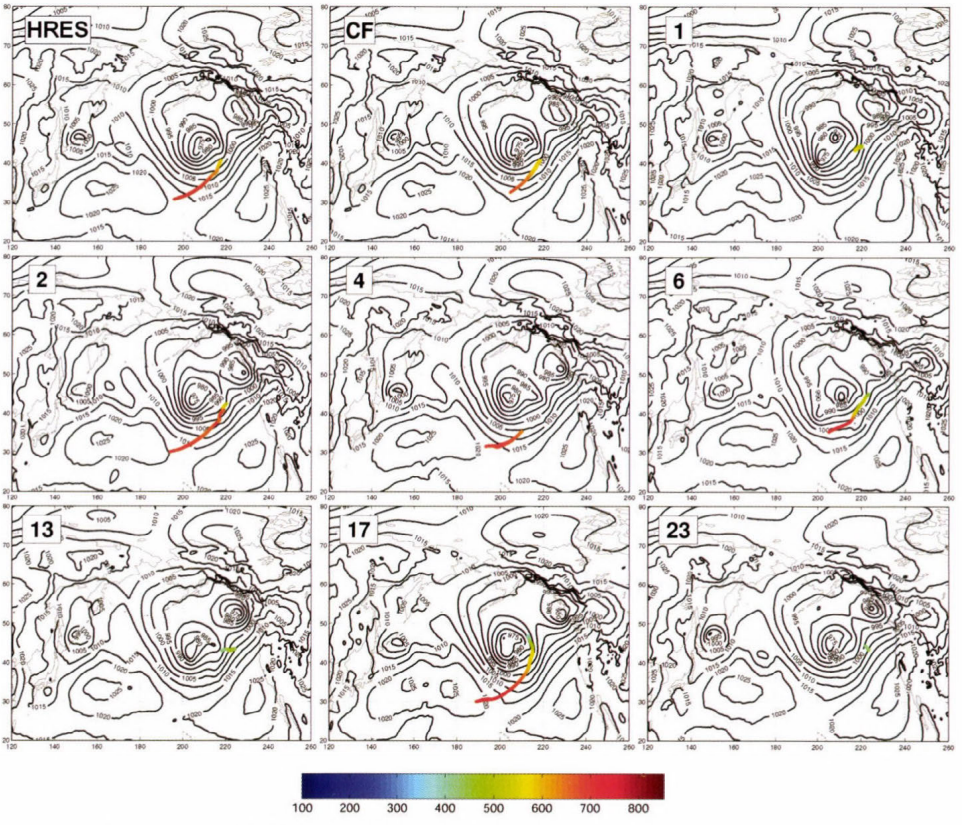

Fig. 2. The distribution of $r = 1$ μm aerosol particles 2.5 day after the emission using the high-resolution forecast (HRES), the control forecast (CF), and the perturbed ensemble members, respectively. Only some representative members of the whole ensemble dispersion simulation are presented. Color bar indicates the height of the particles in hPa. Black contours denote the mean sea level pressure in hPa.

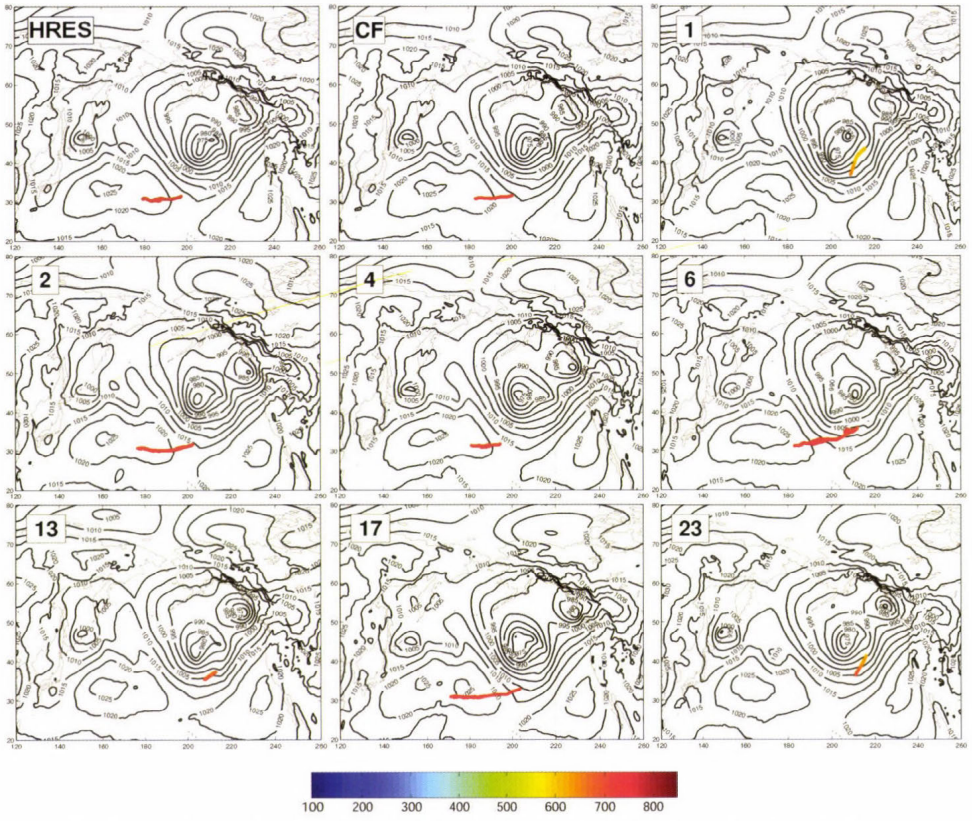

Fig. 3. The distribution of $r = 4$ μm aerosol particles 2.5 day after the emission using the high-resolution forecast (HRES), the control forecast (CF), and the perturbed ensemble members, respectively. Only some representative members of the whole ensemble dispersion simulation are presented. Color bar indicates the height of the particles in hPa. Black contours denote the mean sea level pressure in hPa.

Without any quantitative characterization of the location or extension of the pollutant clouds, just by visual inspection, different types of dispersion events can be distinguished. In *Fig. 2* for the $r = 1$ μm particles in some of the ensemble members, the pollutant cloud is hardly lengthened during the 2.5 days and remains located in the 600–350 hPa layer of the atmosphere (like no. 1, 13, 23, 43, 46[1]). Another class may be formed by dispersion members HRES and no. 2, 5, 10, 11, 14, 27, 29, etc.[1] characterized principally by orange color (750–600 hPa) and strong stretching. A similar, but distinct group can be detected e.g., from members no. 4, 20, 24, 34, 44[1] with a stretched, but less expanded shape (compared to the previous group). As mentioned before, there are

[1] Only some of the listed ensemble members are shown in *Figs. 2* and *3*.

dispersion members (e.g., no. 17, 28, 48[1]) in which the pollutant cloud is strongly influenced by the cyclonic flow, and thus, particles form a spiral towards the center of the cyclone, and the vertical extent of the pollutant cloud covers a wide region from 800 to 300 hPa (red to light blue colors). Finally, there is a similar class of members with particles lifted high in the atmosphere, where the pollutant cloud starts to turn away from the center of the western low pressure system near the North American coast due to the flow of the eastern cyclone (e.g., member no. 6, 16, 33[1]).

An analogous "visual" clustering can be carried out for the $r = 4$ μm particles based on *Fig. 3*. However, in this case fewer groups can be identified. Especially, the vertical distribution of the particles is much narrower, since these particles have 16 times greater terminal velocity than that of the $r = 1$ μm ones (based on Eq. (2)), and therefore, most of them reach the bottom level of the simulation, on which they are formally deposited, within 2.5 days. Almost all of the dispersion members can be classified into two groups: one characterized by slightly or moderately stretched shape in the west–east direction (e.g., HRES, CF, no. 2, 3, etc.[1]), and one including clouds with shorter extension and southwest–northeast direction close to the second low pressure area from North America (member no. 13, 21, 28, 46[1]). It is interesting to note that there are two "outlier" pollutant clouds in *Fig. 3* (member no. 1 and 23). Member 1 has almost all of its particles in the 750–700 hPa layer, while member 23 has half of its particles in the 800–750 hPa and 750–700 hPa layers, respectively. For both members, particles get much higher than those of the other dispersion clouds.

4.1.2. "Outlier" dispersion forecast – "outlier" meteorological forecast?

In connection with the above-mentioned "outlier" predictions for the $r = 4$ μm particles, the question arises whether dispersion member no. 1 and/or 23 is related to a strongly atypical meteorological event. The mean sea level pressure contour lines of the postage stamps charts in *Fig. 2* and *3* do not seem to confirm the idea of a likewise "outlier" meteorological forecast: the general circulation patterns of member 1 and 23 do not appear to differ much more from that of the others than the other members from each other.

Even without computing any statistical quantity, the question may be answered by comparing the $r = 1$ μm and $r = 4$ μm pollutant clouds. In the case of $r = 1$ μm particles in *Fig. 2,* both member no. 1 and no. 23 are characterized by short clouds. However, in contrast to the $r = 4$ μm particles in *Fig. 3*, they are not the only members with these properties; members no. 12, 13, 43, 46 show the same features (and possibly member 3 and 35 also can be included into the group). In the case of $r = 4$ μm particles, these members differ significantly from the two "outlier" predictions with lower and, in certain cases, longer clouds.

Based on these arguments, we cannot claim that the "outlier" members for $r = 4$ μm particles would be the consequence of considerably different meteorological forecasts. In fact, the phenomenon can be attributed to the result of the chaotic advection due to which small differences can produce significantly different dispersion patterns.

It is noted here that it would be a natural idea to run the dispersion calculations only with the representative members of the meteorological ensemble clusters in order to reduce the computational cost of the dispersion prediction. However, some studies suggest that there is not a one-to-one correspondence between the meteorological ensemble clustering and the dispersion clustering (see, e.g., *Straume*, 2001). Therefore, using only the meteorological representatives for a dispersion forecast may not necessarily give a general overview of the possible dispersion scenarios.

4.1.3. Probabilistic evaluation

It is illustrated in Section 4.1.1, that a dispersion calculation run by an ensemble meteorological forecast may result in pollutant clouds which deviate both in location and extension from each other even within 2.5 days. The difference among the pollutant clouds can be quantified by various statistical measures and probability information, see e.g. *Haszpra et al.* (2013), *Scheele* and *Sigmund* (2001), *Straume et al.* (1998), *Straume* (2001). One of the most elegant probability information is demonstrated in *Fig. 4.*

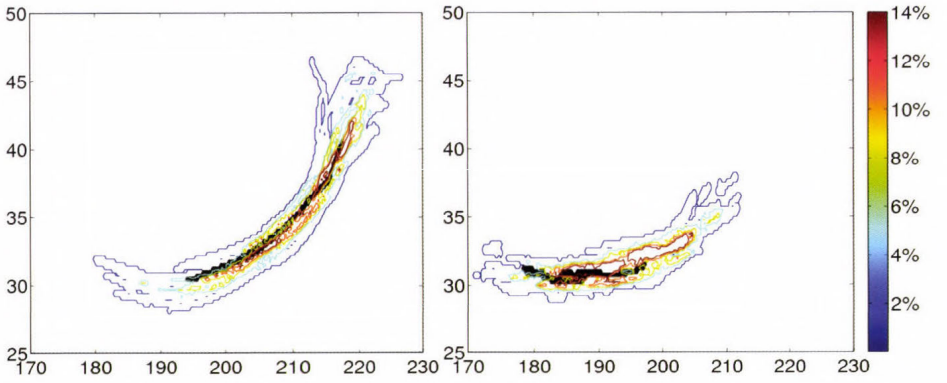

Fig. 4. Horizontal distribution of the ensemble of pollutant clouds after 2.5 days. Contours (at 2, 5, 8, 11 and 14%) indicate the percentage of the dispersion calculations predicting at least one particle in 0.25°×0.25° air columns for particles of $r = 1$ μm remained in the free atmosphere (left) and in 0.25°×0.25° cells for deposited particles of $r = 4$ μm (right). Black color denotes the pollutant cloud obtained by using the high-resolution forecast.

The particle number in 0.25°×0.25° air columns is determined for particles remained above 850 hPa, and this quantity is also calculated in 0.25°×0.25° cells in the "deposition field" for particles which subside below this level, respectively, in each member of the ensemble of pollutant clouds. The left panel of *Fig. 4* demonstrates the horizontal distribution of the ensemble of pollutant clouds in the case of $r = 1$ μm for particles remaining in the simulation range, and the right panel is the same for $r = 4$ μm for particles "deposited" within 2.5 days. Contour lines indicate areas where certain proportion of the ensemble dispersion members predicts at least one particle. Black cells demonstrate the location of the pollutant cloud given by the high-resolution forecast. Both panels of *Fig. 4* point to the fact (as expected) that the area covered by the cloud of the high-resolution forecast is much smaller than the region where at least one ensemble member predicts any particles.

This kind of information is rather useful in risk assessment when one would like to estimate the potential area in the deposition field or the region in air where the concentration of the pollutant exceeds a certain threshold.

4.2. The impact of the resolution of the meteorological data

Comparing the results of the simulations which use the unperturbed high-resolution forecast (HRES) and control forecast (CF), it is possible to study the impact of the resolution of the meteorological forecasts on the dispersion calculation. *Fig. 5* illustrates the horizontal location of the center of mass of the HRES and CF clouds for different particle radii (denoted by the numbers in μm) both for particles in the air (left) and in the deposition field (right). Neither the HRES cloud nor the CF cloud with particles of $r \geq 5$ μm have any particles in the air after 2.5 days, and similarly, clouds consisting of small particles (HRES: $r \leq 1$ μm, CF: $r \leq 2$ μm) have no particles in the deposition field.

As a general rule, it can be concluded that for all particle sizes, differences can be observed between the HRES and CF cloud centers. For those particles of the pollutant clouds that remain in the free atmosphere during the observation period (left panel), the distance between the centers of mass varies between 500 and 1400 km. In the deposition field, the distances range from about 300 km (small particles) down to the order of 10 km (large particles). This is due to the fact that larger particles have larger terminal velocities, hence they deposit sooner and the clouds have less time to separate in the different meteorological fields. *Fig. 5* reveals that also the extension of the HRES and CF pollutant cloud differs somewhat. The rate of the standard deviation values of the HRES and CF clouds in most of the cases is found to be greater than 1 (between 1.1 and 2.5). This implies that the dependence of the dispersion calculation on the resolution of the meteorological data used in the simulation is still significant, especially for pollutants consisting of small particles.

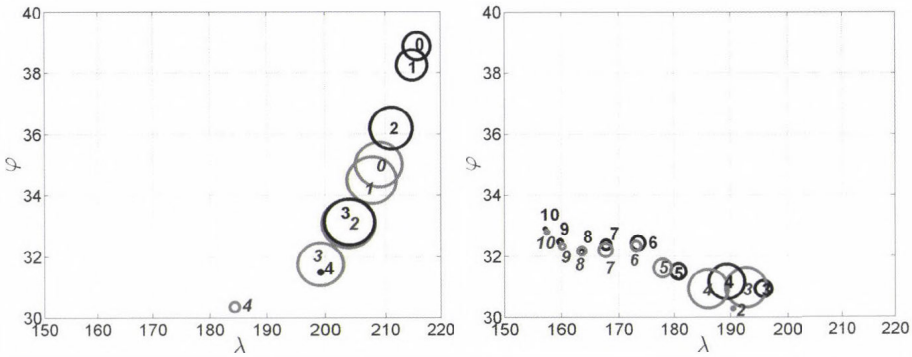

Fig. 5. The horizontal location of the center of the pollutant clouds using the high-resolution forecast (grey, italic font) and the control forecast (black, normal font). Left: center of the pollutant clouds consisting only particles remained in the air for 2.5 days. Right: the same for particles deposited during the 2.5 days. Numbers indicate the particle radius r of the clouds. The radii of the circles are proportional to the standard deviation of the particles within the cloud.

5. Final remarks

In this paper, the case study of a hypothetical emission illustrates that significant deviations may appear among the pollutant clouds of an ensemble of dispersion forecast, and also between the simulations using unperturbed forecasts with different resolutions, even in the simplest case when only advection influences the dispersion of the pollutants. Presumably, in simulations that take into account the impact of turbulent diffusion and precipitation on the particles, even more remarkable differences could be found, since in that case the uncertainties in the dispersion model would be enhanced.

In practice, dispersion models are usually run by a single forecast which is considered to be the best one (i.e., the high-resolution forecast). However, as the paper demonstrates, it can be useful to perform simulations using a whole ensemble of forecasts, i.e., producing an ensemble dispersion prediction in order to get a detailed and more reliable overview of the uncertainties and possible hazards related to the dispersion event.

Acknowledgements: The authors thank *T. Tél* for useful suggestions. This work was partially supported by the European Union and the European Social Fund through the project FuturICT.hu (grant no. TAMOP-4.2.2.C-11/1/KONV-2012-0013), and by the Hungarian Science Foundation (grant no. OTKA NK100296).

References

Aref, H., 1984: Stirring by chaotic advection. *J. Fluid. Mech. 143*, 1–21.

Dee, D.P., Uppala, S.M., Simmons, A.J., Berrisford, P., Poli, P., Kobayashi, S., Andrae, U., Balmaseda M. A., Balsamo, G., Bauer, P., Bechtold, P., Beljaars, A.C.M., van de Berg, L., Bidlot, J., Bormann N., Delsol, C., Dragani, R., Fuentes, M., Geer, A. J., Haimberger, L., Healy, S.B., Hersbach, H., Hólm, E.V., Isaksen, L., Kållberg, P., Köhler, M., Matricardi, M., McNally, A.P., Monge-Sanz, B.M., Morcrette, J.-J., Park, B.-K., Peubey, C., de Rosnay, P., Tavolato, C., Thépaut, J.-N., Vitart, F., 2011: The ERA-Interim reanalysis: Configuration and performance of the data assimilation system. *Q. J. Roy. Meteor. Soc. 137(656)*, 553–597.

Galmarini, S., Bianconi, R., Klug, W., Mikkelsen, T., Addis, R., Andronopoulos, S., Astrup, P., Baklanov, A., *Bartniki, J., Bartzis, J., Bellasio, R., Bompay, F., Buckley, R., Bouzom, M., Champion, H., D'Amours, R., Davakis, E., Eleveld, H., Geertsema, G., Glaab, H., Kollax, M., Ilvonen, M., Manning, A., Pechinger, U., Persson, C., Polreich, E., Potemski, S., Prodanova, M., Saltbones, J., Slaper, H., Sofiev, M., Syrakov, D., Sørensen, J., der Auwera, L., Valkama, I., Zelazny, R.*, 2004: Ensemble dispersion forecasting – Part I: concept, approach and indicators. *Atmos. Env. 38(28)*, 4607-4617.

Haszpra, T., Lagzi, I., and *Tél, T.*, 2013: Dispersion of aerosol particles in the free atmosphere using ensemble forecasts. *Nonlinear Proc. Geoph. 20*, 759–770.

Haszpra, T. and *Tél, T.*, 2013: Escape rate: a Lagrangian measure of particle deposition from the atmosphere. *Nonlinear Proc. Geoph. 20*, 867–881.

Holt, T., Pullen, J. and *Bishop, C.H.*, 2009: Urban and ocean ensembles for improved meteorological and dispersion modelling of the coastal zone. *Tellus A 61*, 232–249.

Lee, J.A., Peltier, L.J., Haupt, S.E., Wyngaard, J.C., Stauffner, D.R., and Deng, A., 2009: Improving SCIPUFF dispersion forecasts with NWP ensembles. *J. Appl. Meteorol. Climatol. 48*, 2305–2319.

Leutbecher, M. and *Palmer, T.N.*, 2008: Ensemble forecasting. *J. Comput. Phys. 227*, 3515–3539.

Molteni, F., Buizza, R., Palmer, T.N., and *Petroliagis, T.*, 1996: The ECMWF ensemble prediction system: Methodology and validation. *Q. J. Roy. Meteor. Soc. 122*, 73–119.

Scheele, M.P. and *Siegmund, P.C.*, 2001: Estimating errors in trajectory forecasts using ensemble predictions. *J. Appl. Meteorol. 40*, 1223–1232.

Straume, A.G., 2001: A more extensive investigation of the use of ensemble forecasts for dispersion model evaluation *J. Appl. Meteorol. 40*, 425–445.

Straume, A.G., Koffi, E.N.D. and *Nodop, K.*, 1998: Dispersion modeling using ensemble forecasts compared to ETEX measurements. *J. Appl. Meteorol. 37*, 1444–1456.

IDŐJÁRÁS

Quarterly Journal of the Hungarian Meteorological Service
Vol. 118, No. 4, October – December, 2014, pp. 349–378

Statistical analysis of relationships between road accidents involving personal injury and meteorological variables in Hungary

Pál Vécsei[*1] and **Kálmán Kovács**[2]

[1] *Senior research adviser,*
Denevér köz 2, H-1121 Budapest, Hungary
pvecsei@t-online.hu

[2] *Director, Federated Innovation and Knowledge Centre of Budapest*
University of Technology and Economics,
Egry József utca 18, V1 C201, H-1111 Budapest, Hungary
kovacsk@mail.bme.hu

**Corresponding author*

(Manuscript received in final form September 10, 2014)

Abstract— Public opinion and certain human meteorological communications assume close relationship between meteorological variations and human conditions, especially the development of traffic accidents. This paper presents a detailed statistical analysis between domestic road accidents involving personal injury and relevant meteorological conditions for the period of 1990–2010 in Hungary. Approximately 431 thousand accidents were analyzed based on official statistical data. In general, a significant but weak interrelation was found between the absolute change – calculated from the previous day – of road traffic accidents involving personal injury and meteorological conditions. The results of multivariate linear regression analysis show that meteorological variations affected only nearly four percent of the variation of accidents relative to traffic. We demonstrated, however, that together with the significant variation of certain meteorological parameters, the number of accidents also significantly varies. Days with extreme meteorological variations explain the development of accidents in 9.8 percent, while in the case of days with non-extreme variations, this value was only 2.6 percent.

Key-words: road accidents with personal injury, multivariate regression, main component analysis, discriminant analysis, climate variation

1. Introduction

There is little scientifically grounded understanding of the effect of climatic variations on everyday living conditions, notwithstanding the numerous studies based on rather limited evidence – looking mainly at the relationship of accident rescue and weather (*Andersson* and *Chapman,* 2011; *Edwards*, 1999; *Jaroszweski et al.*, 2010; *Suarez et al.*, 2005). In spite of this, public opinion and certain human meteorological communications assume close relationship between meteorological variations and human conditions, especially the development of traffic accidents. During the past fifty years, significant results were achieved in the field of the investigation of relationship between road traffic conditions and meteorological parameters. The research activity carried out so far focused only on selected meteorological variables (*Sándor*, 2013). Present paper is aimed at exploring, as far as possible, complex statistical interrelations between road accidents involving personal injury and related meteorological parameters in Hungary.

Due to relatively advantageous circumstances, an opportunity presented itself to perform the joint statistical analysis of all domestic road traffic accidents involving personal injury between 1990 and 2010 (source: KSH data collection, data provider: police OSAP1009) and the relatively detailed data of selected meteorological observatory sites of the Hungarian Meteorological Service (Budapest, Pécs, Szeged, Debrecen, Szombathely, Győr, Nagykanizsa, and Siófok) for the same period. Nearly 13 million data of the approximately 431 thousand accidents were analyzed in details. The statistical analyses were done mostly on the basis of daily averages of the originally hourly data and absolute changes calculated from the previous day.

The key studies were completed with the temperature data of the eight meteorological observatory stations, the measured values of precipitation, wind speed, air pressure, relative humidity of the first five stations, and the average values of cloud cover data, as well as the daily average values of road traffic accidents involving personal injury and partially determined by estimation values for traffic on account of absent factual data. Beyond the interrelations between variations in meteorological conditions and the totality of accidents, the analysis touched upon the study of relations among key accident situations and locations.

2. Relationship between traffic accidents and complex variations of meteorological conditions

In general, it can be concluded, that there is significant but weak interrelation between the absolute change – calculated from the previous day – of road traffic accidents involving personal injury and meteorological conditions. The completed multivariate linear regression analysis shows that climatic variations affected only nearly four percent the variation of accidents relative to traffic as summarized in *Table 1* and *Fig. 1.*

Among the analyzed meteorological variations, the variation of precipitation patterns (1.9% points, nearly half of the total impact) had the most significant impact on the development of accidents, followed by temperature variation (0.7% points). Besides the aforementioned components, the variation of cloud cover and relative humidity influenced the development of accidents to 0.5 percentage points, while air pressure variation to 0.4 percentage points. The impact of wind speed was not statistically significant.

*Table 1.*Multivariate regression interrelations of daily variation of accidents (dependent variable) for estimated traffic between 1990 and 2010 with daily meteorological variation indicators (independent variables), (Stepwise method)

Model summary*									
Model	R	R-squared	Adjusted R-squared	Std. error of the estimate	Change statistics				
					R-squared Change	F change	df1	df2	Sig. F change
1	0.137[a]	0.019	0.019	0.59959	0.019	147.540	1	7668	0.000
2	0.162[b]	0.026	0.026	0.59738	0.007	57.832	1	7667	0.000
3	0.177[c]	0.031	0.031	0.59585	0.005	40.217	1	7666	0.000
4	0.191[d]	0.036	0.036	0.59434	0.005	40.071	1	7665	0.000
5	0.199[e]	0.040	0.039	0.59337	0.003	25.996	1	7664	0.000

* Dependent variable: Daily variation of the number of accidents per estimated traffic

[a] Predictors: (constant), variation of daily mean precipitation amount

[b] Predictors: (constant), variation of daily precipitation amount, variation of daily mean temperature

[c] Predictors: (constant), variation of daily mean precipitation amount, variation of daily mean temperature, variation of daily mean cloud cover

[d] Predictors: (constant), variation of daily mean precipitation amount, variation of daily mean temperature, variation of daily mean cloud cover, variation of daily mean relative humidity

[e] Predictors: (constant), variation of daily mean precipitation amount, variation of daily mean temperature, variation of daily mean cloud cover, variation of daily mean relative humidity, variation of daily mean air pressure

Besides the diverse significance of climatic component variations, their direction of effect was also differentiated (*Fig. 1*).

In general – regarding the measured interrelations, the increase of the amount of precipitation, temperature, and relative humidity, the thinning of the cloud cover and the decrease of the air pressure resulted in an increasing number of accidents. Resulting from the foregoing, opposite meteorological processes impacted on or became characteristic of the moderation of accidents. Therefore, nearly parallel with the decrease of precipitation, temperature, and relative humidity, and with the increase of cloud cover and the rise of air pressure, the number of traffic accidents involving personal injury decreased.

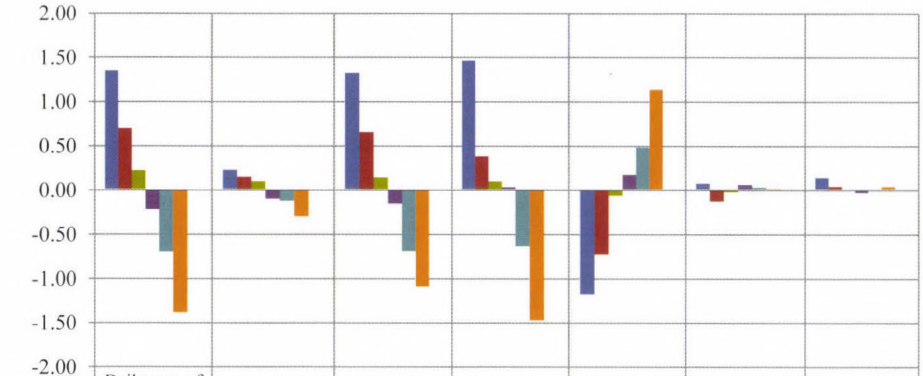

	Daily var. of the number of accidents for estimated traffic [accident / hundred thousand vehicles]	Var. of daily mean temperature [°C]	Var. of daily mean precipitation amount [mm]	Var. of daily mean relative humidity [% points]	Var. of daily mean air pressure [hPa]	Var. of daily mean cloud cover [okta]	Var. of daily mean wind speed [m/s]
1.0 – X increase	1.35	0.23	1.32	1.46	-1.19	0.07	0.14
0.5 – 1.0 increase	0.70	0.15	0.65	0.38	-0.73	-0.13	0.04
0.0 – 0.5 increase	0.22	0.10	0.14	0.10	-0.07	-0.03	0.00
0.0 – 0.5 decrease	-0.23	-0.10	-0.16	0.03	0.17	0.06	-0.04
0.5 – 1.0 decrease	-0.70	-0.13	-0.70	-0.63	0.48	0.03	-0.01
1.0 – X decrease	-1.39	-0.30	-1.10	-1.48	1.14	0.01	0.04
Total	0.00	0.00	0.00	0.00	0.00	0.00	0.00

Fig 1. Daily variation of average values of key meteorological features and of accidents involving personal injury per estimated traffic, calculated from the previous day by categorized values of daily variation of accidents between 1990 and 2010.

Analyses concluded with indicators expressing the daily variation of accidents (not standardized with traffic) and with variants (estimated factor and discriminant function values) obtained from multivariate statistical (factor and discriminant) analysis of the original meteorological indicators led to results almost perfectly identical with the above-mentioned findings.

In contrast with this interrelation, that can be considered generally weak, there are significant differences in the relationship of significantly differing components, types, and categories according to the content and factors, direction and intensity of meteorological variations – separated with multivariate statistical procedures (factor, cluster, and discriminant analysis) – with traffic accidents involving personal injury.

The score of factor analysis of daily meteorological variations represents 87.5% of the variance of the original variants with four relatively well identifiable components (variation of cloud cover, temperature, precipitation, and wind force), and these components well reflect the variation of relative humidity and air pressure, as well (*Table 2*).

Table 2. Scores of key components and factor analysis of indicators representing the absolute variation of meteorological features calculated from the previous day, for days between 1990 and 2010

Component Matrix					
	Component 1	**Component 2**	**Component 3**	**Component 4**	**Communalities**
Variation of daily mean temperature	–0.001	0.787	–0.492	–0.110	0.874
Variation of daily mean precipitation amount	0.714	–0.145	0.246	–0.588	0.936
Variation of daily mean wind speed	0.279	0.557	0.738	0.149	0.956
Variation of daily mean air pressure	–0.671	–0.498	0.22	0.082	0.753
Variation of daily mean humidity	0.746	–0.468	–0.254	0.037	0.842
Variation of daily mean cloud cover	0.787	–0.046	–0.056	0.515	0.889
Extraction sums of squared Loadings in % of variance	36.87	23.68	16.07	10.88	
Extraction sums of squared Loadings in cumulative %	36.87	60.55	76.62	87.50	
Rotated Component Matrix					
	Component 1	**Component 2**	**Component 3**	**Component 4**	**Communalities**
Variation of daily mean temperature	–0.131	**0.914**	–0.150	0.007	0.874
Variation of daily mean precipitation amount	0.181	–0.008	**0.943**	0.118	0.936
Variation of daily mean wind speed	0.041	0.079	0.096	**0.969**	0.956
Variation of daily mean air pressure	–0.403	–0.667	–0.328	–0.195	0.753
Variation of daily mean humidity	0.735	–0.091	0.445	–0.310	0.842
Variation of daily mean cloud cover	**0.919**	0.069	0.068	0.186	0.889
Extraction sums of squared Loadings in % of variance	26.64	21.66	20.51	18.69	
Extraction sums of squared Loadings in cumulative %	36.87	60.55	76.62	87.50	

Extraction method: principal component analysis.
Rotation Method: varimax with Kaiser normalization.

The separation of types, essentially different in the content, structure, and direction of climatic variations, was completed with the so-called K-mean cluster analysis of rotated components obtained from factor analysis, in five variations, incrementally expanding the number of possible types (clusters). The applied procedure resulted in typologies of 7, 10, 15, 20, and 25 numbers of element, the reliability and final content of which were tested partially with four climate change components from factor analysis, and partially with discriminant analyses run on the original variants (*Table 3*).

Table 3. Tests of equality of group means

	Wilks' lambda	F	df1	df2	Sig.
Daily meteorological variations, 25 clusters					
Variation of daily mean precipitation amount	0.208	1215	24	7645	0.00
Variation of daily mean cloud cover	0.313	698	24	7645	0.00
Variation of daily mean wind speed	0.317	688	24	7645	0.00
Variation of daily mean temperature	0.394	491	24	7645	0.00
Variation of daily mean humidity	0.413	452	24	7645	0.00
Variation of daily mean air pressure	0.487	336	24	7645	0.00

Although both approaches hold statistically significant classifications, corresponding to approaches searching less types, the 25-cluster solution represents more reliable and detailed diversity of day-to-day climatic variations of the period, both in total and in the various components. The above is confirmed furthermore by the fact, that the discriminant analyses qualified the distribution of daily variations by 25 types to be rather good – namely, cross classification with four components was matched in 96.5%, and with six original meteorological variations it matched 92.8% of the original classification, therefore, it qualified the classification as correct. The minor difference between the scores of cluster analysis and the discriminant analyses is partially due to that factor analysis and discriminant analysis which defined the significance hierarchy of meteorological variation components somewhat differently.

According to discriminant analyses, in the period between 1990 and 2010, the key determinant, the component of day-to-day climatic variations was the development of precipitation patterns (34.3% variance explained), followed by – with nearly identical weight – cloud cover (24.1%), wind force (21.2%), and temperature change (19.7%).

The rather detailed classification offered empirical opportunity to a more aggregate categorization by intensity and directions of multidimensional variations, to the separation of extreme or non-extreme variations considering the general trend, furthermore, to differentiate extremities according to their direction – appearing, rising or moderating, disappearing. The categorization of the 25 clusters was mainly based on the automatic classification (K-mean clustering) of the group average of estimated values of discriminant functions obtained from the discriminant analysis, but the result from the former ones was supplemented by the content analysis of factor values calculated for the clusters and of the original variants. Finally, 5 groups (9 percent of days) of the 25 cluster solution fell in the appearing-rising extremes category, 6 groups (9.7 percent of days) fell in the disappearing-moderating extremes category, and the remaining 14 groups with 81.3 percent of the days of the 20 years form the group of changes not classified as extreme (*Table 4*). The category of extreme changes is, naturally, the result of the pooling of rising and moderating extremes.

Table 4. Group means of rotated components and discriminant functions of groups separated by the direction and intensity of day-to-day meteorological variations

	Rotated factors from factor analysis of day-to-day meteorological variations				**Value of discriminant functions from the discriminant analysis based on rotated factors of the 25-cluster solution of meteorological variations**				**Days**	
	Meteorological variation component				**Discriminant function**					
	3. Var. of precipitation amount	**1. Var. of cloud cover**	**4. Var. of wind speed**	**2. Var. of temperature**	**1. Var. of daily precipitation amount**	**2. Var. of daily cloud cover**	**3. Var. of daily wind speed**	**4. Var. of daily temperature**	**Number of**	**Distribution of (%)**
	Factor score				**Discriminant scores**					
	Group means									
Rising extreme	1.67	0.00	0.72	–0.70	3.71	–0.35	1.16	–0.87	694	9.0
Decreasing extreme	–1.18	–0.61	–0.68	–1.02	–2.60	–1.50	–0.52	–1.83	741	9.7
Extreme variation	0.20	–0.31	0.00	–0.86	0.45	–0.94	0.29	–1.37	1435	18.7
Non-extreme variation	–0.05	0.07	0.00	0.20	–0.10	0.22	–0.07	0.31	6235	81.3
Days total in 1990–2010	0.00	0.00	0.00	0.00	0.00	0.00	0.00	0.00	7670	100.0

(The plus and minus 0.5, and especially, the above and below (plus and minus) 1.0 group means resulting from the standardizing and normalizing procedure applied in the construction of factor values resulting from factor analyses can be clearly regarded as extremes.) Daily variation of the average values of key meteorological features, and of accidents involving personal injury per estimated traffic, calculated from the previous day by extremity of meteorological variation are shown in *Figs. 2, 3.* and *4.*

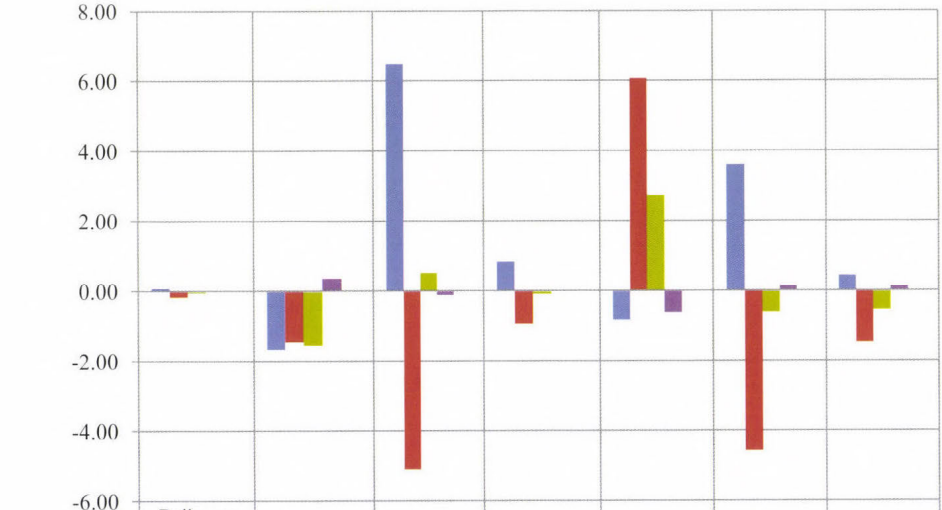

	Daily var. of accidents for estimated traffic	Var. of daily mean temperature [°C]	Var. of daily mean precipitation amount [mm]	Var. of daily mean wind speed [m/s]	Var. of daily mean air pressure [hPa]	Var. of daily mean relative humidity [% points]	Var. of daily mean cloud cover [okta]
Rising extremes	0.08	-1.67	6.49	0.84	-0.83	3.61	0.43
Moderating extremes	-0.17	-1.45	-5.09	-0.95	6.06	-4.57	-1.46
Extreme variations total	-0.05	-1.56	0.51	-0.08	2.73	-0.61	-0.55
Non-extreme variations total	0.01	0.36	-0.12	0.02	-0.63	0.14	0.13
1990 – 2010 total	0.00	0.00	0.00	0.00	0.00	0.00	0.00

Fig 2. Daily variation of the average values of key meteorological features, and of accidents involving personal injury per estimated traffic, from the previous day calculated by extremity of meteorological variation between 1990 and 2010.

The aggregate categorization of meteorological variations by the intensity and direction of the extremes, according to the prepared statistics, is significant for all meteorological indicators especially for the variation of precipitation, then air pressure, wind speed and temperature, however, not nearly to the extent as in the case of the 25 categories.

Because of the complexity and type richness of climatic variations, it may seem a problematic endeavor to condense in three categories the result of a classification based on four independent components of different significances, because even allowing 25 types will leave significant heterogeneities within the different types (clusters). Despite the above reservations, statistical control examinations qualified the classification as satisfactorily reliable. For example, the discriminant analyses - based on the original variables as well as on the factors formed from these - qualified the conformity of the three-category classification to be correct in 89 percent – pertaining to the same category as the initial classification. In terms of content, the only difference is that reclassifications drew somewhat broader borders for the extremes, and this directly resulted in a lower (down to 72 percent of days) proportion of non-extreme days (*Table 5*).

Table 5. Results of classification

Classification results[b,c]						
Meteorological extremes 1990–2010			Predicted group membership			Total
			Rising extremes	Moderating extremes	Non-extreme days	
Original	Count	Rising extremes	602	19	73	694
		Moderating extremes	10	675	56	741
		Non-extreme days	250	460	5525	6235
	%	Rising extremes	86.7	2.7	10.5	100.0
		Moderating extremes	1.3	91.1	7.6	100.0
		Non-extreme days	4.0	7.4	88.6	100.0
Cross-validated[a]	Count	Rising extremes	601	19	74	694
		Moderating extremes	10	674	57	741
		Non-extreme days	252	460	5523	6235
	%	Rising extremes	86.6	2.7	10.7	100.0
		Moderating extremes	1.3	91.0	7.7	100.0
		Non-extreme days	4.0	7.4	88.6	100.0

[a] Cross validation is done only for the cases in the analysis. In cross validation, each case is classified by the functions derived from all cases other than that case.
[b] 88.7% of original grouped cases correctly classified.
[c] 88.6% of cross-validated grouped cases correctly classified.

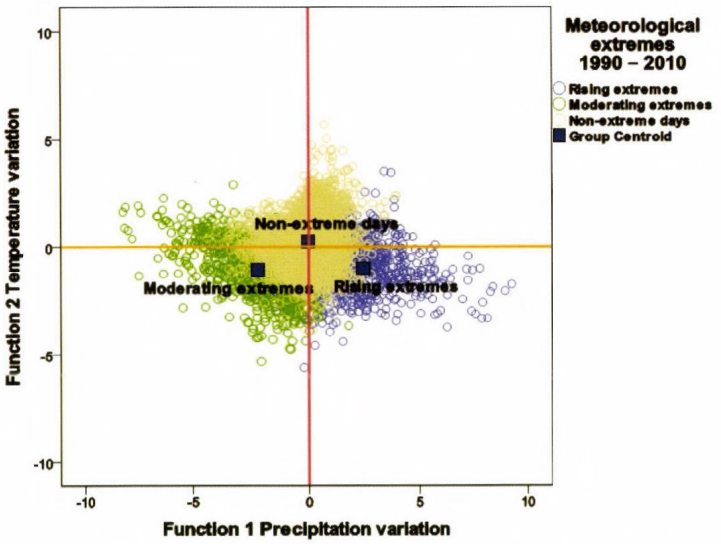

Fig 3. Meteorological extremes for the period 1990–2010 (canonical discriminant functions).

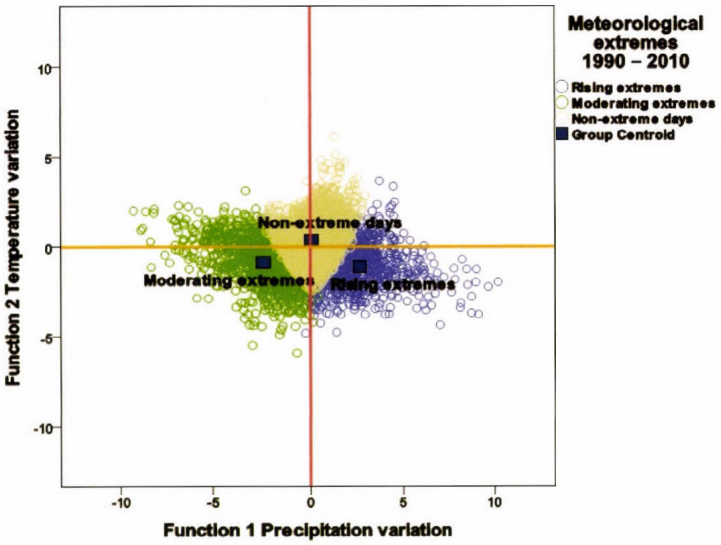

Fig 4. Meteorological extremes for the period 1990–2010 (canonical discriminant functions reclassified).

The grouping of day-to-day meteorological variations by intensity and direction created the opportunity of in-detail analysis of accidents involving personal injury by the indicated categories. The development of multivariate linear regression analysis relation (R-squared) calculated between traffic accidents involving personal injury per estimated traffic and day-to-day variation of meteorological features by meteorological change extremes can be seen in *Fig. 5*.

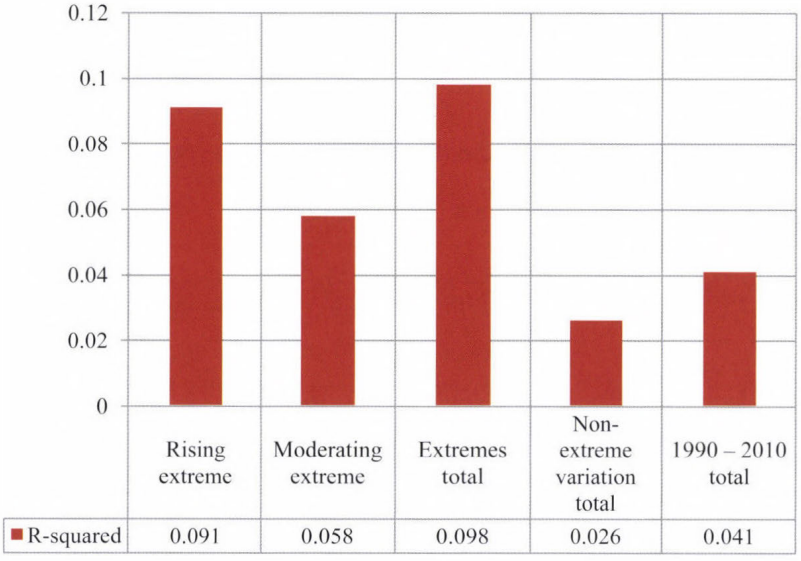

	Rising extreme	Moderating extreme	Extremes total	Non-extreme variation total	1990 – 2010 total
R-squared	0.091	0.058	0.098	0.026	0.041

Fig. 5. The development of multivariate linear regression analysis relation (R-squared) calculated between traffic accidents involving personal injury per estimated traffic and day-to-day variation of meteorological features by meteorological change extremes.

Analyses and classifications in the case of days qualified as extreme in meteorological change show marked interrelations between accidents and climatic variations. Moreover, the more intense the variation, the more powerful the correlation formed with the variation (rise or modification) of accidents.

In accordance with the multivariate linear regression calculated between the extreme meteorological change and accident variation, meteorological variations explained already 9.8 percent of accident variation. In contrast, road traffic accidents involving personal injury under non-extreme meteorological variation conditions can only be attributed in 2.6 percent – more than three and half times smaller proportion than in case of extreme variations – to climatic changes from the previous day. Results of stepwise method applied are summarized in *Table 6*.

Among the components of extreme meteorological variation conditions, the variation of accidents (increase or decrease) was most fundamentally affected by the combination of relative humidity and precipitation (nearly 8.4 percentage point), followed by, together with the previous factors, or independently from them, the nearly 1.0 percentage point effect of temperature variation. The moderated decrease of cloud cover only slightly modified the combined effect of the former factors, and the variation of wind force did not have significant effect. The significance and direction of the partial effect of the various climatic factors were also varied. The decrease of relative humidity and especially of temperature moderated, while the increase of precipitation and the decrease of cloud cover increased the probability of accidents.

Table 6. Multivariate regression interrelations of daily variation of accidents (dependent variable) for estimated traffic with daily meteorological variation indicators (independent variables) (Stepwise method), between 1990 and 2010

Model summary*									
					Change statistics				
Model	R	R-squared	Adjusted R-squared	Std. error of the Estimate	R-squared change	F change	df1	df2	Sig. F change
1	0.262[a]	0.069	0.068	0.64266	0.069	106.043	1	1433	0.000
2	0.290[b]	0.084	0.083	0.63761	0.015	23.830	1	1432	0.000
3	0.307[c]	0.094	0.093	0.63424	0.010	16.235	1	1431	0.000
4	0.313[d]	0.098	0.095	0.63327	0.003	5.384	1	1430	0.020

* Dependent variable: daily variation of the number of accidents for estimated traffic

[a] Predictors: (constant), variation of daily mean relative humidity

[b] Predictors: (constant), variation of daily mean relative humidity, variation of daily mean precipitation amount

[c] Predictors: (constant), variation of daily mean relative humidity, variation of daily mean precipitation amount, variation of daily mean temperature

[d] Predictors: (constant), variation of daily mean relative humidity, variation of daily mean precipitation amount, variation of daily mean temperature, variation of daily mean cloud cover

In the case of non-extreme – slightly deviating from the mean – meteorological changes, only very weak partial relation prevailed among accident variations and the variations in precipitation, cloud cover, air pressure, and temperature, and there was no significant relation with the variation of relative humidity and wind force.

The mutually neutralizing character of the various meteorological factors played significant role in the weakness of the effect on accident variations, because the accident increasing effect of the rise of temperature and the decrease

of air pressure was largely compensated by the accident risk moderating effect of the decrease of precipitation and the growth of cloud cover.

The extreme and non-extreme categories only expressed deviations from the general trend of climatic processes – and not with equal accuracy –, however, they did not reflect the direction of the changes. Consequently, these are not appropriate for the separate examination of interrelations between the development of accidents and the appearance and rising or moderation and disappearance of extremes. Furthermore, they do not offer opportunity to consider and prognosticate the possible consequences on the development of accidents, and in general, on the human and social relations if, in the future, the frequency of appearance and rise, or temporal durability of extreme meteorological conditions should increase compared to non-extreme days and periods. Variation of the daily mean values of the meteorological features by the rate and direction of extremes between 1990 and 2010 is presented in *Fig. 6*.

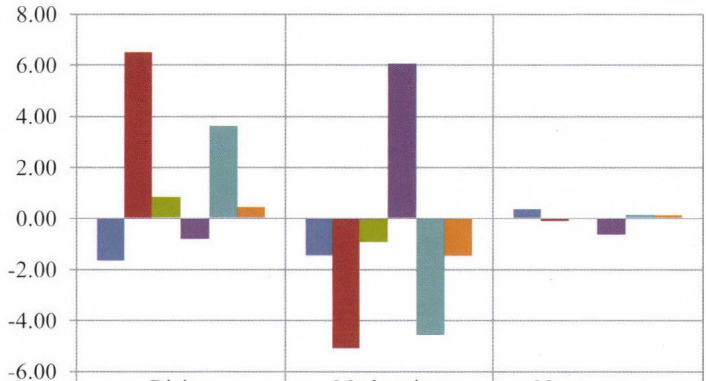

	Rising extreme	Moderating extreme	Non-extreme variation total
Var. of daily mean temperature [°C]	-1.67	-1.45	0.36
Var. of daily mean precipitation amount [mm]	6.49	-5.09	-0.12
Vari. of daily mean wind speed [m/s]	0.84	-0.95	0.02
Var. of daily mean air pressure [hPa]	-0.83	6.06	-0.63
Var. of daily mean relative humidity [% points]	3.61	-4.57	0.14
Var. of daily mean cloud cover [okta]	0.43	-1.46	0.13

Fig. 6. Variation of the daily mean values of the meteorological features by the rate and direction of extremes between 1990 and 2010.

Regarding the direction of extremes in the various categories among the mean values of examined meteorological indicators – excluding temperature variation –, usually significant and partially symmetric differences were developed. For example, while on days with rising extremes, precipitation increased by a mean of 6.5 mm, relative humidity by 3.6% points, wind force by 0.84 m/s, compared to the previous day, then on days with moderating extremes, precipitation decreased by 5.1 mm, relative humidity by 4.6% points, and wind force by 0.95 m/s. However, the variation of air pressure and cloud cover significantly deviated from the generic trend only in the case of moderating extremes. The air pressure increased rather significantly, and cloud cover decreased. However, temperature usually fell in the course of both rising and moderating extremes.

Applied statistical tests have shown that the most significant difference among the various categories by the direction of the extremes appeared in the precipitation amount variation, but the deviations of air pressure, cloud cover and wind force are also rather characteristic. The differences in the variations of relative humidity, and especially that of temperature, are less relevant than the above-mentioned components.

The appearing and rising meteorological extremes already impacted the increase of accidents by nearly 9.1 percentage. The rise of humidity (in nearly 80 percent), the decrease of temperature, and the strengthening of wind had the most significant impact. The effect of the various meteorological components was not restricted to one-way only. The rise of relative humidity (and of the mostly well correlated precipitation amount) and the increase of wind force impacted the increase of accidents, while the moderation of temperature impacted the decrease of accidents. According to the results of regressive analysis, the effect of temperature decrease slowed the increase of the number of accidents by nearly one third.

In the moderating and disappearing extreme periods the relation between the climatic variations and the variation of accidents is significantly weaker (5.8% R-Square) than in the period of rising extremes, yet still more than twice stronger than in the case of non-extreme variations. It may lay behind the relative weakness of the interrelation that the temporal processes of appearing, rising, and moderating, disappearing are not necessarily of the same length. In moderating extreme periods, the moderation of precipitation amount, closely followed by the moderation of temperature and relative humidity had the most significant impact on the characteristic decrease of accidents. At the same time, the decrease of cloud cover affected the increase of accidents, and as a result, the one-third slower moderation of the number of accidents.

3. Relationship between traffic accidents and key meteorological components

More detailed analyses uncovered significantly stronger relations than in case of categories containing the direction and intensity of meteorological variations rather aggregated regarding the extremes. Especially in the case of the most extreme variation of meteorological conditions, and in the autumn and winter periods, strong correlation was formed with the variation of accidents.

Among the meteorological types of variations came from the 25-element solution, in the case of the group carrying the unfolding of the most extreme variation, the number of accidents increased already in nearly one fifth as the effect of the climatic variations (especially the excessively significant increase of precipitation amount and relative humidity, and decrease of air pressure and temperature) to an outstanding level exceeding the mean value of rising extremity nearly two and a half times. The type is particularly characterized by above the average proportion of summer days with rain, rain shower, and thunderstorm. The number of rainy days is six times, and those with rain shower, and thunderstorm is nearly three times higher than the national average. The climatic determination of accident locations and situations also shows characteristic features. Meteorological variation had particularly significant effect on the development of the frequency of accidents involving slight injuries, hitting pedestrians, oncoming traffic, road bends, and residential area. The effects on accidents involving slight injury nearly ten times, and on accidents involving hitting pedestrians and occurring in road bends over eight times exceeded the general impact.

The strengthening of the interrelation between the intensity of meteorological extremes and the increase of the frequency of accidents can be typically explained by the grouping by direction and intensity of the variation of the analyzed primary meteorological features. In a method identical with multidimensional classifications, the categorization of the various meteorological indicators was also performed with automatic classification technique (K-mean clustering) – in order that the result of classification factually express the spatial distance among the groups as regards their content.

Seven search groups were conventionally determined, therefore because of the differences among the distributions, the number of days significantly differs in the various categories. For example, barely one percent of the days of the examined 21 years was classified into the category of the most intensive precipitation increase, and nearly identically with this proportion, the element number of the most extreme temperature variation (increase and decrease) categories increasing (*Figs. 7* and *8*).

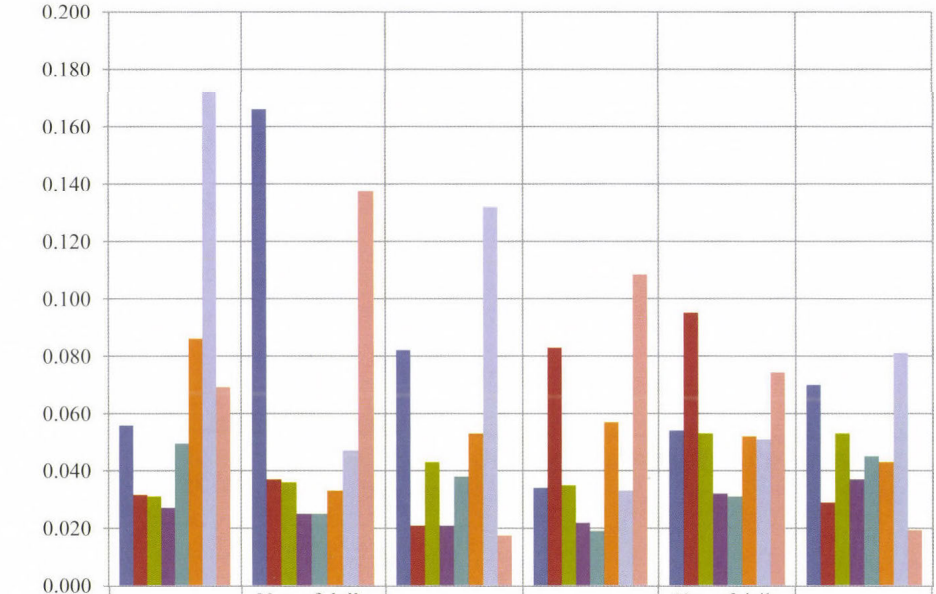

	Var. of daily mean temperature [°C]	Var. of daily mean precipitation amount [mm]	Var. of daily mean wind speed [m/s]	Var. of daily mean air pressure [hPa]	Var. of daily mean relative humidity [% points]	Var. of daily mean cloud cover [okta]
Cluster 1	0.056	0.166	0.082	0.034	0.054	0.070
Cluster 2	0.032	0.037	0.021	0.083	0.095	0.029
Cluster 3	0.031	0.036	0.043	0.035	0.053	0.053
Cluster 4	0.027	0.025	0.021	0.022	0.032	0.037
Cluster 5	0.050	0.025	0.038	0.019	0.031	0.045
Cluster 6	0.086	0.033	0.053	0.057	0.052	0.043
Cluster 7	0.172	0.047	0.132	0.033	0.051	0.081
Total	0.069	0.137	0.017	0.108	0.074	0.019

Fig. 7. Multivariate linear interrelation of daily variation of accidents for traffic with the totality of daily meteorological variations (R-squared) calculated by clusters obtained by automatic classification of certain meteorological variation components.

The offered charts clearly indicate that progressing from the general trend of variations towards the intensification of extremities by an approximately U-shaped curve the effect of the various meteorological factors is increasingly stronger on the development of accidents, and depending on the direction of the variation, increasingly more significant scale variation (rise or decrease) occurred in the number of accidents, as well.

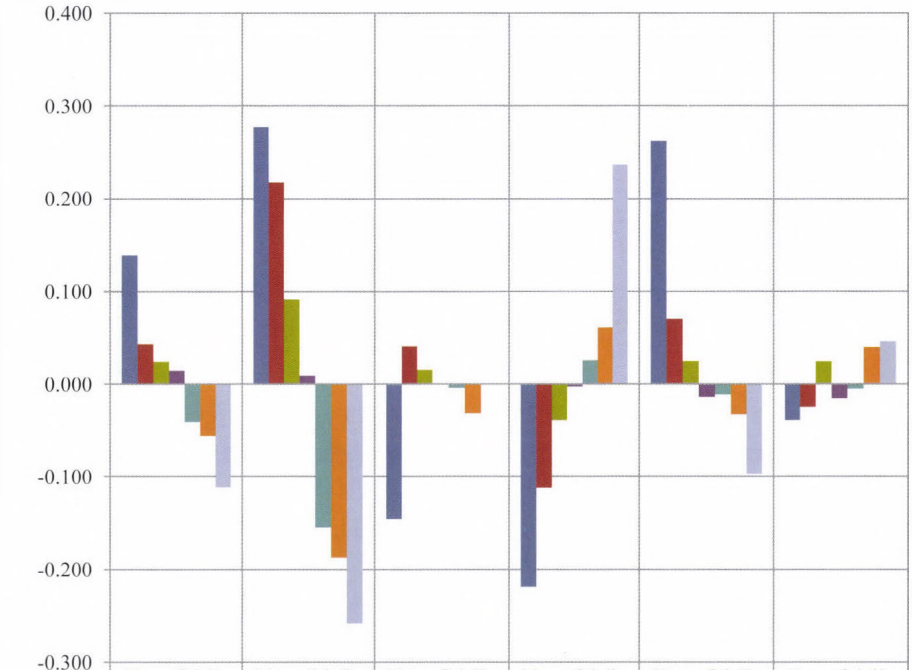

	Var. of daily mean temperature [°C]	Var. of daily mean precipitation amount [mm]	Var. of daily mean wind speed [m/s]	Var. of daily mean air pressure [hPa]	Var. of daily mean relative humidity [% points]	Var. of daily mean cloud cover [okta]
Cluster 1	0.139	0.277	-0.146	-0.219	0.263	-0.039
Cluster 2	0.043	0.217	0.041	-0.112	0.070	-0.025
Cluster 3	0.024	0.091	0.015	-0.039	0.024	0.024
Cluster 4	0.015	0.009	0.000	-0.003	-0.014	-0.016
Cluster 5	-0.041	-0.155	-0.004	0.025	-0.011	-0.005
Cluster 6	-0.056	-0.187	-0.031	0.061	-0.033	0.040
Cluster 7	-0.111	-0.258	-0.001	0.236	-0.097	0.046

Fig. 8. Mean of daily variation of accidents for traffic calculated by clusters obtained by automatic classification of certain meteorological variation components.

In the case of the most extreme categories according to the increase of precipitation amount and the decrease of temperature, the combined effect of all the meteorological factors exceeds four times the average, and more than six times the average of non-extreme days. It can be said of all the above-mentioned categories, that the significant scale variation of accidents (increase in the case of precipitation variation and decrease in the case of temperature variation) was already induced in a proportion of one-sixth by meteorological change or inappropriate accommodation to these.

Besides the above mentioned facts, the combined effect of meteorological variation factors was very significant in the most extreme categories as regards wind force strengthening (8.2 and 13.2 percent) but in the frames of both extremes the accident moderating effect became dominant. Furthermore, this effect was significant on the opposing poles of the variation of cloud cover (7, and 8.1 percent determination). The relationship between the variation of accidents and cloud cover – jus as that of air pressure variation – essentially developed inversely as temperature and precipitation variation, because the increase of cloud cover and air pressure amount correlates with the moderation of accidents, while the decrease of these factors correlates with the increase of accidents.

In contrast to the most extreme – mostly containing the rise – categories of air pressure and relative humidity variation, the relationship of one degree less extreme categories was the strongest with the variation of accidents, while accident variation was the most intensive in the most extreme categories. It cannot be excluded, that the use of multidimensional, nonlinear methods or the proper transformation of variants should lead to different results.

4. Relationship between traffic accidents and extreme meteorological variations

The determination by meteorological variations of accident development changed extraordinarily differently by the seasons. The spring and summer period determination does not reach even half of the average, and only in the period of the moderation of extremes does remarkable relationship manifest itself. In contrast, in the second half-year, meteorological extremes had significant – 17.4 percent in autumn, 13.4 percent in winter – effect on the development of accidents. The linear regressive interrelations (R-squared) between the daily variations by seasons of road traffic accidents involving personal injury and meteorological conditions are shown in *Fig. 9.*

The differences can be partially explained by the unequal distribution of extreme meteorological conditions, according to which, in the second half-year, the frequency of extreme variations characteristically exceeded the average in winter, typically because of the excessive proportion of moderating extremes, while in spring, it significantly fell short of it. The proportion of rising extreme days, on the other hand, exceeded the prorated distribution, especially in summer and autumn. Distribution of daily variations categorized by the type of meteorological extremity across the seasons is presented in *Fig. 10*, while seasonal averages of road accidents involving personal injury for estimated traffic, between 1990 and 2010 can be found in *Fig. 11.*

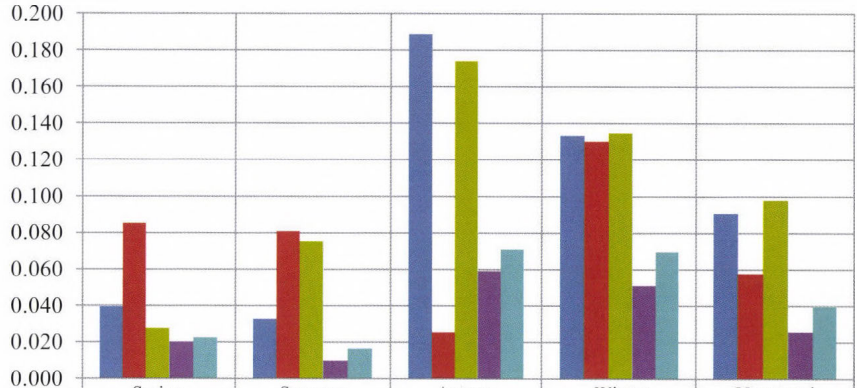

	Spring	Summer	Autumn	Winter	Year total
Rising extreme	0.040	0.033	0.189	0.134	0.091
Moderating extreme	0.085	0.081	0.026	0.130	0.058
Extreme days total	0.028	0.075	0.174	0.135	0.098
Non-extreme days total	0.020	0.010	0.059	0.051	0.026
1990 – 2010 days total	0.023	0.017	0.071	0.070	0.040

Fig. 9. Linear regressive interrelations (R-squared) between the daily variations by seasons of road traffic accidents involving personal injury and meteorological conditions, between 1990 and 2010.

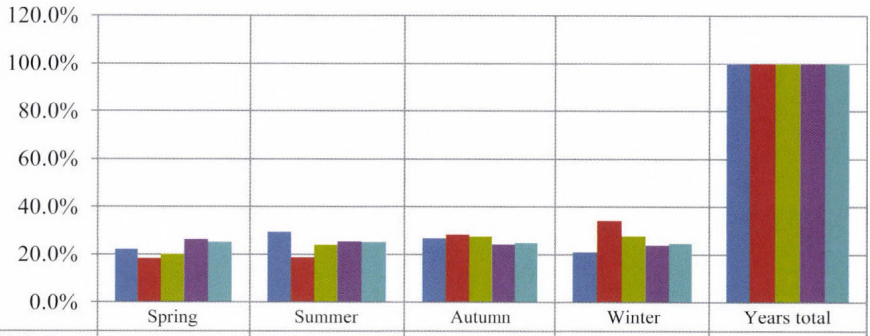

	Spring	Summer	Autumn	Winter	Years total
Rising extreme	22.3%	29.7%	26.8%	21.2%	100.0%
Moderating extreme	18.4%	18.8%	28.6%	34.3%	100.0%
Extreme days total	20.3%	24.0%	27.7%	27.9%	100.0%
Non-extreme days total	26.3%	25.5%	24.3%	24.0%	100.0%
1990 – 2010 days total	25.2%	25.2%	24.9%	24.7%	100.0%

Fig. 10. Distribution of daily variations categorized by the type of meteorological extremes across the seasons.

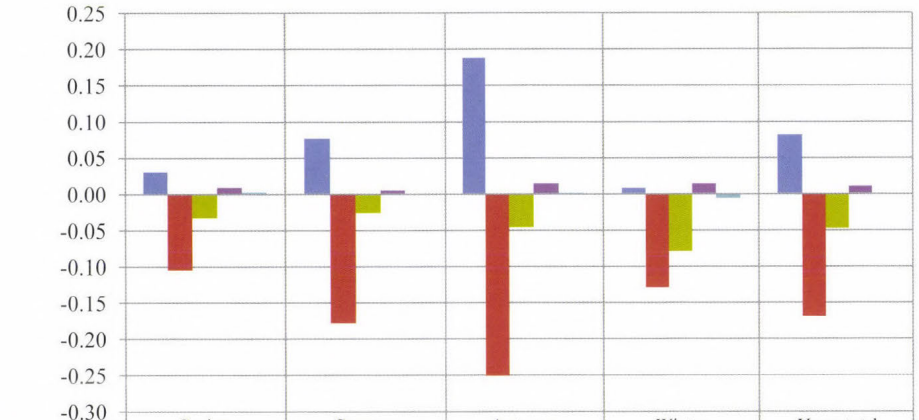

	Spring	Summer	Autumn	Winter	Years total
Rising extreme	0.03	0.08	0.19	0.01	0.08
Moderating extreme	-0.10	-0.18	-0.25	-0.13	-0.17
Extreme days total	-0.03	-0.03	-0.05	-0.08	-0.05
Non-extreme days total	0.01	0.01	0.01	0.01	0.01
1990 – 2010 days total	0.00	0.00	0.00	-0.01	0.00

Fig. 11. Seasonal averages of road accidents involving personal injury for estimated traffic between 1990 and 2010.

The variation in the number of accidents under unfolding and rising extreme conditions increased in autumn – more than twofold – above the average, and the relationship between accidents and climate variations was the strongest in this season, as well. To an extent nearly one-fifth, the complex impact of climate variation, but especially, the variation of relative humidity (and behind this, the mostly well correlated cloud cover and precipitation amount variation) and the variation of temperature and wind force impacted the development of accidents. The increase of relative humidity and strengthening of wind force impacted the increase of accidents, while the decrease of temperature impacted the decrease of accidents, however, it could only partially slow the increase of accidents. Variation of daily average value of the main meteorological features and the traffic accidents related to estimated traffic density due to previous day in case of rising extremes by seasons is shown in *Fig. 12,* while the development of the calculated standardized Beta coefficient between the daily variations of the traffic accidents with personal injury related to estimated traffic density and the daily variations of the meteorological features in case of rising extremes by seasons is presented in *Fig. 13.*

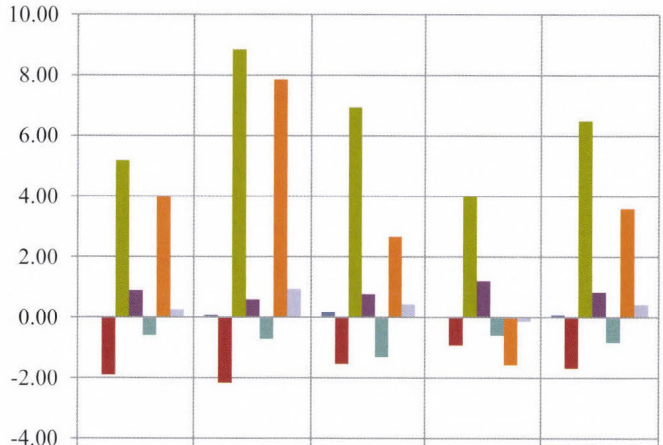

	Spring	Summer	Autumn	Winter	Rising extremes total
Daily var. of the number of accidents for estimated traffic [accident / hundred thousand vehicles]	0.03	0.08	0.19	0.01	0.08
Var. of daily mean temperature [°C]	-1.90	-2.16	-1.53	-0.92	-1.67
Var. of daily mean precipitation amount [mm]	5.18	8.85	6.94	4.00	6.49
Var. of daily mean wind speed [m/s]	0.90	0.59	0.76	1.21	0.84
Var. of daily mean air pressure [hPa]	-0.60	-0.72	-1.31	-0.60	-0.83
Var. of daily mean relative humidity [% points]	3.99	7.87	2.66	-1.56	3.61
Var.of daily mean cloud cover [okta]	0.27	0.94	0.44	-0.14	0.43

Fig. 12. Variation of daily average value of the main meteorological features and the traffic accidents related to estimated traffic density due to previous day in case of rising extremes by seasons between 1990 and 2010.

Opposed to the autumn periods of rising extremes, the increase of accident numbers in winter reached only one tenth of the average of this type; despite that the totality of meteorological effects directed toward it was relatively significant (13.4 percent). The increase of precipitation amount and the strengthening of wind were especially impacting the increase of accidents, while its decrease was affected characteristically by decreasing relative humidity and decrease of temperature (unlike the rest of the seasons). The moderate increase in the number of accidents is primarily explained by that, in total, in the winter, the intensity of the variation of components of climatic conditions – with the exception of wind force, which increased in a rate exceeding that of the other seasons – was far below the 1990–2010 average of rising extreme variation.

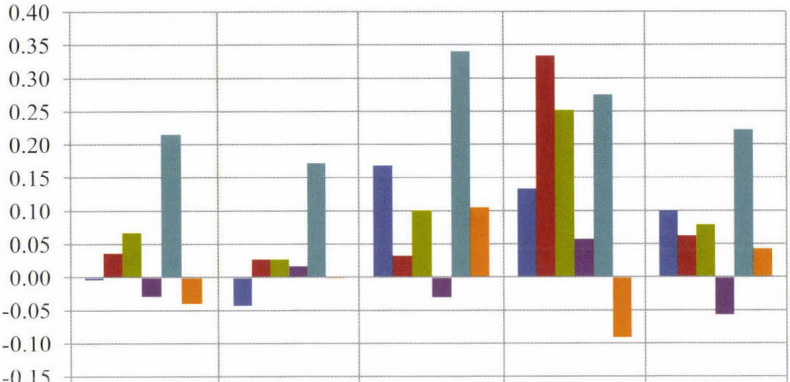

	Spring	Summer	Autumn	Winter	Rising extreme total
Var. of daily mean temperature [°C]	0.00	-0.04	0.17	0.13	0.10
Var. of daily mean precipitation amount [mm]	0.04	0.03	0.03	0.33	0.06
Var. of daily mean wind speed [m/s]	0.07	0.03	0.10	0.25	0.08
Var. of daily mean air pressure [hPa]	-0.03	0.02	-0.03	0.06	-0.06
Var. of daily mean relative humidity [% points]	0.22	0.17	0.34	0.28	0.22
Var. of daily mean cloud cover [okta]	-0.04	0.00	0.11	-0.09	0.04

Fig. 13. Development of the calculated standardized Beta coefficient between the daily variations of the traffic accidents with personal injury related to estimated traffic density and the daily of the meteorological features in case of rising extremes by seasons.

In the spring and summer periods of appearing, rising extremes, only relatively weak (4 and 3.3%, respectively) multivariate linear relationship prevailed between the variation of accidents and climatic conditions; and the change in the number of accidents developed below the average of the category averages, especially in spring, however, still exceeding nearly three times the extent of winter variation. In both seasons, only the increase of relative humidity (or, behind that, the increase of cloud cover and precipitation) had substantial effect on the increase of accidents, yet this effect was much weaker than in autumn or – with different sign – in winter. The different extent increase of accidents was basically brought about by the significantly different intensity of meteorological variations. While springtime variations developed in an extent nearly identical with the annual average of the category, then the relative humidity and cloud cover increased with more than double, and precipitation amount more than one third above the average in the summer period of rising extremes. Only the extent of the increase of wind force fell below the average.

5. *Relationship between traffic accidents and extreme meteorological variations by accident severity, and situation*

Looking at the whole of the 1990–2010 period, the relationship of climatic variations with a more detailed breakdown of accidents – with the development by outcomes involving persons, gravity, accident locations and situations – is rather weak, falling behind the already described overall effect (*Table 7*).

Table 7. Development of multivariate linear regression relationships of the daily variation of meteorological variations and accidents involving personal injury per accident consequences, locations, and situations, and the extremity of meteorological change

Absolute variation from the previous day	Rising extreme days	Moderating extreme days	Extreme days total	Non-extreme days total	Days total in 1990–2010
	R-squared				
Variation of number of accidents	0.104	0.063	0.097	0.027	0.041
Variation of number of fatal accidents	0.026	0.021	0.015	0.005	0.006
Variation of number of serious accidents	0.062	0.036	0.052	0.013	0.020
Variation of number of slight accidents	0.076	0.045	0.079	0.022	0.032
Variation of number of accidents in residential areas	0.061	0.049	0.049	0.025	0.029
Variation of number of accidents outside residential areas	0.121	0.035	0.111	0.016	0.036
Variation of number of accidents on straight paths	0.074	0.038	0.063	0.014	0.023
Variation of number of accidents in road bends	0.117	0.056	0.120	0.014	0.035
Variation of number of accidents in road crossings	0.040	0.046	0.037	0.028	0.027
Variation of number of accidents in other road sections	0.022		0.010		0.003
Variation of number of accidents due to head-on collision of vehicles	0.160	0.053	0.150	0.027	0.055
Variation of number of accidents due to collision of vehicles travelling in the same direction	0.008	0.050	0.023	0.010	0.012
Variation of number of accidents due to collision of vehicles crossing paths	0.006	0.033	0.013	0.022	0.018
Variation of number of accidents due to slipping, skidding, tipping on road	0.015	0.017	0.012	0.003	0.004
Variation of number of accidents involving hitting pedestrian	0.077	0.013	0.049	0.012	0.021

(Note: The table contains only significant statistics.)

Interrelation stronger than the average can we observed only in the case of accidents due to collision of vehicles travelling towards each other ; however, this is not explained by the effects characterized days without meteorological extremes, but by the extremely strong consequences of the appearance and rise of extremes affecting the whole category. The increase in the number of accidents due to the collision of vehicles travelling towards each other in the period of appearing and rising extreme meteorological conditions – beyond all other categories shown in the table – was determined by climatic variations in a proportion of nearly one sixth, or at least developed synchronously with those in this degree. The formation of the interrelation and the significant increase of accidents in scale were primarily (in nearly 90 percent) impacted by the increase of relative humidity of air, and, in the remaining proportion, by the decrease of air pressure.

Besides the above category, meteorological change had particularly significant impact on the increase of accidents outside residential areas and in road bends in an extent exceeding the average of the category of the total appearing and rising extremes (nearly 12 percent). The overall effect was, however, less significant; but in the case of accidents involving hitting pedestrians – in general slight and serious accidents –, on straight paths and in residential areas, the effect of climatic variations in the period of rising extremes exceeds multiple times those prevailing in non-extreme periods. (For example: in the case of hitting pedestrians, nearly six times, and three-four times in the case of accidents involving slight and serious injuries and on straight path, and over twice in case of accidents in residential areas.) Although, in total, the determination of the variation of fatal accidents by climatic variations can be regarded to be modest, it was nearly five times stronger among extreme meteorological conditions than in other periods.

6. Future expected tendencies between traffic accidents and key meteorological variations

The time series data of the endeavor to differentiate extreme and non-extreme meteorological changes show, that between 1990 and 2010 the climatic variations became somewhat more extreme. This is supported by the data expressing the annual proportions of extreme, and appearing and rising extreme days, and the linear trends calculated on their basis. The relatively detailed classification and the reclassified – giving a broader sense to extremity – categorization essentially led to the same result. According to both approaches, the linear trend of extremity and rising extremes – in spite of fluctuations – took a decidedly upward direction. Proportion of extreme days as well as that of rising extreme days is shown in *Figs. 14* and *15*.

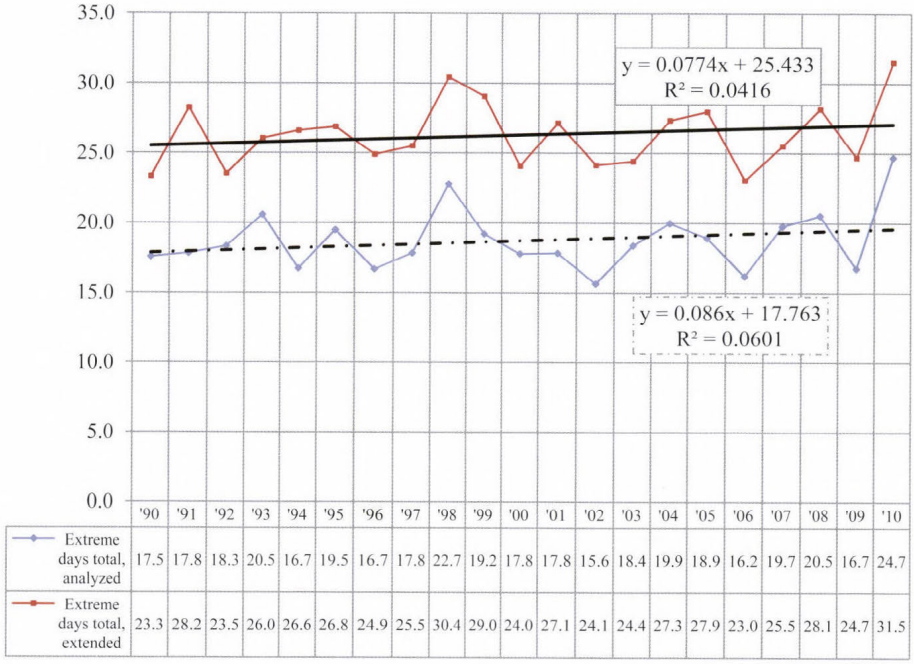

	'90	'91	'92	'93	'94	'95	'96	'97	'98	'99	'00	'01	'02	'03	'04	'05	'06	'07	'08	'09	'10
Extreme days total, analyzed	17.5	17.8	18.3	20.5	16.7	19.5	16.7	17.8	22.7	19.2	17.8	17.8	15.6	18.4	19.9	18.9	16.2	19.7	20.5	16.7	24.7
Extreme days total, extended	23.3	28.2	23.5	26.0	26.6	26.8	24.9	25.5	30.4	29.0	24.0	27.1	24.1	24.4	27.3	27.9	23.0	25.5	28.1	24.7	31.5

Fig. 14. Proportion of extreme days between 1990 and 2010 (%).

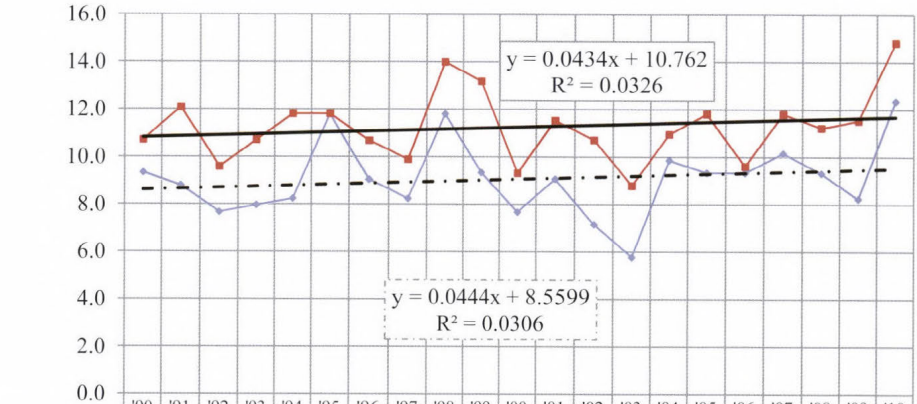

	'90	'91	'92	'93	'94	'95	'96	'97	'98	'99	'00	'01	'02	'03	'04	'05	'06	'07	'08	'09	'10
Rising extreme, analyzed	9.3	8.8	7.7	7.9	8.2	11.8	9.0	8.2	11.8	9.3	7.7	9.0	7.1	5.8	9.8	9.3	9.3	10.1	9.3	8.2	12.3
Rising extreme, extended	10.7	12.1	9.6	10.7	11.8	11.8	10.7	9.9	14.0	13.2	9.3	11.5	10.7	8.8	10.9	11.8	9.6	11.8	11.2	11.5	14.8

Fig. 15. Proportion of rising extreme days between 1990 and 2010 (%).

The variability trends of the various meteorological features mostly support the picture painted by the typologies. The linear trends of temperature, precipitation, air pressure, and relative humidity – although to varying extent – refer to the rising of extremes, while that of wind force and cloud cover to moderating extremes. Absolute deviation (range) by the year of the daily variation of the meteorological indicators between 1990 and 2010 is presented in *Fig. 16.*

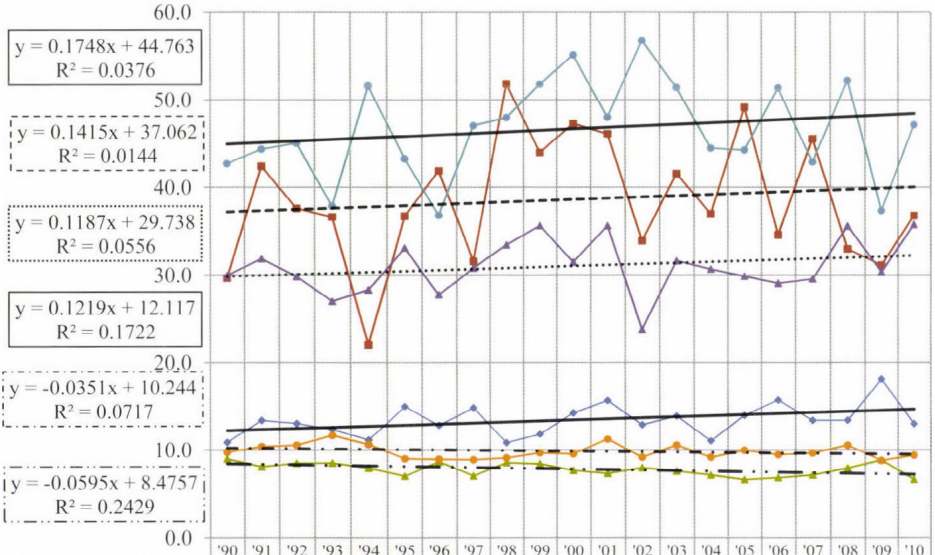

	'90	'91	'92	'93	'94	'95	'96	'97	'98	'99	'00	'01	'02	'03	'04	'05	'06	'07	'08	'09	'10
Var. of daily mean temperature [°C]	10.9	13.5	13.1	12.4	11.2	15.0	12.9	14.9	10.9	11.9	14.3	15.7	12.9	13.9	11.1	14.0	15.8	13.4	13.5	18.2	13.1
Var. of daily mean precipitation amount [mm]	29.7	42.4	37.6	36.7	22.1	36.8	41.9	31.6	51.9	44.0	47.3	46.1	33.9	41.6	37.0	49.2	34.6	45.6	33.0	31.2	36.8
Var. of daily mean wind speed [m/s]	9.0	8.1	8.5	8.6	8.0	7.1	8.7	7.1	8.6	8.5	7.7	7.4	8.0	7.6	7.2	6.7	6.9	7.2	8.0	8.9	6.7
Var. of daily mean air pressure [hPa]	30.0	31.9	29.9	27.0	28.3	33.1	27.8	30.9	33.5	35.7	31.5	35.7	23.8	31.7	30.7	29.9	29.1	29.6	35.6	30.4	35.8
Var. of daily mean relative humidity [% points]	42.8	44.4	45.1	37.9	51.7	43.3	36.9	47.1	48.0	51.8	55.2	48.1	56.8	51.5	44.5	44.3	51.4	42.9	52.3	37.4	47.2
Var. of daily mean cloud cover [okta]	9.8	10.4	10.6	11.7	10.7	9.1	9.0	8.9	9.2	9.7	9.6	11.3	9.2	10.6	9.2	10.0	9.5	9.7	10.6	8.8	9.4

Fig. 16. Absolute deviation (range) by the year of the daily variation of the meteorological indicators between 1990 and 2010.

On the basis of interrelationships seen between the slight extremization of meteorological variations, furthermore the extreme climatic variations and the variation of traffic accidents involving personal injury, it could be assumed that approaching our days, the connection would be further strengthened. This

hypothesis, however, was supported neither by the totality of meteorological variations, nor the statistical analyses of the various extremity categories.

According to the linear regression analysis of the annual (and three-year period) relationships of accident and meteorological variations, the correlation essentially did not change between 1990 and 2010, however, compared to 1993, the correlation weakened, and there were significant fluctuations within the period. (Note, that statistically not significant relations are not shown in the diagrams.) Results are shown in *Figs. 17, 18,* and *19.*

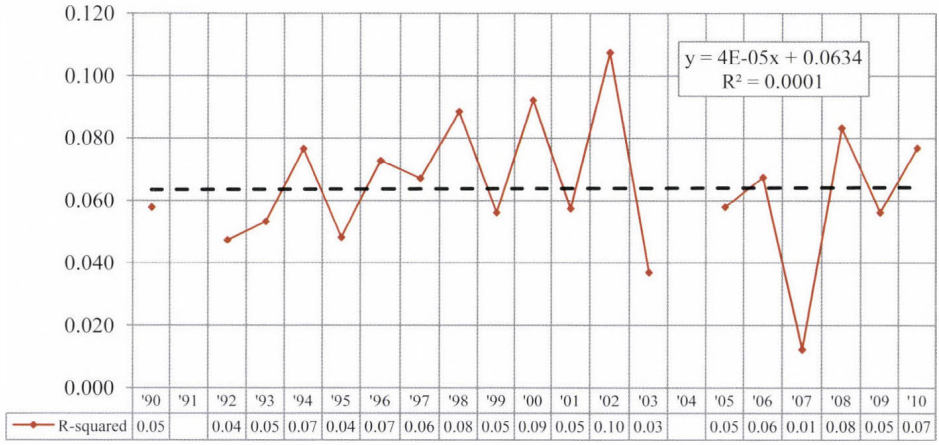

	'90	'91	'92	'93	'94	'95	'96	'97	'98	'99	'00	'01	'02	'03	'04	'05	'06	'07	'08	'09	'10
R-squared	0.05		0.04	0.05	0.07	0.04	0.07	0.06	0.08	0.05	0.09	0.05	0.10	0.03		0.05	0.06	0.01	0.08	0.05	0.07

Fig. 17. The multivariate linear regression analysis interrelation (R-squared) calculated among the daily variation of traffic accidents involving personal injury with the daily variation of analyzed meteorological characteristics between years 1990 and 2010.

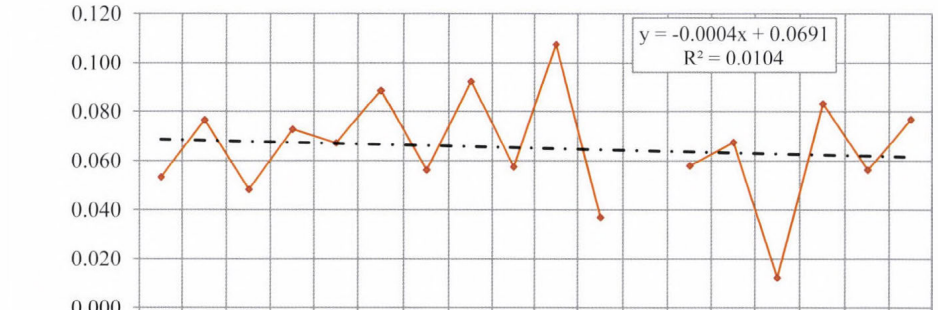

	'93	'94	'95	'96	'97	'98	'99	'00	'01	'02	'03	'04	'05	'06	'07	'08	'09	'10
R-squared	0.053	0.076	0.048	0.073	0.067	0.088	0.056	0.092	0.057	0.107	0.037		0.058	0.067	0.012	0.083	0.056	0.077

Fig. 18. The multivariate linear regression analysis interrelation (R-squared) calculated among the daily variation of traffic accidents involving personal injury with the daily variation of analyzed meteorological characteristics between years 1993 and 2010.

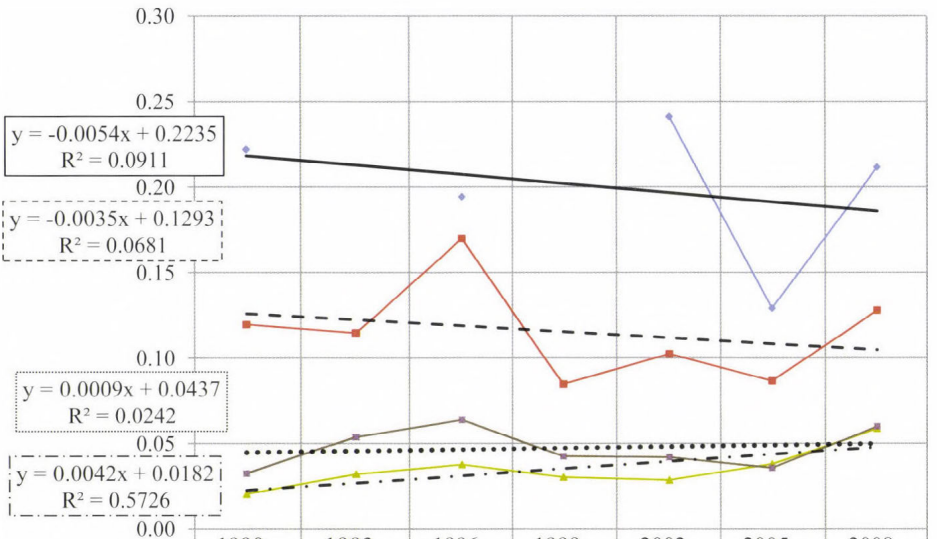

	1990 - 1992	1993 - 1995	1996 - 1998	1999 - 2001	2002 - 2004	2005 - 2007	2008 - 2010
Rising extremes	0.22		0.19		0.24	0.13	0.21
Extreme days total	0.12	0.11	0.17	0.08	0.10	0.09	0.13
Non-extreme days	0.02	0.03	0.04	0.03	0.03	0.04	0.06
Days total	0.03	0.05	0.06	0.04	0.04	0.04	0.06

Fig. 19. The multivariate linear regression interrelations (R-squared) calculated among the daily variation of traffic accidents involving personal injury with the daily variation of analyzed meteorological features, between 1990 and 2010, in three years breakdown.

Presumably, the weakness and weakening of relationships can primarily be explained by the rather significant moderation of total traffic accidents involving personal injury, by their relatively hectic development, and by economic processes and regulatory environment affecting the above. In 2010, the number of accidents was nearly forty percent lower than in 1990, primarily on account of the decrease of fatal and serious accidents. At the same time, the number of slight accidents fell only by 21.8% compared to 1990; what's more, between 1993 and 2010, it moreover even increased. On account of the above circumstances, it seemed appropriate to extend the analysis to slight accident data between 1993 and 2010. The result of this shows that interrelation between extreme climatic variations and the variation of traffic accidents involving slight personal injury strengthened in the analyzed epoch (*Figs. 20* and *21*).

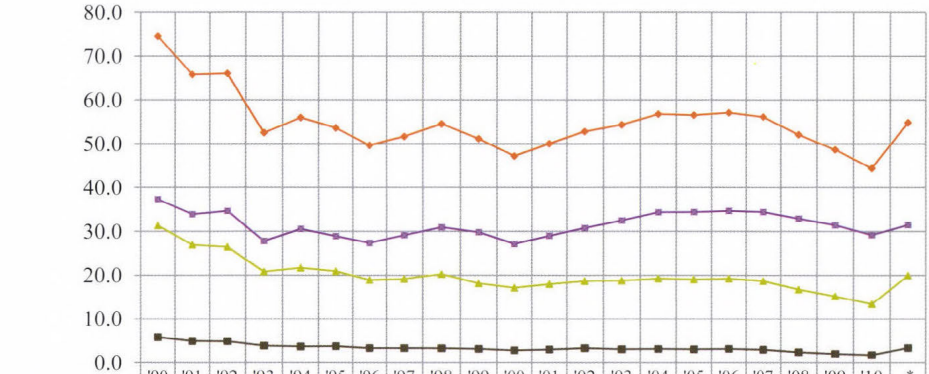

	'90	'91	'92	'93	'94	'95	'96	'97	'98	'99	'00	'01	'02	'03	'04	'05	'06	'07	'08	'09	'10	*
Number of accidents	74.6	65.9	66.1	52.6	56.0	53.7	49.7	51.7	54.6	51.2	47.2	50.1	52.9	54.4	56.8	56.6	57.2	56.2	52.1	48.7	44.4	54.9
Number of fatal accidents	5.8	5.0	4.9	3.9	3.7	3.8	3.4	3.4	3.3	3.2	2.8	3.0	3.3	3.1	3.2	3.1	3.2	3.0	2.4	2.0	1.8	3.4
Number of serious injury accidents	31.4	27.0	26.5	20.8	21.7	20.9	18.9	19.2	20.3	18.2	17.2	18.0	18.7	18.8	19.3	19.1	19.2	18.7	16.8	15.2	13.4	20.0
Number of slight injury accidents	37.4	34.0	34.7	27.9	30.6	29.0	27.4	29.2	31.0	29.9	27.2	29.0	30.8	32.5	34.4	34.5	34.7	34.5	33.0	31.5	29.2	31.5

*1991–2010 annual average

Fig. 20. Road traffic accidents involving personal injury between 1900 and 2010.

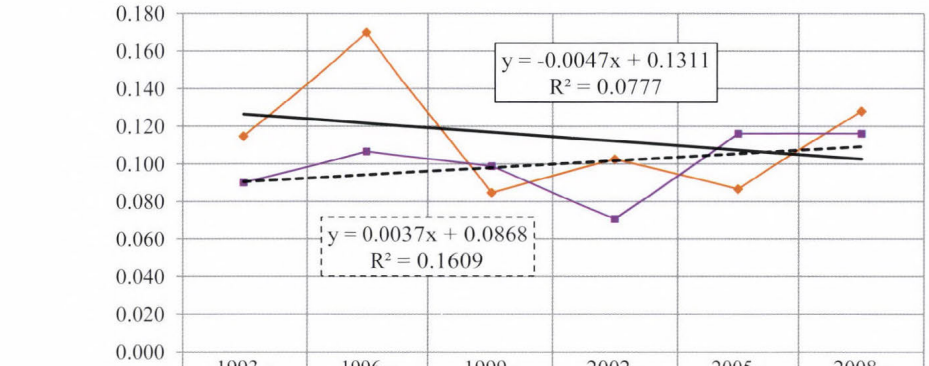

	1993 - 1995	1996 - 1998	1999 - 2001	2002 - 2004	2005 - 2007	2008 - 2010
Daily var. of accident numbers	0.115	0.170	0.085	0.103	0.087	0.128
Daily var.of slight accident numbers	0.090	0.107	0.099	0.071	0.116	0.116

Fig. 21. Three-year multivariate linear interrelations of day-to-day variation of accidents and meteorological conditions between 1993 and 2010 (R-squared) in case of extreme variation.

Naturally, the above described results will provide little guidance to the prognosticability of future developments; however, on the basis of the analysis results, it can be said that the significant future rise of extreme meteorological conditions, and, possibly as a result, the appearing and rising climate change will have significant effect on the development, on the number of accidents, or on the deceleration of the rate of moderation, and, in general, on the development of social relations, which are generally relatively well represented by accident conditions.

7. Conclusions

Compared to other economically and socially important sectors such as energy, water resources, agriculture, and human health (*Törő et al.*, 2010), the assessment of the potential impacts of climate change on transport and road accidents is an area with very limited investigations so far. The increased demand for personal mobility, the dependence on reliable movement of goods and components in the supply chain, and the observed disruption effect of the weather (*Koetse* and *Rietveld*, 2009) make the study of current and future transport resilience essential.

The investigations presented above might provide a potential guidance to the expectation of future developments in the forthcoming decades. On the basis of the results, it can probably be said that the expected increase in the number and intensity of extreme meteorological conditions can have a visible effect on the increase of the number of road accidents. The problem is rather complex, since the future climate change is expected to influence several layers of the social conditions as well, which is also going to be reflected in the road accident conditions.

Acknowledgements: This work is connected to the scientific project „Infocommunication technologies and the society of the future – Project ID: TÁMOP-4.2.2.C-11/1/KONV-2012-0013" of BME VIKING Zrt. (Budapest, Magyar tudósok körútja 2. H-1117) supported by European Social Fund. The assisstance of the Hungarian Meteorological Service in providing surface meteorological data for this research is also highly acknowledged.

References:

Andersson, A. and *Chapman, L.*, 2011: The impact of climate change on winter road maintenance and traffic accidents in West Midlands, UK. *Accident Anal. Prev. 43*, 284–289.

Edwards, J.B., 1999: The temporal distribution of road accidents in adverse weather. *Meteorol. Appl. 6*, 59–68.

Jaroszweski, D., Chapman, L. and *Petts, J.*, 2010: Assessing the potential impact of climate change on transportation: the need for an interdisciplinary research. *J. Transp. Geogr. 18*, 331–335.

Koetse, M.J. and *Rietveld, P.*, 2009: The Impact of climate change and weather on transport: an overview of empirical findings. *Transport. Res. Part D, 14*, 205–221.

Sándor, Zs.P., 2013: Az esőzés hatása a hazai autópályák forgalmi jellemzőire. *Közlekedéstudományi Szemle 63*, 25–35. (In Hungarian)

Suarez, P., Anderson, W., Mahal, V. and *Lakshmanan, T.R.*, 2005. Impacts of flooding and climate change on urban transportation: A systemwide performance assessment of the Boston Metro Area. *Transport. Res. Part D 10*, 231–244.

Törő. K., Bartholy. J., Pongrácz. R., Kiss. Zs., Keller. É. and *Dunay. Gy.*, 2010: Evaluation of meteorological factors on sudden cardiovascular death. *J. Forensic Legal Med. 17*, 236–242.

IDŐJÁRÁS

VOLUME 118 * 2014

BUDAPEST, HUNGARY

AUTHOR INDEX

TABLE OF CONTENTS

SUBJECT INDEX

A

V

W

INSTRUCTIONS TO AUTHORS OF *IDŐJÁRÁS*

The purpose of the journal is to publish papers in any field of meteorology and atmosphere related scientific areas. These may be

- research papers on new results of scientific investigations,
- critical review articles summarizing the current state of art of a certain topic,
- short contributions dealing with a particular question.

Some issues contain "News" and "Book review", therefore, such contributions are also welcome. The papers must be in American English and should be checked by a native speaker if necessary.

Authors are requested to send their manuscripts to

Editor-in Chief of IDŐJÁRÁS
P.O. Box 38, H-1525 Budapest, Hungary
E-mail: journal.idojaras@met.hu

including all illustrations. MS Word format is preferred in electronic submission. Papers will then be reviewed normally by two independent referees, who remain unidentified for the author(s). The Editor-in-Chief will inform the author(s) whether or not the paper is acceptable for publication, and what modifications, if any, are necessary.

Please, follow the order given below when typing manuscripts.

Title page: should consist of the title, the name(s) of the author(s), their affiliation(s) including full postal and e-mail address(es). In case of more than one author, the corresponding author must be identified.

Abstract: should contain the purpose, the applied data and methods as well as the basic conclusion(s) of the paper.

Key-words: must be included (from 5 to 10) to help to classify the topic.

Text: has to be typed in single spacing on an A4 size paper using 14 pt Times New Roman font if possible. Use of S.I. units are expected, and the use of negative exponent is preferred to fractional sign. Mathematical formulae are expected to be as simple as possible and numbered in parentheses at the right margin.

All publications cited in the text should be presented in the *list of references*, arranged in alphabetical order. For an article: name(s) of author(s) in Italics, year, title of article, name of journal, volume, number (the latter two in Italics) and pages. E.g., *Nathan, K.K.,* 1986: A note on the relationship between photo-synthetically active radiation and cloud amount. *Időjárás 90,* 10-13. For a book: name(s) of author(s), year, title of the book (all in Italics except the year), publisher and place of publication. E.g., *Junge, C.E.,* 1963: *Air Chemistry and Radioactivity.* Academic Press, New York and London. Reference in the text should contain the name(s) of the author(s) in Italics and year of publication. E.g., in the case of one author: *Miller* (1989); in the case of two authors: *Gamov* and *Cleveland* (1973); and if there are more than two authors: *Smith et al.* (1990). If the name of the author cannot be fitted into the text: *(Miller,* 1989); etc. When referring papers published in the same year by the same author, letters a, b, c, etc. should follow the year of publication.

Tables should be marked by Arabic numbers and printed in separate sheets with their numbers and legends given below them. Avoid too lengthy or complicated tables, or tables duplicating results given in other form in the manuscript (e.g., graphs).

Figures should also be marked with Arabic numbers and printed in black and white or color (under special arrangement) in separate sheets with their numbers and captions given below them. JPG, TIF, GIF, BMP or PNG formats should be used for electronic artwork submission.

Reprints: authors receive 30 reprints free of charge. Additional reprints may be ordered at the authors' expense when sending back the proofs to the Editorial Office.

More information for authors is available: journal.idojaras@met.hu

Published by the Hungarian Meteorological Service

Budapest, Hungary

INDEX 26 361

HU ISSN 0324-6329